Synthesis, Characterization and Photophysical Properties of Lanthanide Carboxylates

Thesis submitted to
The University of Kerala
for the award of the degree of

Doctor of Philosophy
in Chemistry
Under The Faculty of Science

BY
SHYNI RAPHAEL M

**NATIONAL INSTITUTE FOR INTERDISCIPLINARY
SCIENCE AND TECHNOLOGY
COUNCIL OF SCIENTIFIC AND INDUSTRIAL RESEARCH
THIRUVANANTHAPURAM-695 019
KERALA, INDIA**

2012

Dedicated to my Parents
and sumetan...

DECLARATION

I hereby declare that Ph.D thesis entitled "**Synthesis, Characterization and Photophysical Properties of Lanthanide Carboxylates**" is an independent work carried out by me at the Chemical Sciences and Technology Division, National Institute for Interdisciplinary Science and Technology (NIIST), CSIR, Thiruvananthapuram, under the supervision of Dr. M. L. P. Reddy, Chief Scientist, and it has not been submitted anywhere else for any other degree, diploma or title.

SHYNI RAPHAEL M

Thiruvanathapuram
September, 2012

NATIONAL INSTITUTE FOR INTERDISCIPLINARY SCIENCE AND TECHNOLOGY (NIIST)

Council of Scientific & Industrial Research (CSIR)
(Formerly Regional Research Laboratory)
Industrial Estate P.O., Thiruvananthapuram – 695 019
Kerala, INDIA

ISO 9001 REGISTERED

DNV
MGMT. SYS.
RvA C024
DNV Certification B.V., The Netherlands

Dr. M. L. P. Reddy
Chief Scientist
Chemical Sciences and Technology Division

Tel: 91-471-2515 360
Fax: +91-471-2491 712
E-mail: mlpreddy55@gmail.com

CERTIFICATE

This is to certify that the work embodied in the thesis entitled "**Synthesis, Characterization and Photophysical Properties of Lanthanide Carboxylates**" has been carried out by **Mrs. Shyni Raphael M** under my supervision and guidance at the Chemical Sciences and Technology Division of National Institute for Interdisciplinary Science and Technology (Formerly Regional Research Laboratory), Council of Scientific and Industrial Research, Thiruvananthapuram and the same has not been submitted elsewhere for any other degree.

Dr. M. L. P. Reddy
(Thesis Supervisor)

Thiruvananthapuram
September, 2012

iii

Acknowledgements

CONTENTS

CHAPTER 4   **79-106**

2-Thiopheneacetato-based one-dimensional coordination polymer of Tb^{3+}: Enhancement of terbium-centered luminescence in the presence of bidentate nitrogen donor ligands

List of Tables

List of Figures

maximum emission wave lengths

List of Abbreviations

1) Ln^{3+} — Lanthanide

2) Xe — Xenon

3) S_1 — Singlet

4) T_1 — Triplet

5) ISC — Intersystem crossing

6) IR — Infrared

7) EM — Luminescence emission

8) ET — Energy transfer

9) XRD — X-Ray Diffraction

10) FT-IR — Fourier Transform Infra-Red

11) PMMA — poly(methyl methacrylate)

12) *p*-CZBA — 4-(9H-carbazol-9-yl) benzoic acid

13) UV-Vis — Ultra Violet-Visible

14) MeOBB — 2-(4-methoxybenzoyl)benzoate

15) pabaH — *p*-amiobenzoic acid

16) terpy — terpyridine

17) bpy — 2,2′- bipyridine

18) phen — 1,10-phenanthroline

19) BAA — benzyl acetic acid

20) 2-FBA — 2-flourobenzoate

21) HL — 4-[4-(9H-carbazol-9-yl)butoxy]benzoic acid

22) tmphen — 3,4,7,8-tetramethyl-1,10-phenanthroline

23) ILCT — Intraligand Charge Transfer

24) DMA — N,N-dimethyl acetamide

25) $CHCl_3$ — Chloroform

26) NMR — Nuclear Magnetic Resonance

27) $CDCl_3$ — Chloroform-d

28)	DMSO	Dimethyl sulphoxide
29)	Alq$_3$	tris-8-hydroxyquinolinolato aluminum
30)	FAB-MS	Fast Atom Bombardment Mass Spectrometer
31)	TGA	Thermogravimetric analysis
32)	CN	Coordination number
33)	HXA	xanthene-9-carboxylic acid
34)	CSD	Cambridge Structural Database
35)	HTPAC	2-thiophene acetic acid
36)	TPAC	2-thiopheneacetate
37)	FUR	2-furanecarboxylate
38)	bath	4,7-diphenyl-1,10-phenanthroline

PREFACE

Luminescent lanthanide coordination complexes dsplay unique line-like emission bands, exhibit substantial Stokes shifts, possess very long luminescence lifetimes, and emit over the visible and near-IR (NIR) spectral domains. Furthermore, the fascinating photophysical properties of lanthanide molecular materials render them appropriate for a host of photonic applications such as tunable lasers, amplifiers for optical communications, luminescent probes for biomedical analysis, and as emitting materials in multilayer organic light emitting diodes. Unfortunately, due to the Laporte forbidden character and intraconfigurational nature of the $4f$ transitions, the molar absorption coefficients of lanthanide transitions are typically very small (less than 10 M^{-1} cm^{-1}). To obviate this problem, over the past few years, efforts have been made to augment the absorption coefficients and thereby obtain significantly more intense lanthanide ion emission. Fortunately, this objective can be accomplished by prudent selection and synthesis of organic ligands with conjugated motifs. Aromatic carboxylates and β-diketonates are particularly valuable in this context because such ligands can absorb ultraviolet light and transfer the absorbed energy to the central lanthanide ions in an appropriately effective manner (the so-called ''antenna effect''). In particular when aromatic carboxylates are employed as the antenna ligands, the coordinated lanthanide ions exhibit higher luminescent stabilities than those ligated with other organic ligands. This enhanced stability is of obvious practical importance in terms of device performance and stability. Thus, the primary objective of the present work is to design and develop novel visible-light sensitized lanthanide antenna complexes based on aromatic carboxylate ligands and to investigate their structure-property relationships. The thesis comprises of four chapters.

  The introductory chapter highlights the need for the development of new class of lanthanide molecular materials based on aromatic carboxylate ligands for the sensitization of Eu^{3+} and Tb^{3+} ions. Further, a detailed literature review on the recent developments in the photophysical properties of lanthanide-carboxylates has been brought out towards the end of this chapter.

A new aromatic carboxylate ligand, 4-[4-(9H-carbazol-9-yl)butoxy]benzoic acid (HL), has been synthesized by replacement of the hydroxyl hydrogen of 4-hydroxy benzoic acid with a 9-butyl-9H-carbazole moiety. The anion derived from HL has been used for the support of a series of lanthanide coordination compounds [Ln = Eu (1), Gd (2) and Tb (3)]. The new lanthanide complexes have been characterized by a variety of spectroscopic techniques and investigated their photophysical properties. These results have been incorporated in chapter 2. Complex 3 was structurally authenticated by single-crystal X-ray diffraction and found to exists as a solvent-free 1D coordination polymer with the formula $[Tb(L)_3]_n$. The structural data reveal that the terbium atoms in compound 3 reside in an octahedral ligand environment that is somewhat unusual for a lanthanide. It is interesting to note that each carboxylate group exhibits only a bridging-bidentate mode, with a complete lack of more complex connectivities that are commonly observed for extended lanthanide-containing solid-state structures. Examination of the packing diagram for 3 revealed the existence of two-dimensional molecular arrays held together by means of CH-π interactions. Aromatic carboxylates of the lanthanides are known to exhibit highly efficient luminescence, thus offering the promise of applicability as optical devices. However, due to difficulties that arise on account of their polymeric nature, their practical application is somewhat limited. Accordingly, synthetic routes to discreet molecular species are highly desirable. For this purpose, a series of ternary lanthanide complexes was designed, synthesized and characterized, namely $[Eu(L)_3(phen)]$ (4), $[Eu(L)_3(tmphen)]$ (5), $[Tb(L)_3(phen)]$ (6) and $[Tb(L)_3(tmphen)]$ (7) (phen = 1,10-phenanthroline and tmphen = 3,4,7,8-tetramethyl-1,10-phenanthroline). The photophysical properties of the foregoing complexes in the solid state at room temperature have been investigated. The quantum yields of the ternary complexes 4 (9.65%), 5 (21.00%), 6 (14.07%) and 7 (32.42%),

were found to be significantly enhanced in the presence of bidentate nitrogen donors

when compared with those of the corresponding binary compounds 1 (0.11%) and 3 (1.45%). Presumably this is due to effective energy transfer from the ancillary ligands. (These results were communicated to *Dalton Trans.*, **2012**).

The third chapter describes the results on the synthesis, characterization and photophysical properties of Ln^{3+}-Xanthene-9-carboxylate complexes $[Ln_2(XA)_6(DMSO)_2(H_2O)_2]$ (Ln = Eu (1), Tb (2) and Gd (3); HXA = xanthene-9-carboxylic acid; DMSO = dimethylsulfoxide). The compounds 1 and 2 were structurally characterized by single-crystal X-ray diffraction. The crystal structures of 1 and 2 consist of homodinuclear species that are bridged by two oxygen atoms from two carboxylate ligands. Each lanthanide ion is coordinated by eight oxygen atoms in an overall distorted square-prismatic geometry. Six of the oxygen atoms are furnished by the carboxylate moieties, and the remaining two oxygen atoms are provided by water and DMSO molecules. The photophysical properties of these complexes in the solid state at room temperature have been investigated. The quantum yields were found to be 0.06 ± 0.01 and $7.30 \pm 0.73\%$ for 1

and 2, respectively. (These results were published in *Inorg. Chem.*, **2007, 11025-11030**).
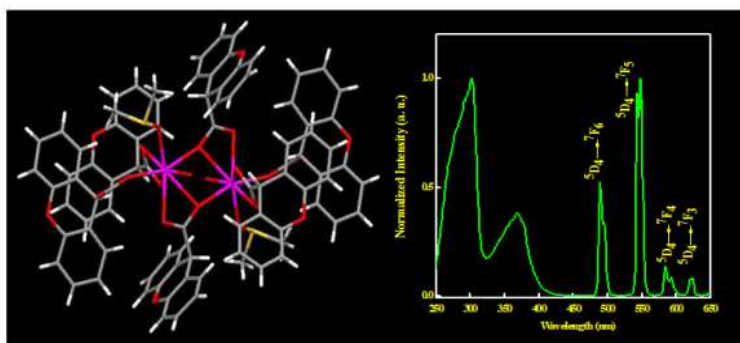
Four new Ln^{3+} complexes of 2-thiopheneacetic acid (HTPAC), $[Tb(TPAC)_3 \cdot H_2O]_n$ (1), $[Gd(TPAC)_3 \cdot H_2O]_n$ (2), $[Tb(TPAC)_3(phen)]_2$ (3) and $[Tb(TPAC)_3(bath)]_2$ (4) (phen = 1,10-phenanthroline; bath = bathophenanthroline) have been synthesized and characterized by various spectroscopic techniques and these results are disclosed in chapter 4. The X-ray structure of 1 reveals that each Tb^{3+} ion is connected to two neighboring ions by six thiopheneacetic acid ligands via the carboxylate groups to form an infinite one-dimensional polymer. The unit cell contains only one independent crystallographic site for the Tb ions. The carboxylate groups of the six molecules of the thiopheneacetate ligands are coordinated in both bidentate bridging

and tridentate chelate-bridging modes. Each Tb^{3+} ion is coordinated by nine oxygen atoms in an overall distorted tricapped trigonal-prismatic geometry. Eight of the oxygen atoms are furnished by the carboxylate moieties, and the remaining oxygen atom is provided by the water molecule. The quantum yields of 3 ($4.43 \pm 0.44\%$) and 4 ($9.06 \pm 0.90\%$) were found to be significantly enhanced by the presence of the bidentate nitrogen donor ligands in comparison with that of 1 ($0.07 \pm 0.01\%$) due to effective energy
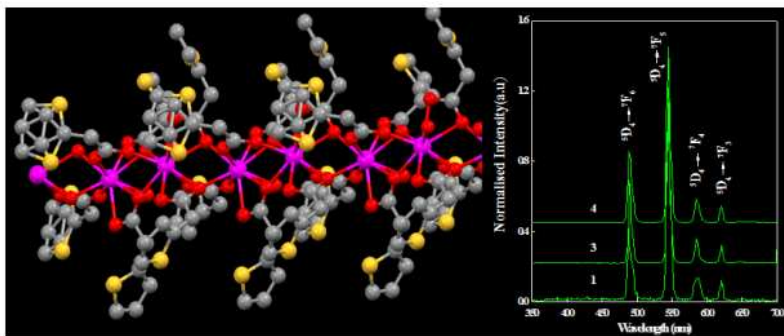
transfer from the secondary ligands. (These results were published in *Eur. J. Inorg. Chem.*, **2008, 4387-4394**).

The relevant references have been cited towards the end of the thesis.

Chapter 1

Chapter1

Introduction

1.1. Photoluminescence of trivalent lanthanides

Recent startling interest for lanthanide luminescence is stimulated by the continuously expanding need for luminescent materials meeting the stringent requirements for telecommunication, lighting, electroluminescent devices, bio-analytical sensors and bio-imaging set-ups [Eliseeva and Bünzli 2010] (Figure 1.1). In 1937, J. H. van Vleck wrote an article entitled *"The Puzzle of Rare-Earth Spectra in Solids"* which perfectly reflects the fascination exerted by the intricate optical properties of the trivalent lanthanides (Ln^{3+}) [van Vleck 1937]. The electronic $[Xe]4f^n$ configurations ($n = 0\text{-}14$) indeed generate a rich variety of electronic levels as shown in Figure 1.2.
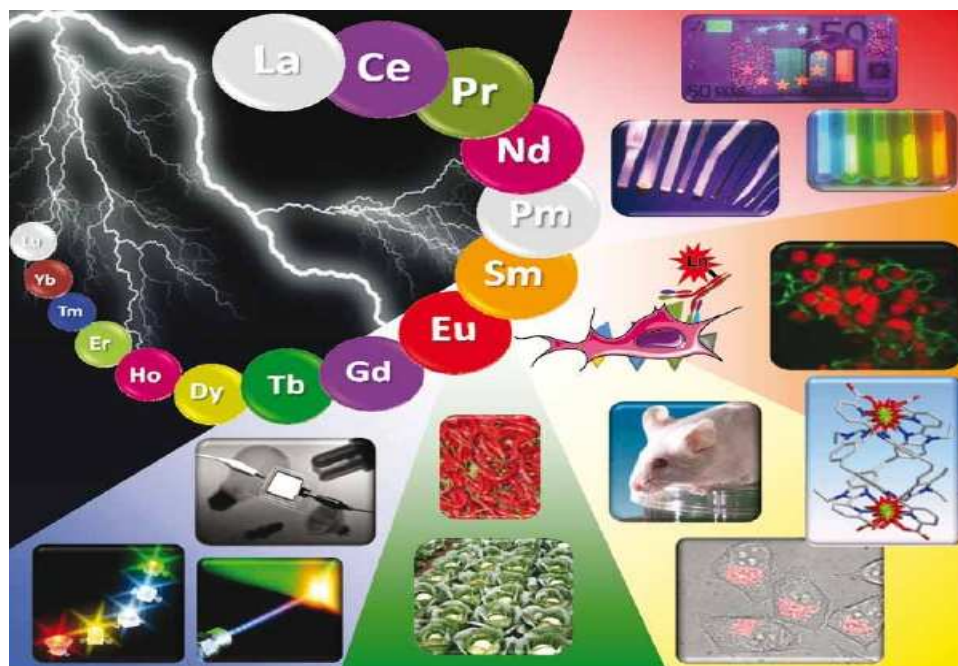
Figure 1.1. Type of emission and related applications of lanthanides.

The energies of these levels are well defined due to the shielding of the 4f orbitals by the filled $5s^2 5p^6$ sub-shells and, in addition, they do not vary much with the chemical environments in which the lanthanide ions are inserted. As a corollary, inner-shell 4f-4f transitions are sharp and the excited state life-times are relatively

long (usually within the micro-to-millisecond range, depending on the ion). However, because they are forbidden, these transitions exhibit low extinction coefficients ($\varepsilon < 1$ M^{-1} cm^{-1}) [Sabbatini *et al*. 1993; Samuel *et al*. 2009]. The weak absorbance can be overcome by coordinating chromophore-containing ligands to the metal ion, which, upon irradiation, transfer energy to the metal center, typically *via* the ligand triplet excited state, populating the Ln^{3+} emitting levels in a process known as the "antenna effect" (Figure 1.3) [Lehn 1990].
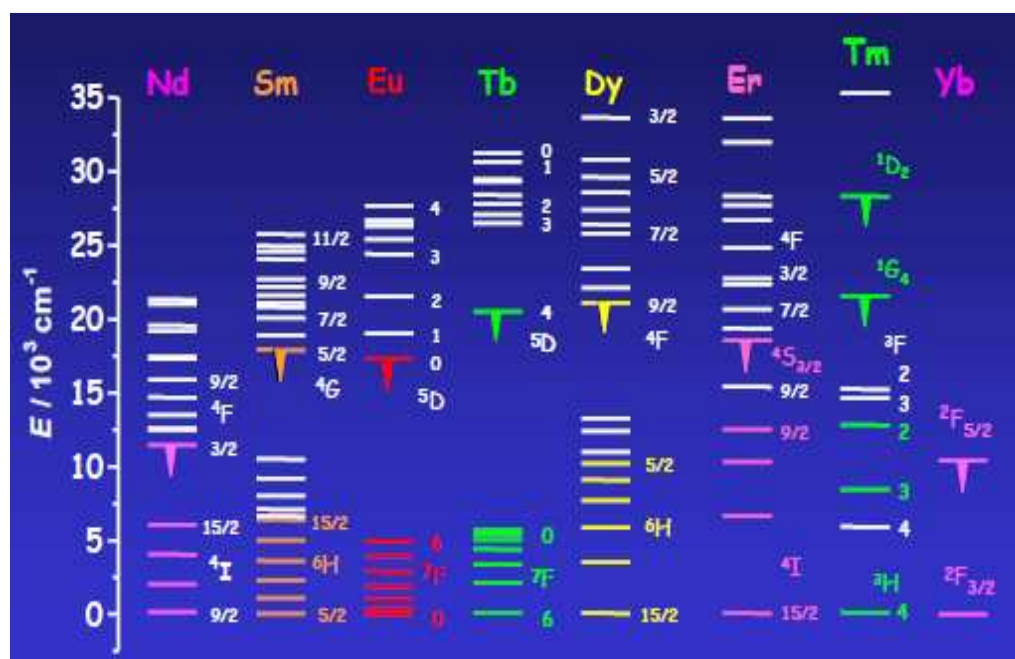
Figure 1.2. A summary of electronic excited state levels for Ln^{3+} ions.

According to the well-known Jablonski diagram (Figure 1.4), the sensitization pathway in luminescent Ln^{3+} complexes consists of the following steps: (i) excitation of the coordinated ligand leading to population of the ligand's singlet state (S$_1$), (ii) singlet excited state subsequently decays through intersystem crossing (ISC) to a triplet state of the ligand, (iii) the triplet state finally through a Förster-type dipole-dipole exchange mechanism leads to the population of the emissive f excited state of the Ln^{3+} ion, (iv) a radiative transition in the visible or near-IR domains, *i.e.*, luminescence emission (EM), which is usually characterized by the specific emission of Ln^{3+} ions. Among which, the energy transfer from the triplet energy level of the ligands to the metal ions plays a leading role in the luminescence

of the lanthanide complexes, affecting the luminescent intensity, lifetime and quantum yields. Thus, the energy level's match of the triplet state of the ligands to the corresponding Ln^{3+} ion's exciting states, is one of the key factors having impact on the luminescent properties of the complexes, and affords an essential in the design and modulation of ligands, other than their conformation and coordination characters [Gutierrez *et al*. 2004; Pan *et al.* 2009].
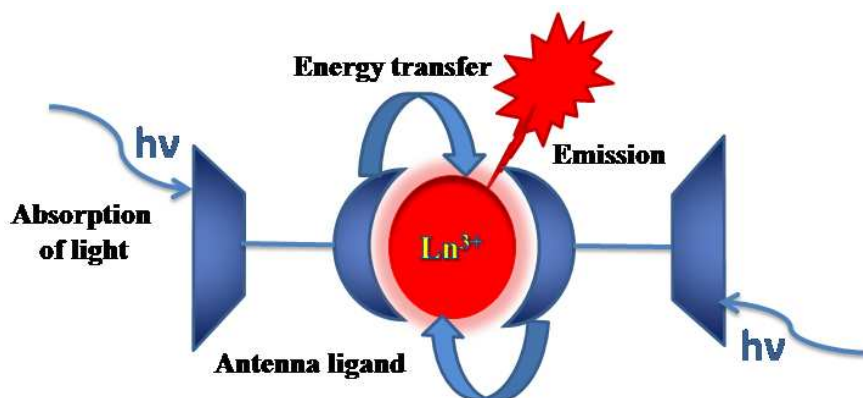
Figure 1.3. Pictorial representation of antenna effect.

A wide array of antenna chromophores that yield emissive Ln^{3+} complexes have been studied extensively, including bipyridines [[a]Alpha *et al.* 1987; [b]Alpha *et al.* 1987; Mukkala and Kankare 1992; Sabbatini *et al*. 1993], calixarenes [Bünzli *et al*. 1993; Bünzli and Ihringer 1996; Charbonniere *et al*. 1998], dipicolinic acids [Lamture *et al.* 1995; George *et al*. 2006] and β-diketonates [de Sa *et al*. 2000; Binnemans 2005; Binnemans 2009], to highlight a few. Carboxylate anions are hard Lewis bases and are known to bind strongly to Ln^{3+} cations which possess a pronounced hard Lewis acid character [de Bettencourt-Dias and Viswanathan 2006; Viswanathan and de Bettencourt-Dias 2006; Sivakumar *et al*. 2011]. Commonly, due to possessing large conjugated π-electron systems and strong carboxyl absorption groups, aromatic carboxylic acids are good activators for the luminescence of lanthanide ions [Li *et al.* 2000; Seward *et al.* 2001; Barja *et al.* 2003; Wang *et al.* 2003; Lam *et al.* 2003; Wang *et al.* 2004; de Bettencourt-Dias 2005; Zhou *et al.* 2008]. As a consequence, a variety of carboxylate ligands have been used as antenna chromophore ligands.
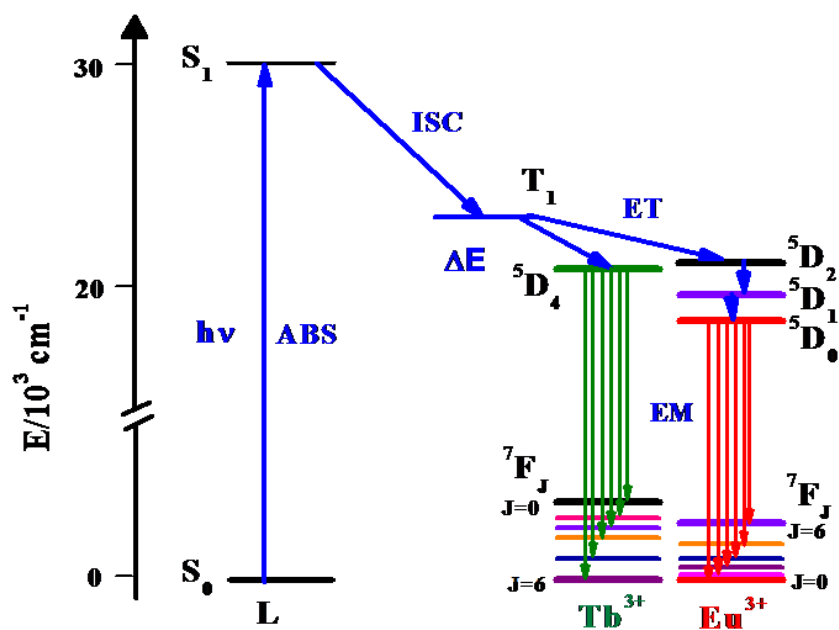
Figure 1.4. Jablonski diagram for the sensitization pathway in luminescent Ln^{3+} complexes.

The overall quantum yield ($\Phi_{overall}$) for a sensitized Ln^{3+} complex is given by the equation:

$$\Phi_{overall} = \Phi_{ISC}\Phi_{ET}\Phi_{Ln} \qquad (1)$$

where Φ_{ISC} and Φ_{ET} are the respective efficiencies of intersystem crossing (ISC) and ligand-to-Ln^{3+} energy transfer (ET), and Φ_{Ln} is the intrinsic quantum yield of the Ln^{3+} ion. In terms of ligand design, this means that the antenna chromophore should

(i)   be efficient at absorbing light (i.e., have large ε values),

(ii)   have an ISC quantum yield near unity,

(iii)   have a triplet state that is close enough in energy to the Ln^{3+} emitting state to allow for effective ligand-to-Ln^{3+} energy transfer (but not so close that thermal back transfer competes effectively with Ln^{3+} emission), and

(iv)   protect the Ln^{3+} from the quenching effects by preventing the non-radiative deactivation by O-H, N-H, or C-H oscillators in the coordination environment or in close proximity of the metal.

1.2. Overview on the visible emitting luminescent carboxylates

The luminescent properties of Ln^{3+}-benzene carboxylate complexes have been extensively investigated and these data are well documented in many review articles [Hilder *et al.* 2009, Latva *et al.* 1997]. Excellent correlation between the lowest triplet state energy level of the various carboxylate ligands and Ln^{3+} luminescence quantum yield has been reported by Latva and co-workers [Latva *et al.* 1997].

Recent developments in the photoluminescence properties of lanthanide benzoates: The photophysical properties of lanthanide benzene carboxylates in the solid state were systematically investigated by Peter. C. Junk and coworkers and the results are summarized in an excellent review article [Hilder *et al.* 2009]. Eu^{3+} and Tb^{3+} complexes of benzoic acid, 9-anthracenecarboxylic acid, 1-naphthoic acid, 2-naphthoic acid, cinnamic acid, *o*-phenylbenzoic acid, *p*-phenylbenzoic acid, *o*-methylbenzoic acid, *m*-methylbenzoic acid, *p*-methylbenzoic acid, *p-tert*-butylbenzoic acid, phthalic acid, isophthalic acid and terephthalic acid were synthesized by aqueous metathesis reactions and the compositions were determined by microanalysis and volumetric methods. The structural conclusions were drawn from the powder XRD patterns and FT-IR spectral data. It showed that most of the corresponding Eu^{3+} and Tb^{3+} complexes were isomorphous, thus isostructural. The luminescent properties were determined in the solid state, including the excitation and emission efficiency, complemented by considering triplet state energies. The triplet state energies of the alkyl-substituted carboxylates and dicarboxylates are suitable to populate the emission level $^5D_4$ of Tb^{3+} directly while higher energetic excited $^5D_{1-4}$ levels of Eu^{3+} are populated, resulting in a comparatively low light output. Conjugation lowers the triplet state energies to such an extent that at some stage only the lower energy $^5D_0$ state of Eu^{3+} can be populated. Further conjugation lowers the triplet state to energies below the excited $^5D_0$ emission level, not being able to sensitize Eu^{3+} emission. It has been shown that a crucial criterion affecting ligand sensitized lanthanide emission is the energy of the triplet state. Observations suggest that the triplet state should be around 3,000 cm^{-1} higher than the lanthanoid resonance level to result in efficient emission. An additional carboxylate substituent also results in efficiently populated ^5D states of Eu^{3+} and Tb^{3+}. The light output of

the dicarboxylate complexes seems to be determined by multiphonon relaxation and Ln-Ln energy transfer rather than inefficient population of the Ln^{3+} resonance levels.

Recently, a series of 4-benzyloxybenzoic acid derivatives have been designed in our laboratory and investigated their structure property relationships with respect to the photophysics of the lanthanide complexes [Sivakumar *et al.* 2010]. The benzoate ligand was modified by including electron-releasing (-OCH$_3$) and electron-withdrawing (-NO$_2$) substituents to produce three novel ligands: 4-benzyloxybenzoic acid, 3-methoxy-4-benzyloxy benzoic acid, and 3-nitro-4-benzyloxy benzoic acid (Figure 1.5). The molecular structures of the lanthanide 4-benzyloxybenzoates were characterized by crystallography and shown to be formed by dimeric metallic units that are bridged by two oxygen atoms from two benzoate ligands. It was demonstrated that the photosensitization of the lanthanide centers was strongly affected by the type of substituents; while the electron-releasing group improves the emission, and the electron-withdrawing moiety quenches it by way of an energy dissipation channel.
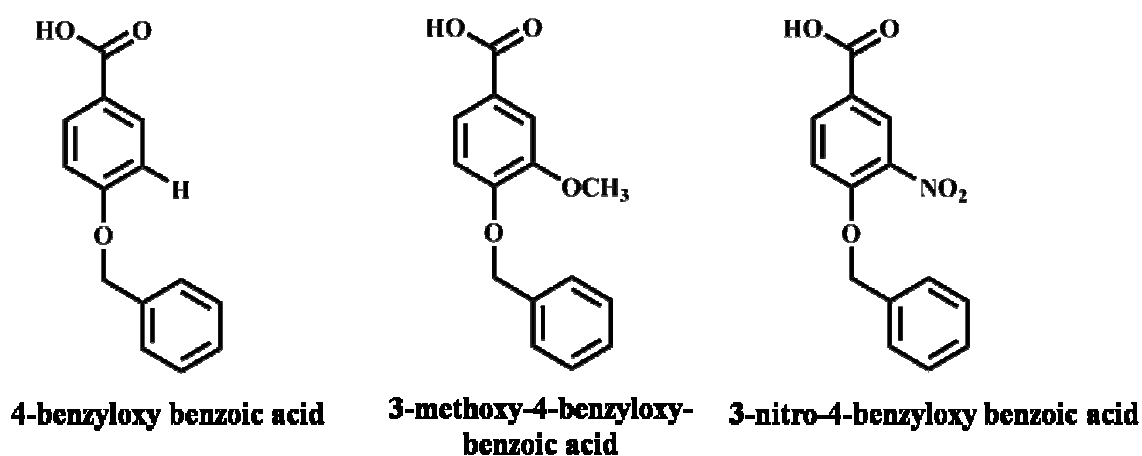
Figure 1.5. Structural formulae of ligands used by Sivakumar *et al.* 2010.

In the subsequent studies Sivakumar *et al.* have designed two new aromatic carboxylic acids namely, 3,5-bis(benzyloxy)benzoic acid and 3,5-bis(pyridine-2-ylmethoxy)benzoic acid by replacing the hydroxyl hydrogens of 3,5-dihydroxy benzoic acid with benzyl and pyridyl moieties (Figure 1.6), respectively [Sivakumar *et al.* 2011]. The anions derived from these ligands have been used for the support of

3,5-bis(benzyloxy)benzoic acid

3,5-bis(pyridine-2-ylmethoxy)-benzoic acid
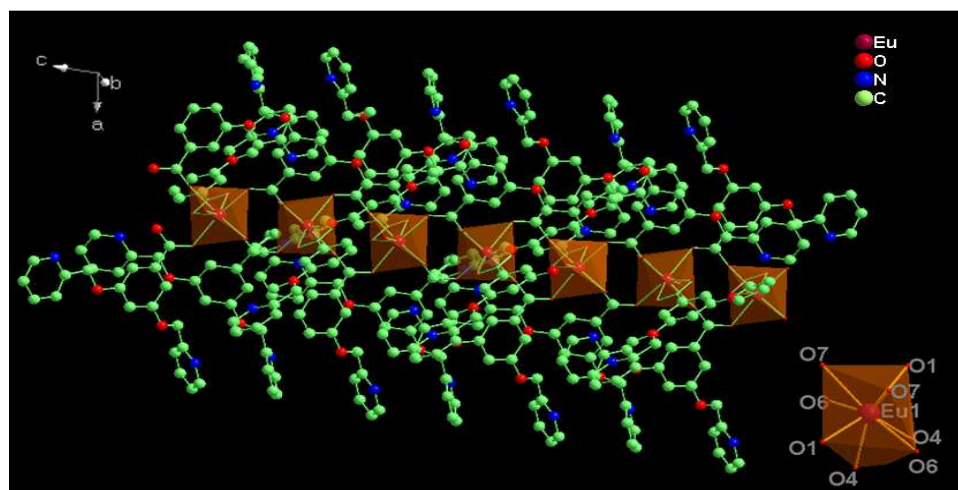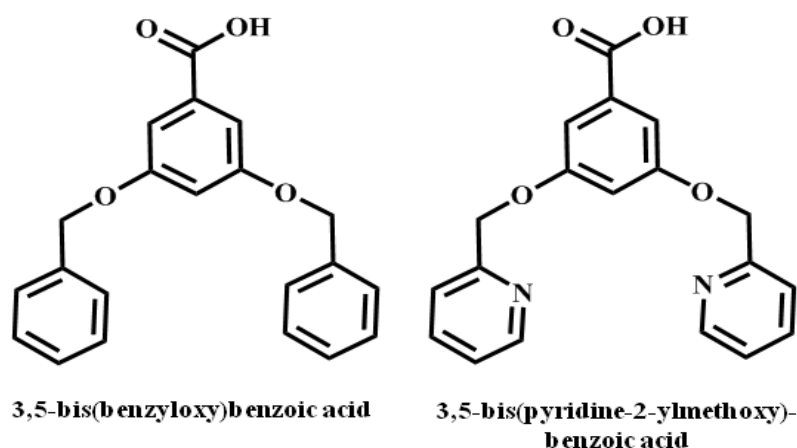
Figure 1.6. Structural formulae of ligands and complex reported by Sivakumar *et al.* 2011.

a series of lanthanide coordination compounds. All these compounds are found to exist as infinite one-dimensional coordination polymers and sensitize their luminescence in the visible region. Furthermore, 3,5-bis(pyridine-2-ylmethoxy)benzoic acid forms unique luminescent coordination polymers with both Eu^{3+} and Tb^{3+} ions. These polymers features free Lewis basic pyridyl sites and may therefore proved to be useful for the sensing of heavy metal ions. The newly designed benzoate ligands are adequate sensitizers for the Tb^{3+} ion. Indeed, their excited states lie at sufficiently high energies in comparison with that of the $^5D_4$ state to obviate back transfer of energy. As a result, even in the presence of metal-bound water molecules, the solid state quantum yields of the sensitized Tb^{3+} complexes are

9

appreciable (as high as 60%). On the other hand, these ligands sensitize Eu^{3+} luminescence inefficiently, because of the larger energy gap between the triplet states of the ligands and $^5D_0$ level of Eu^{3+} ion.

Very high quantum yields (88%) have been reported with terbium-aminobenzoate complexes, which is somewhat surprising in view of the coordination of both -NH_2 and OH_2 ligands, since such moieties usually function as vibrational deactivators of the excited state [Fiedler *et al.* 2007]. In the later studies, Ramya et al. demonstrated that the replacement of hydrogens of the NH_2 moiety of *p*-aminobenzoic acid by benzyl groups (Figure 1.7) had a significant influence on the distribution of π- electron density within the ligand system and resulted in the development of a novel photosensitizer for Tb^{3+} with an overall quantum yield of 82% [Ramya *et al.* 2010]. On the other hand, poor luminescence efficiency has been noted for the Eu^{3+}-4-(dibenzylamino)benzoate complex. The molecular structures of these compounds consist of homodinuclear species that are bridged by two oxygen atoms from two carboxylate ligands via different coordination modes.
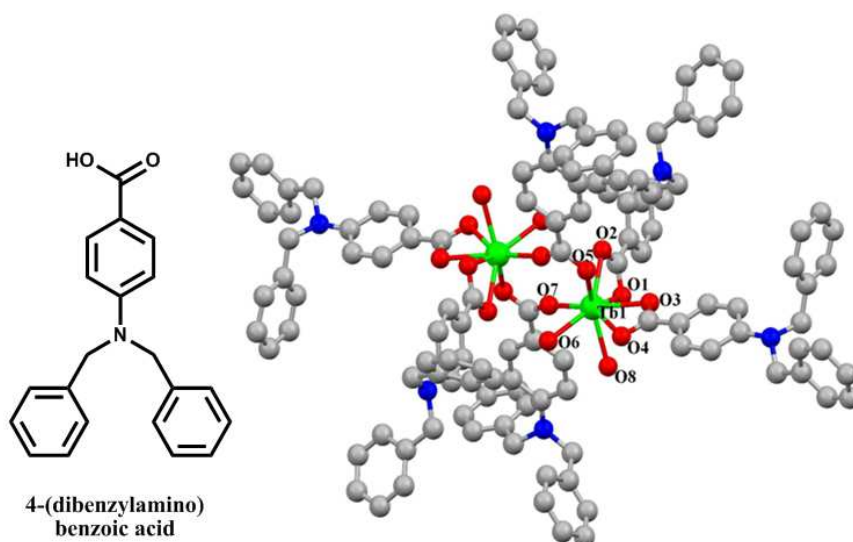
Figure 1.7. Structural formula of ligand and complex reported by Ramya *et al.* 2010.

In order to modulate the light harvesting properties of the benzoic acid ligand, benzimidazole moiety has been anchored at the 4[th] position of the benzoic acid through an alkyl linkage and designed a new ligand namely, 4-((1H-benzo[d]imidazol-1- yl)methyl)benzoic acid and utilized for the synthesis of a series

of lanthanide complexes [Lucky *et al.* 2011]. The single crystal X-ray diffraction analysis of the synthesized Eu^{3+} complex indicated that it exists as a one dimensional helical chain like coordination polymer consisting of unique unsymmetrical dinuclear lanthanide building blocks (Figure 1.8). The 1D chains are further linked by the significant intermolecular hydrogen-bonding interactions to form a two-dimensional supramolecular network. The Tb^{3+} complex exhibits bright green luminescence efficiency in the solid state with a quantum yield of 15%. On the other hand, poor luminescence efficiency has been noted for Eu^{3+}-benzoate complex.
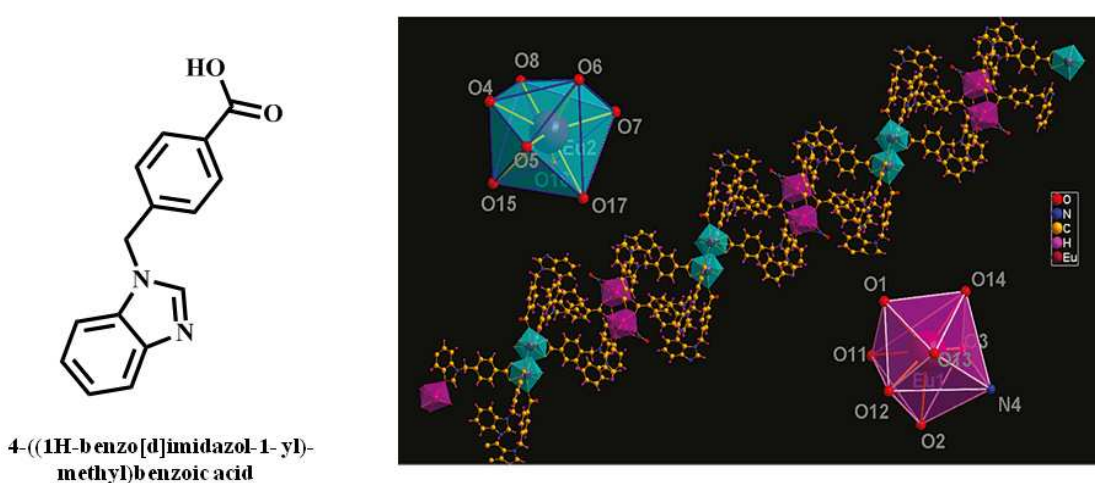
Figure 1.8. Structure of 4-((1H-benzo[d]imidazol-1-yl)methyl)benzoic acid and Eu^{3+} complex.

Recently, a novel antenna chromophore ligand for the photosensitization of Tb^{3+} has been designed based on the highly fluorinated carboxylate ligand 3,5-bis(perfluorobenzyloxy)benzoic acid [Sivakumar *et al.* 2012] (Figure 1.9). The results demonstrated that the replacement of high-energy C–H vibrations with fluorinated phenyl groups in the 3,5-bis(benzyloxy)benzoate effectively improves the luminescence intensity and lifetimes of lanthanide complexes. It is interesting to note that the designed fluorinated carboxylate is well suited for the sensitization of Tb^{3+} emission ($\Phi_{sen} = 52\%$), thanks to a favourable position of the triplet state of the ligand as investigated in the Gd^{3+} complex. On the other hand, the corresponding Eu^{3+} complex shows weak luminescence efficiency ($\Phi_{sen} = 24\%$) due to poor match of the triplet state of the ligand with the emissive excited states of the metal ion. In

the present work, efforts have also been made to isolate luminescent molecular terbium plastic materials by combining the unique optical properties of lanthanides with the mechanical characteristics, thermal stability, flexibility and film-forming tendency of polymers (PMMA). The photoluminescence quantum yields of polymer–lanthanide hybrid materials are significantly enhanced (53–65%) as compared to that of the Tb^{3+}–3,5-bis(perfluorobenzyloxy)benzoate complex.

3,5-bis(perfluorobenzyloxy)benzoic acid
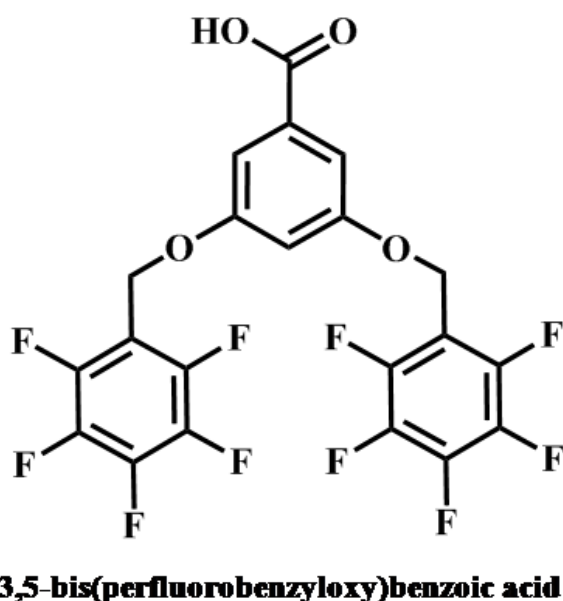
Figure 1.9. Structure of 3,5-bis(perfluorobenzyloxy)benzoic acid.

Previous results suggest that derivatizing benzoic acid analogues with thiophene has a beneficial tuning effect on the triplet state of the antenna leading to a higher emission quantum yield resulting from a better match between the ligand and lanthanide ion excited states, as derivatization of isophthalic acid with thiophene leads to an average lowering of the triplet state energy by 5000 cm^{-1} [de Bettencourt-Dias 2005]. The photophysical characterization of the solutions shows the effect of the presence of the thiophene-derivatization in the antenna on the emission behavior of the coordinated lanthanides. In the later studies thiophene derivatized nitrobenzoic acid ligands have been evaluated as possible sensitizers for Eu^{3+} and Tb^{3+} luminescence [Viswanathan and de Bettencourt-Dias 2006] (Figure 1.10). All of the isolated compounds are molecular, in contrast with previously isolated nitrobenzoic acid complexes, which are coordination polymers [Viswanathan and de

Bettencourt-Dias 2006]. Relatively short Ln-Ln distances are seen in the complexes which display a triply coordinated carboxylate as bridging-bidentate ligand. The complexes are weakly luminescent in the solid state with a metal-to-ligand ratio of 1:3. In solution, only 1:1 species form. Solution quantum yields between 0.9 and 3.1% for Eu(III)-containing and 4.7 and 9.8% for Tb(III)-containing solutions were obtained. Although moderate, they are the highest reported so far for nitrobenzoato-type ligands. Their magnitude can be explained by the small stability constants of the species in solution, as well as the unfavorable energy gaps between singlet and triplet levels of the ligand and the triplet level of the ligand and emissive excited state of the lanthanide ion. The strong electron-withdrawing effect of the nitro group and its position relative to the coordinating carboxylate moiety do not seem to influence strongly the photophysical properties of the sensitizer, as its effect is counter balanced by the moderate electron-donating thiophene moiety.
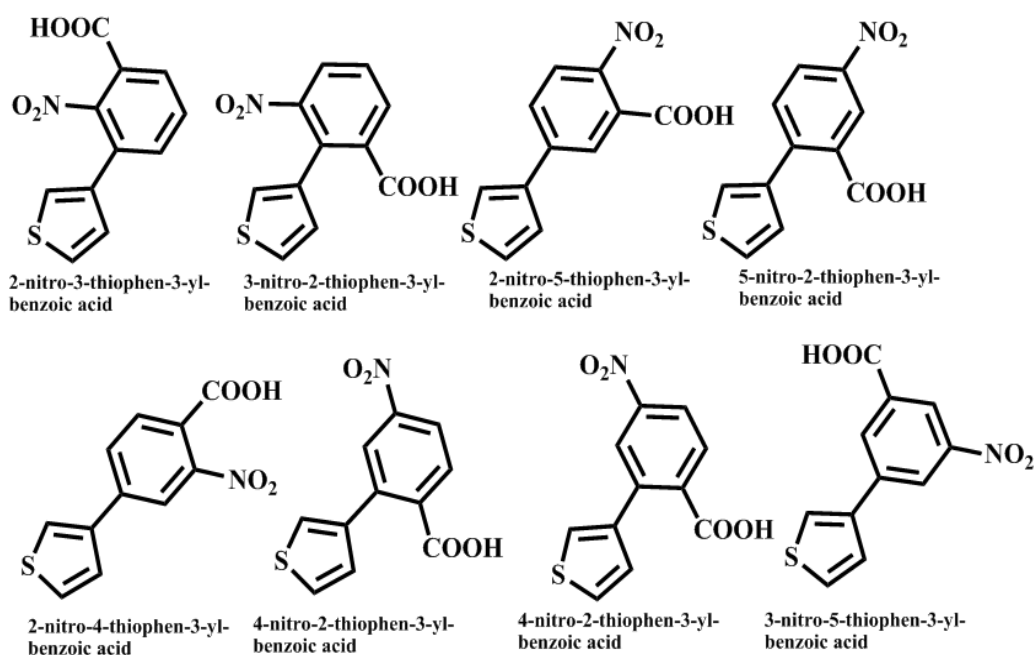
Figure 1.10. Ligands studied as sensitizers in de Bettencourt-Dias work.

With the graft of carbazolyl group as a hole-transport group to benzoic acid molecule, a new organic ligand, *p*-CZBA, and two novel complexes Eu(*p*-CZB)$_3$(H$_2$O)$_2$ and Tb(*p*-CZB)$_3$(H$_2$O)$_2$ have been synthesized [Juan *et al.* 2006] (Figure 1.11). Photoluminescence measurements indicated that *p*-CZBA itself is a

blue emitter under UV radiation. When the effective energy transfer from the organic ligand to the central Tb^{3+} ions occurs in the binary complex, strong and characteristic green emission appears due to the $^5D_4 \rightarrow {}^7F_j$ transitions of the 4f electrons of the central Tb^{3+} ions. Based on the enhanced luminescence intensity and good thermal stability of $Tb(p\text{-}CZB)_3(H_2O)_2$, it would be considered as a candidate material for fabrication of OLEDs. $Eu(p\text{-}CZB)_3(H_2O)_2$ hardly has fluorescence property, this is because the energy of the triplet state of the ligand is not matchable with the energy of the lowest excited state of Eu^{3+}.

p-**CZBA**
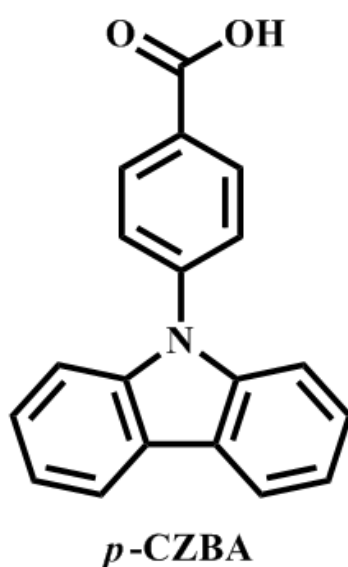
Figure 1.11. The structure of the ligand used by Juan *et al.* 2006.

New thermally stable luminescent lanthanide-(methoxybenzoyl)benzoate complexes, $Tb(MeOBB)_3$ and $Eu(MeOBB)_3$, were synthesized and their absorption and luminescent properties were reported [Edwards *et al.*1997] (Figure 1.12). Single layer LEDs were fabricated from the Tb or Eu complex combined with PVK and butyl-PBD, and these devices showed EL spectra that are attributed to emission from the Tb^{3+} or operating voltage of 24V. The higher brightness values of $Tb(MeOBB)_3$ devices compared to $Eu(MeOBB)_3$ LEDs is due to the higher PL quantum efficiency of the Tb complex and the higher luminous efficiency of the eye in the green region of the spectrum.
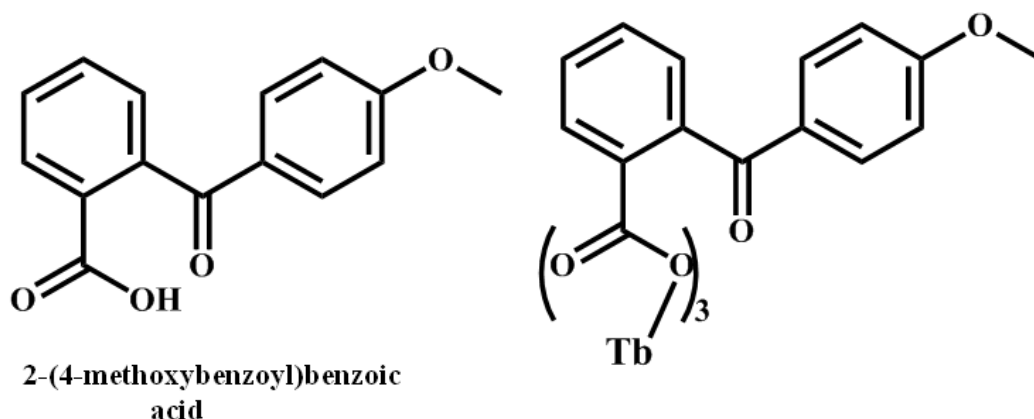
Figure 1.12. Structure of 2(4'-methoxy-benzoyl)benzoic acid and Tb^{3+}-Tris[2(4'-methoxybenzoyl)benzoate].

Remarkable thermal stability of Eu^{3+}-(4-phosphonobenzoate) and its luminescent properties have been reported [Rueff *et al.* 2009]. The molecular structure of the complex has been solved by X-ray diffraction on a powder sample and is described as an inorganic network in which both carboxylic and phosphonic acid groups are linked to Eu^{3+} ions forming a three dimensional architecture. Thermal analysis performed on this compound has underlined its remarkable thermal stability upto 510°C. Finally the luminescent properties of the compound have been related to the structure of the material.

Lanthanide heterocyclic carboxylates: The synthesis, characterization and the molecular structure of the Eu^{3+}-thiophene carboxylate complex indicated that thiophene carboxylate ligand chelates to the lanthanoid ions via the carboxylic oxygen donors (Figure 1.13) and it also functions as a bridge ligand in the formation of a dimeric complex where two identical Eu^{3+} centers are involved [Malta *et al.* 2004]. The coordination polyhedron can be described as a distorted square antiprism. A rather weak intersystem crossing (singlet-to-triplet) in the thiophene carboxylate ligand is suggested by the high luminescent intensity of the bands arising from the allowed $S_1 \rightarrow S_0$ transitions in the emission spectrum of the Gd^{3+} complex at 77 K. The absence of these bands in the emission spectrum of the Eu^{3+}

and Tb^{3+} complexes indicates that probably the singlet state of the ligand plays a role in the energy transfer from the ligand to the Ln^{3+} ions.
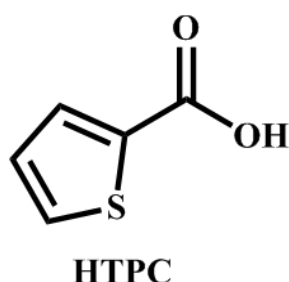
Figure 1.13. The structure of the ligand used by Malta *et al.* 2004.

In the subsequent studies, Malta and coworkers has also introduced 2-thiophene acetic acid as a photosensitizer for Ln^{3+} ions [Teotonio *et al.* 2005]. According to the single crystal X-ray analysis Eu^{3+}-thiophene acetate complex consists of asymmetric units forming infinite parallel chains. The unit cell contains two independent crystallographic sites for Eu^{3+} ions, labeled Eu(1) and Eu(2a), each coordinated to three thiophene acetate ligands (Figure 1.14). The emission spectra of lanthanoid ions displayed only narrow bands, indicating an efficient luminescent sensitization by the thiophene acetic acid antenna.
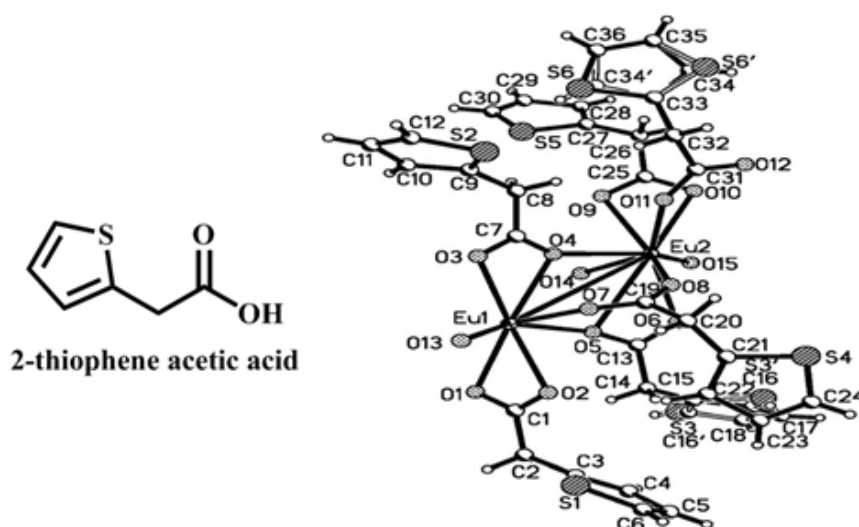
Figure 1.14. Structure of 2-thiophene acetic acid and Eu^{3+}-2-thiophene acetate complex.

Two series of lanthanide complexes coordinated with aromatic chromophore-containing pyrrole-derivatized carboxylate ligands were successfully synthesized (Figure 1.15), characterized and investigated their photophysical properties [Ga-Lai Law *et al.* 2007]. The X-ray diffraction studies reveal that the lanthanide complexes that incorporate bidentate carboxylate ligands (1-methylpyrrole-2-carboxylic acid and *N*-methyl-3-indoleglyoxylic acid) could attain highly symmetrical polymeric structures without any coordination with luminescence-quenching solvent or water molecules. The europium and terbium complexes derived from pyrrole carboxylates were found to be capable of exhibiting solid-state luminescence of high intensity, long lifetimes and high efficiency.

1-methylpyrrole-2-carboxylic acid   *N*-methyl-3-indoleglyoxylic acid
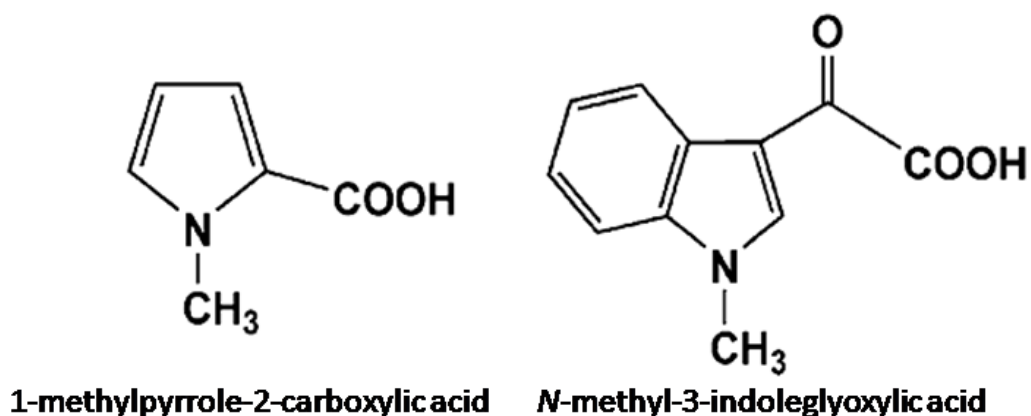
Figure 1.15. Structural formulae of ligands used by Ga-Lai Law *et al.* 2007.

Sterically hindered N-aryl-benzimidazole pyridine-2-carboxylic acids (aryl = phenyl, 4-biphenyl, 2-naphthyl) (Figure 1.16) readily form homoleptic, neutral, nine-coordinate europium complexes which display efficient sensitized luminescence in solid state and in dichloromethane solution with quantum yields reaching 59% and have monoexponential and nearly temperature-independent lifetimes as long as 2.7 ms [Shavaleev *et al.* 2010]. The ligand-centered absorption band with a maximum at 321-342 nm and intensity $(50\text{-}56) \times 10^3$ $M^{-1}cm^{-1}$ ensures efficient harvesting of excitation light by the complexes. Variation of N-aryl chromophore enhances the ligand absorption at 250-350 nm without changing its triplet state energy which amounts to $(19.2\text{-}21.3) \times 10^3$ cm^{-1}. Photophysical properties of europium complexes benefit from adequate protection of the metal by

the ligands against non-radiative deactivation and efficient ligand-to-metal energy transfer exceeding 70%.

HL1: R'=CH$_3$, R=H
HL4Me: R'=C$_4$H$_9$, R=CH$_3$
HL4O1: R'=C$_4$H$_9$, R=OCH$_3$
HL8: R'=C$_8$H$_{17}$, R=H
HL8R: R'=C$_8$H$_{17}$, R=F, Cl, Br
HL8Me: R'=C$_8$H$_{17}$, R=CH$_3$
HL8O8: R'=C$_8$H$_{17}$, R=OC$_8$H$_{17}$

HLPh: R=H
HLPhBr: R=Br
HLPhBu: R='Bu
HLPhO8: R=OC$_8$H$_{17}$

HLPhOX

HLBiphX

HLNapX
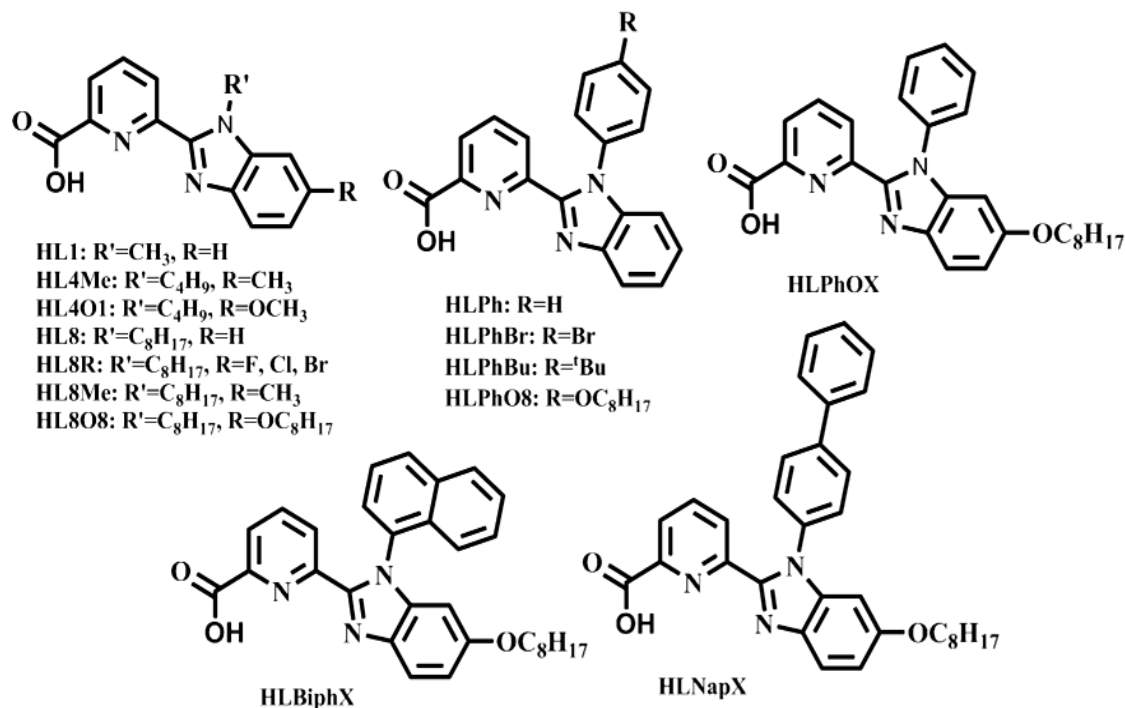
Figure 1.16. Structural formulae of N-Aryl-Benzimidazole Pyridine-2-Carboxylic Acids used by Shavaleev *et al*. 2010.

Luminescent lanthanide carboxylates with neutral donors: Lanthanide 2-flourobenzoate complexes containing 2,2'-bipyridyl/4,4'-bipyridyl or phenanthroline have interesting structures (Figure 1.17), with both high stability and intense fluorescence [Polynova *et al.* 1987; Ma *et al.* 1993; Jin *et al.* 2001; Li and Zou 2003; Li *et al.* 2004; Li *et al.* 2005]. It is interesting to note that these coligands generate Tb^{3+} complexes with various structures.

The use of phenanthroline functionalized organic compounds in promoting Ln^{3+} ion emission has been reported [Quici *et al.* 2004; Quici *et al.* 2005; [a]Lenaerts *et al.* 2005; [b]Lenaerts *et al.* 2005]. Actually, deduced from the absorption and emission spectra of sodium salt of 4-cyanobenzoic acid and 1,10-phenanthroline, the lowest level triplet energy level is close to that of phenanthroline [Li *et al.* 2006] (Figure 1.18).
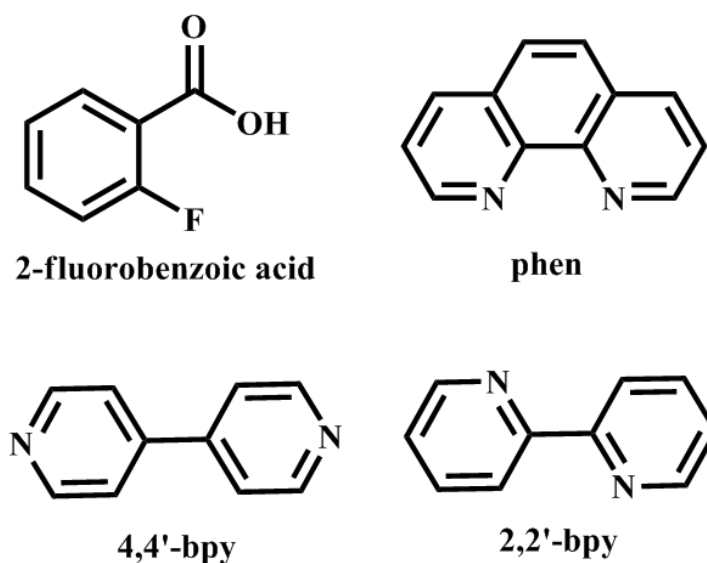
Figure 1.17. Molecular structures of the ligands used by Li *et al.* 2005.
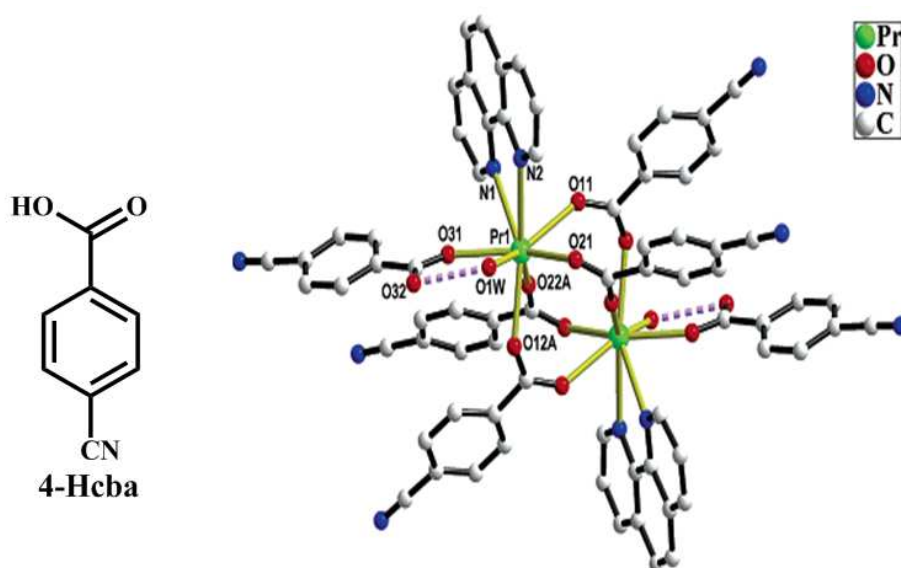
Figure 1.18. Molecular structure of ligand and complex studied by Li *et al.* 2006.

The triplet energy level of phenanthroline can be estimated to be at 21640 cm^{-1}. The lowest lying excited energy levels of Sm^{3+}, Eu^{3+} and Dy^{3+} are 18200, 17500 and 21000 cm^{-1}, respectively. Thus efficient ligand to metal energy transfer takes place for Ln^{3+} complexes and cyanobenzoic acid complexes may act as good candidates for efficient luminescent materials.

The influence of the distortions of the lanthanide coordination polyhedron in dimeric carboxylates with 1,10-phenanthroline on photophysical properties of these compounds was examined in a recent review article [Tsaryuk *et al.* 2010]. The relative contributions of the rates of the radiative and nonradiative processes to the lifetimes were determined. The lifetime of $^5D_0$ of Eu^{3+} in the temperature range 77 to 295 K and the lifetime of $^5D_4$ of Tb^{3+} at low temperatures are mainly determined by radiative processes and depend on details of the charge distribution in the nearest surroundings of the Ln^{3+} ion that are connected with distortions of coordination polyhedron of Ln^{3+} ion. Polyhedron distortions are to a great extent caused by the range of the Ln-O bond lengths related to bridging cyclic carboxylate group that depends on the type and the size of the carboxylate anion. At prominent polyhedron distortions, as in naphthyl carboxylates, benzoates and furan carboxylates, the rates of the radiative processes become higher and the intensity of the Eu^{3+} $^5D_0$-$^7F_2$ hypersensitive transition increases. Multiphonon relaxation is the main nonradiative process in Eu^{3+} compounds at 77 to 295 K and in Tb^{3+} at 77 K. A back energy transfer from $^5D_4$ state of Tb^{3+} ion to the lowest triplet state related to phenanthroline in most of the compounds is the principle nonradiative process contributing noticeably to quenching in Tb^{3+} compounds at high temperatures. To increase the probability of electric dipole transitions, first of all, hypersensitive transitions in the lanthanide carboxylates with phenanthroline, one needs to create substantial distortions of Ln^{3+} coordination polyhedron with the help of voluminous carboxylate ligands. At the same time, to decrease the influence of back energy transfer processes on the quantum yield of luminescence, relatively small changes in the Ln-N bond strengths are sufficient.

Stimulated by high luminescent efficiencies of *p*-aminobenzoates of Tb^{3+} (quantum yield > 80%), detailed structural investigations have been performed to derive luminescent markers [Fiedler *et al.* 2007]. Typically in the series of Ln^{3+} *p*-aminobenzoate coordination polymers are formed, which are broken down to molecular species, which can be accomplished by the use of chelating ligands such as bipyridine, phenanthroline or terpyridine (Figure 1.19). Nevertheless, on coordination with bipyridine a slight increase in quantum yield (>90%) in the case of Tb^{3+}, while phenanthroline reduces the overall efficiency (36%).
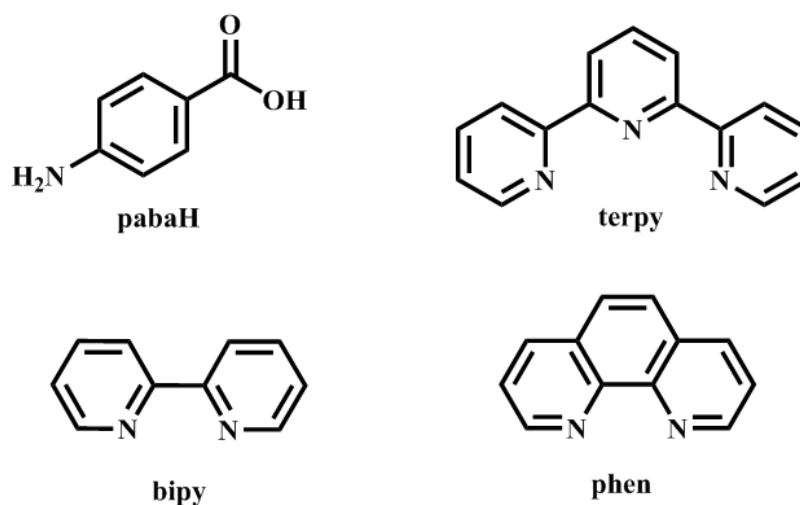
Figure 1.19. Molecular structures of the ligands used by Fiedler *et al.* 2007.

In terms of the molecular fragment principle, a quarternary complex, $[Tb(BAA)_2(Phen)(NO_3)]_2$ is assembled based on benzyl acetic acid and 1,10-phenanthroline, characterized and investigated their photophysical properties [Bai *et al.* 2005]. The Tb^{3+} forms a dimer with a coordination number of nine in which each pair of adjacent Tb^{3+} ions is bridged by four benzyl acetate groups via two types of coordination modes (Figure 1.20). The dimer exhibits strong green luminescence of Tb^{3+}.
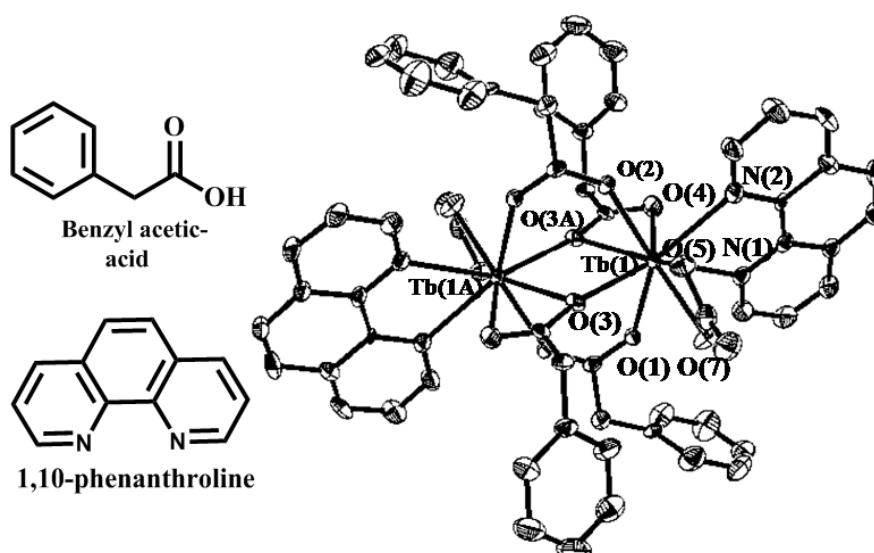
Figure 1.20. Molecular structure of ligands and $[Tb(BAA)_2(Phen)(NO_3)]_2$ complex.

1.3. Scope of the present investigation.

Carboxylate ligands are highly complementary toward lanthanide metal ions because of the oxophilic nature of the later [Bußkamp *et al.* 2007]. Accordingly, lanthanide benzoates are stable and have considerable attention for their potential use in a wide variety of fields because of their novel luminescent and magnetic properties [Li *et al.* 2006, Lam *et al.* 2003, Lucky *et al.* 2011]. In particular, when modified with light-harvesting moieties, benzoates have proven to be efficient sensitizers for Ln^{3+} ions [Ramya *et al.* 2011, Sivakumar *et al.* 2010]. It is well documented that carbazole moiety incorporated into *β*-diketonate ligand acts as an efficient photosensitizer for lanthanides [Ambili Raj *et al.* 2010]. On the other hand, ligands in which carbazol-9-yl grafted to an aromatic carboxylate ligands are scarce [Juan *et al.* 2006]. Carbazoles possess a number of desirable properties, which include good chemical stability, modest cost and the ability to tune the optical and electrical properties by appending with a wide variety of functional groups [Grazulevicius *et al.* 2003; Morin *et al.* 2005]. Inspired by the efficient sensitization of various lanthanide benzoates, herein, a novel ligand, namely, 4-[4-(9H-carbazol-9-yl)butoxy]benzoic acid has been designed and utilized for the support of a series of lanthanide coordination polymers featuring Eu^{3+}, Gd^{3+} and Tb^{3+} cations. The synthesized carbazole appended benzoate complexes of lanthanides were structurally characterized by single-crystal X-ray diffraction. The luminescent properties of designed lanthanide complexes have been evaluated systematically and correlated with the triplet energy level of the developed new benzoate molecule. Further in the present study the effect of bidentate nitrogen donors on the luminescent properties of Ln^{3+}-4-[4-(9H-carbazol-9-yl)butoxy]benzoate has also been investigated and correlated with their structure property relations.

In comparison with the aromatic carboxylic acids mentioned in the forgoing account, the use of xanthene-9-carboxylic acid as a photosensitizer for Ln^{3+} ions has been far less common. Further, xanthenes are highly favorable because of their excellent photophysical properties, such as high extinction coefficients, excellent quantum yields, great photostability, and relatively long emission wavelengths [Chen *et al.* 2012]. With the aims of understanding the coordination chemistry of xanthene-9-carboxylate ligand and preparing new materials with interesting

structural topologies and potential photophysical properties, in the current work, xanthene-9-carboxylate ligand has been chosen as a primary ligand to react with the 4f metal ions.

It is clear from the literature review that a lone electron pair of big S atom in the thiophene carboxylate ligand can be more easily delocalized within the heterocycle, so that the ligand can transfer efficiently the energy of the π, π^* excited state to the Ln^{3+} ions to increase their luminescence quantum yield [Zhan *et al.* 2012]. These factors have motivated to design thiophene acetate based lanthanide coordination compounds and investigate their photophysical properties. Furthermore in the present study the effect of bidentate nitrogen donors on the luminescent properties of Ln^{3+}-thiophene acetate complexes has also been examined.

Chapter 2

Synthesis, crystal structure and photophysical properties of lanthanide coordination polymers of 4-[4-(9H-carbazol-9-yl)butoxy]benzoate: The effect of bidentate nitrogen donors on luminescence
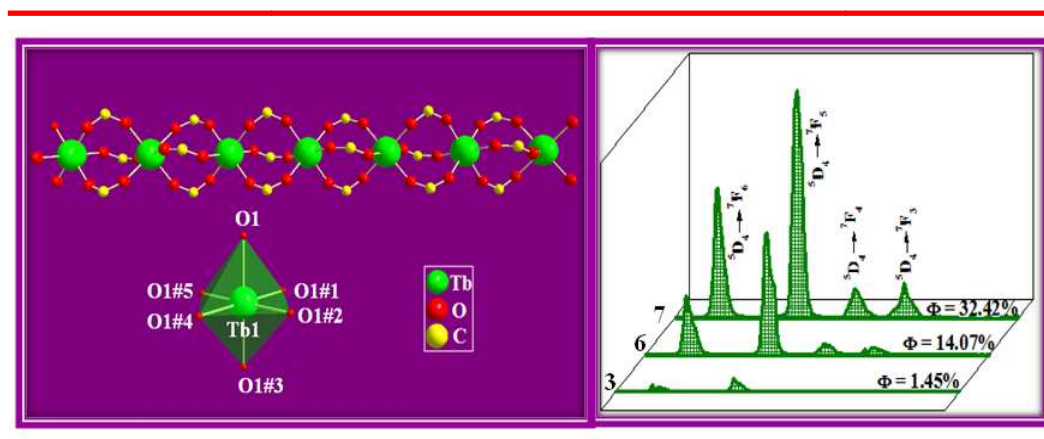
2.1. Abstract. A new aromatic carboxylate ligand, 4-[4-(9H-carbazol-9-yl)butoxy]benzoic acid (HL), has been synthesized by replacement of the hydroxyl hydrogen of 4-hydroxy benzoic acid with a 9-butyl-9H-carbazole moiety. The anion derived from HL has been used for the support of a series of lanthanide coordination compounds [Ln = Eu (1), Gd (2) and Tb (3)]. The new lanthanide complexes have been characterized by a variety of spectroscopic techniques. Complex 3 was structurally authenticated by single-crystal X-ray diffraction and found to exist as a solvent-free 1D coordination polymer with the formula $[Tb(L)_3]_n$. The structural data reveal that the terbium atoms in compound 3 reside in an octahedral ligand environment that is somewhat unusual for a lanthanide. It is interesting to note that each carboxylate group exhibits only a bridging-bidentate mode, with a complete lack of more complex connectivities that are commonly observed for extended lanthanide-containing solid-state structures. Examination of the packing diagram for 3 revealed the existence of two-dimensional molecular arrays held together by means of CH-π interactions. Aromatic carboxylates of the lanthanides are known to exhibit highly efficient luminescence, thus offering the promise of applicability as optical devices. However, due to difficulties that arise on account of their polymeric

nature, their practical application is somewhat limited. Accordingly, synthetic routes to discreet molecular species are highly desirable. For this purpose, a series of ternary lanthanide complexes was designed, synthesized and characterized, namely [Eu(L)$_3$(phen)] (4), [Eu(L)$_3$(tmphen)] (5), [Tb(L)$_3$(phen)] (6) and [Tb(L)$_3$(tmphen)] (7) (phen = 1,10-phenanthroline and tmphen = 3,4,7,8-tetramethyl-1,10-phenanthroline). The photophysical properties of the foregoing complexes in the solid state at room temperature have been investigated. The quantum yields of the ternary complexes 4 (9.65%), 5 (21.00%), 6 (14.07%) and 7 (32.42%), were found to be significantly enhanced in the presence of bidentate nitrogen donors when compared with those of the corresponding binary compounds 1 (0.11%) and 3 (1.45%). Presumably this is due to effective energy transfer from the ancillary ligands.

2.2. Introduction

Recently, several lanthanide benzoate complexes with unique photophysical properties and intriguing structural features have been reported. In general, benzoate ligands are able to sensitize Tb^{3+} better than Eu^{3+} due to a more favorable match of the triplet states of the ligands with that of the $^5D_4$ excited state of the Ln^{3+} ion [Eddaoudi *et al.*2001; Eddaoudi *et al.*2002; Pan *et al.*2004; Li *et al.*2005; de Bettencourt-Dias *et al.*2006; Li *et al.*2006; Zhang *et al.*2011]. Furthermore, the carboxylate groups of the benzoate ligands interact strongly with the oxophilic lanthanides and the delocalized π–electron system results in a strongly absorbing chromophore [Tsaryuk *et al.* 2006; Hilder *et al.*2009; Wu *et al.*2011]. Very recently, our group reported that the replacement of high-energy C–H vibrations by fluorinated phenyl groups in the 3,5-bis(benzyloxy)benzoate moiety significantly improves the luminescence intensity and lifetimes of these lanthanide complexes [Sivakumar *et al.*2012]. It was also demonstrated that replacement of the hydrogens of the NH_2 moiety of *p*-aminobenzoic acid by benzyl groups had a significant influence on the distribution of π-electron density within the ligand system and resulted in the development of a novel solid state photosensitizer for Tb^{3+} with an overall quantum yield of 82% [Ramya *et al.*2010]. Subsequent investigations from our group also revealed that the presence of electron-releasing or electron-withdrawing groups on position 3 of the 4-benzyloxy benzoic acid ligand has a profound effect on the π-electron density of the ligands and consequently on the photosensitization of the Ln^{3+} ions. Specifically, the presence of a methoxy substituent in this position results in a significant improvement in the photoluminescence efficiency of the Tb^{3+}-3-methoxy-4-benzyloxy benzoate complex in comparison with that of the 4-benzyloxy benzoate complex (10-33%). By contrast, the introduction of a nitro group in the 3 position dramatically diminishes the photoluminescence efficiency of the Tb^{3+}-3-nitro-4-benzyloxy benzoate complex due to the existence of a pathway that permits dissipation of the excitation energy *via* the π*-*n* transition of the nitro group in conjunction with the ILCT band [Sivakumar *et al.*2010]. Studies by de Bettencourt-Dias *et al.* [Viswanathan and de Bettencourt-Dias *et al.* 2006] suggest that derivatization of

benzoic acid analogues with thiophene has a beneficial tuning effect on the triplet state of the antenna which results in a higher emission quantum yield. This is a consequence of improved matching of the ligand and lanthanide ion excited states. Inspired by the efficient sensitization of various lanthanide benzoates, herein, the synthesis of new benzoic acid ligand 4-[4-(9H-carbazol-9-yl)butoxy]benzoic acid, which was formed by replacement of the hydroxyl hydrogen of 4-hydroxy benzoic acid with a 9-butyl-9H-carbazole moiety has been reported. Additionally, a series of new lanthanide coordination polymers featuring Eu^{3+}, Gd^{3+} and Tb^{3+} cations was also reported. The presence of the appended carbazole moiety in the ligand molecule widens the absorption profile and serves as a light-harvesting unit, thereby improving the hole-transporting ability. Moreover, there is an increase of solubility in common organic solvents [Zheng *et al.*2008]. The newly synthesized lanthanide benzoates have been fully characterized and their luminescent properties have been investigated in detail.

Aromatic lanthanide carboxylates generally form coordination-polymeric networks with corresponding short-range interactions rather than existing as isolated molecular entities. In general, this results in the formation of poorly soluble and non-volatile species [Ouchi *et al.* 1988]. In turn this prevents the deposition of aromatic lanthanide carboxylate thin films by means of traditional vacuum and solution processing methods [Ouchi *et al.* 1988; Deacon *et al.* 2007; Utochnikova *et al.* 2012]. It is well documented that bidentate nitrogen donors such as bipyridines and phenanthrolines, which can serve as both co-chelating and co-sensitizing ligands, can help to circumvent the aforementioned drawbacks by inhibiting polymer formation and by forming discreet molecular coordination complexes. Such ligands can exclude adventitious solvent molecules from the immediate coordination sphere of the luminescent metal center, thereby avoiding a potential quenching pathway that is frequently encountered in the case of lanthanide carboxylates [Fiedler *et al.* 2007]. In the present work, ternary complexes of Ln^{3+}-4-[4-(9H-carbazol-9-yl)butoxy]benzoates have been prepared by the incorporation of either 1,10-phenanthroline or 3,4,7,8-tetramethyl-1,10-phenanthroline. The new compounds have been fully characterized and their luminescent properties have been investigated.

2.3. Experimental Section

Materials and instrumentation

The commercially available chemicals europium(III) nitrate hexahydrate (Acros Organics; purity 99.9%); gadolinium(III) nitrate hexahydrate (Treibacher; purity 99.9%); terbium(III) nitrate hexahydrate (Acros Organics; purity 99.9%); 4-hydroxy benzoic acid (Aldrich; purity 99%); carbazole (Aldrich; purity 99%); 1,4-dibromobutane (Aldrich; purity 99%); 1,10-phenanthroline (Aldrich; purity 99%) and 3,4,7,8-tetramethy-1,10-phenanthroline (Aldrich; purity 99%) were used without further purification. All additional chemicals were of analytical reagent grade quality.

Elemental analyses were performed with a Perkin-Elmer Series 2 Elemental Analyser 2400. A Nicolet FT-IR 560 Magna Spectrometer using KBr (neat), was used to obtain the IR spectral data and a Bruker 500 MHz NMR spectrometer was used to record the ^{1}H NMR and ^{13}C NMR spectra of the new compounds in DMSO-d_6 media. The mass spectra were recorded on a JEOL JSM 600 fast atom bombardment (FAB) high resolution mass spectrometer (FABMS) and the thermogravimetric analyses were performed on a TGA-50H instrument (Shimadzu, Japan). The diffuse reflectance spectra of the lanthanide complexes and the phosphor standard were recorded on a Shimadzu, UV-2450 UV-Vis spectrophotometer using $BaSO_4$ as a reference. The absorbances of the ligands and the corresponding lanthanide complexes were each dissolved in N,N-dimethyl acetamide (DMA) and were measured with a UV-Vis spectrophotometer (Shimadzu, UV-2450). The X-ray powder patterns (XRD) were recorded in the 2θ range of 10-70° using Cu-K$_α$ radiation (Philips X'pert). The photoluminescence (PL) spectra were recorded on a Spex-Fluorolog DM3000F spectrofluorometer featuring a double grating 0.22m Spex 1680 monochromator and a 450W Xe lamp as the excitation source using the front face mode. The lifetime measurements were carried out at room temperature using a Spex 1040D phosphorimeter. The overall quantum yields ($\Phi_{overall}$) were measured at room temperature using the technique for powdered samples described elsewhere [Bril and De Jager-Veenis 1976], through the following expression:

$$\Phi_{overall} = \frac{1-r_{st}}{1-r_X} \times \frac{A_x}{A_{st}} \times \Phi_{st}$$

31

where r_x and r_{st} represent the diffuse reflectance (with respect to a fixed wavelength) of the complexes and of the standard phosphor, respectively, and Φ_{st} is the quantum yield of the standard phosphor. The terms A_x and A_{st} represent the areas under the complex and the standard emission spectra, respectively. To have absolute intensity values, $BaSO_4$ was used as the reflecting standard. For measuring $\Phi_{overall}$ for Ln^{3+} complexes, Pyrene was employed as a standard, whose emission spectrum comprises an intense broad band peaking around 475 nm, with a constant Φ value (61%) for an excitation wavelength of 313 nm [Melhuish 1964]. Three measurements were carried out for each sample, and each reported $\Phi_{overall}$ value corresponds to the arithmetic mean of the three values. The errors in the quantum yield values associated with this technique were estimated to lie within ±10% [Carlos *et al.* 2003]. The overall quantum yields for the Ln^{3+} complexes were also measured using an integrating sphere in a SPEX Fluorolog spectrofluorimeter. The photoluminescence quantum yields in thin films ($\Phi_{overall}$) were determined using a calibrated integrated sphere system. The Xe-arc lamp was used to excite the thin-film samples placed in the sphere. Samples were prepared by placing the material between two quartz cover slips, the quantum yield was determined by comparing the spectral intensities of the lamp and the sample emission as reported in the literature [de Mello *et al.* 1997; Palsson and Monkman 2002; Shah *et al.* 2006]. Using this experimental setup and the integrating sphere system, the solid-state fluorescence quantum yield of thin film of the standard green OLED material tris-8-hydroxyquinolinolato aluminum (Alq_3) was determined to be 19%, which is consistent with previously reported values [Colle *et al.* 2003; Saleesh Kumar *et al.* 2008]. Each sample was measured several times under slightly different experimental conditions. The estimated error for quantum yields is ±10% [Eliseeva *et al.* 2008].

Crystallographic Characterization. The X-ray diffraction data were collected at 153 K on a Nonius Kappa CCD diffractometer equipped with an Oxford Cryostream low-temperature device and a graphite-monochromated Mo-Kα radiation source ($\lambda = 0.71073$ Å). Corrections were applied for Lorentz and polarization effects. All structures were solved by direct methods (Sheldrick 1994) and refined by full-matrix least-squares cycles on F^2. All nonhydrogen atoms were allowed anisotropic thermal

motion, and the hydrogen atoms were placed in fixed, calculated positions using a riding model (C–H 0.96 Å). Selected crystal data, and data collection and refinement parameters are listed in Tables 2.1 and 2.2. The CCDC number for 3 is 756460.

Synthesis of 4-[4-(9H-carbazol-9-yl)butoxy]benzoic acid.

a) **9-(4-bromobutyl)-9H-carbazole**: A mixture containing carbazole (500 mg, 3.00 mmol), benzene (1.5 mL), benzyl triethyl ammonium chloride (25 mg) and aqueous 50% NaOH (1.5 mL) was prepared. A molar excess (10 fold relative to carbazole) of 1,4-dibromobutane was added, and the reaction mixture was stirred at 40°C for 1 h. The benzene was removed by evaporation and the residue was extracted with CHCl$_3$. The CHCl$_3$ layer was washed with deionized water and dried over Na$_2$SO$_4$ overnight. The CHCl$_3$ layer was then evaporated and excess 1,4-dibromobutane was removed by heating to 80°C under a vacuum. The crude product was recrystallised from benzene. Yield, 831 mg (92%): ^{1}H NMR (500 MHz, CDCl$_3$) δ/ppm: 1.91-1.98 (t, 2H, CH$_2$), 2.03-2.07 (t, 2H, CH$_2$), 3.14-3.18 (t, 1H, CH), 3.36-3.40 (t, 1H, CH), 4.35-4.36 (d, 2H, CH$_2$), 7.21-7.25 (t, 2H, Ph-H), 7.45-7.49 (t, 4H, Ph-H), 8.09-8.12 (d, 2H, Ph-H).

b) **methyl 4-[4-(9H-carbazol-9-yl)butoxy]benzoate**: A mixture of 9-(4-bromobutyl)-9*H*-carbazole (4.95 g, 16 mmol), methyl-4-hydroxybenzoate (2.49 g, 16.0 mmol), potassium carbonate (2.34 g, 17 mmol) and KI (1.00 g) dissolved in anhydrous acetone (90 mL) was stirred vigorously and heated at reflux for 48 h under a nitrogen atmosphere. The solvent was removed by evaporation, and the resulting solid was recrystallized from ethanol to yield a crop of colourless needles. Yield, 4.53 g (74%): ^{1}H NMR (500 MHz, DMSO-d_6) δ/ppm: 1.89-1.92 (t, 2H, CH$_2$), 2.04-2.11 (t, 2H, CH$_2$), 3.82 (s, 3H, O-CH$_3$), 4.11-4.14 (t, 2H, CH$_2$), 4.53-4.56 (t, 2H, CH$_2$), 6.97-6.99 (q, 2H, Ph-H), 7.19-7.22 (m, 2H, Ph-H), 7.44-7.47 (m, 2H, Ph-H), 7.60-7.61 (d, 2H, Ph-H), 7.91-7.93 (q, 2H, Ph-H), 8.14-8.15 (t, 2H, Ph-H).

c) **4-[4-(9H-carbazol-9-yl)butoxy]benzoic acid**: methyl 4-[4-(9H-carbazol-9-yl)butoxy]benzoate (1.12 g, 3 mmol) was refluxed for 12 h with NaOH (0.12 g, 3 mmol) in 50 mL of methanol. The reaction mixture was poured into ice cold water, acidified with dilute HCl, and the resulting precipitate was filtered, washed, dried and recrystallized from methanol (Scheme 2.1). Yield, 0.86 g (80%): ^{1}H NMR (500

MHz, Acetone-d_6) δ/ppm: 1.80-1.83 (t, 2H, CH$_2$), 2.00-2.03 (t, 2H, CH$_2$), 3.26 (s, 2H, CH$_2$), 4.00-4.03 (t, 2H, CH$_2$), 6.91-6.93 (t, 2H, Ph-H), 7.19-7.22 (t, 2H, Ph-H), 7.43-7.47 (m, 2H, Ph-H), 7.55-7.56 (d, 2H, Ph-H), 7.89-7.91 (t, 2H, Ph-H), 8.10-8.12 (d, 2H, Ph-H) (Figure 2.1). FAB: m/z 359.40 [M$^+$]. Elemental analysis (%): calcd for C$_{23}$H$_{21}$NO$_3$: C, 76.86; H, 5.89; N, 3.90. Found: C, 76.81; H, 5.84; N, 4.23. ^{13}C NMR (500 MHz, CDCl$_3$) δ/ppm: 172.30, 167.99, 145.60, 136.79, 130.80, 127.95, 125.30, 123.94, 119.24, 114.08, 72.87, 47.52, 31.82, 30.70. IR (KBr) v_{max}/cm^{-1}: 2941, 1696, 1605, 1485, 1464, 1326, 1294, 1254, 1165, 1066, 1014, 770.
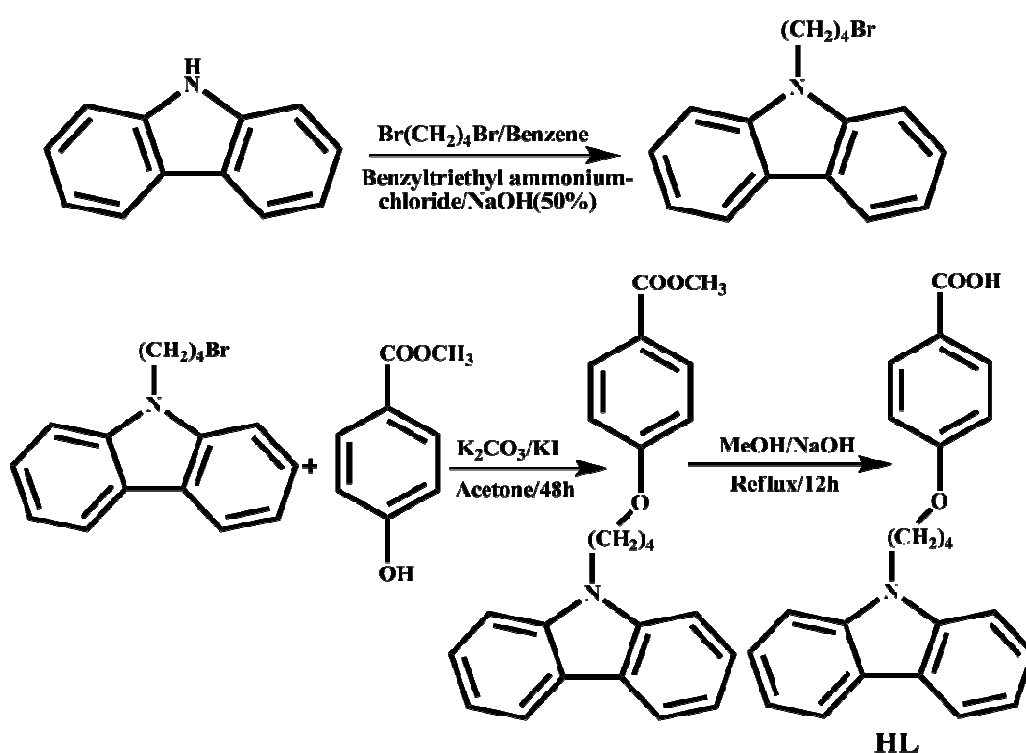
Scheme 2.1. Synthetic procedures for ligand 4-[4-(9H-carbazol-9-yl)butoxy]benzoic acid.

Syntheses of Lanthanide Complexes.

Syntheses of [Ln(L)$_3$]$_n$ [Ln = Eu^{3+}, Gd^{3+} and Tb^{3+}] complexes.

To a stirred ethanolic solution of HL (0.60 mmol), NaOH (0.60 mmol) was added and the resulting mixture was stirred for 5 min. To this solution was added dropwise a saturated ethanolic solution of Ln(NO$_3$)$_3$.6H$_2$O (0.20 mmol) and the reaction mixture was stirred for 10 h. Deionized water was then added to the reaction mixture

and the resulting precipitate was filtered, washed with deionized water and dried (Scheme 2.2). Single crystals of the Tb complex were grown from a solution of N,N-dimethyl acetamide (DMA).
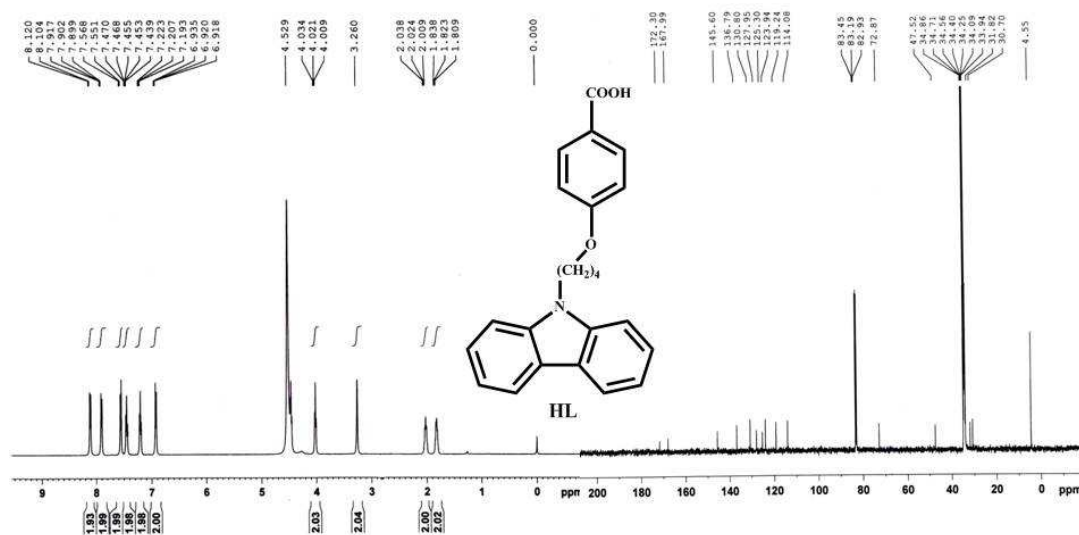
Figure 2. 1. ^{1}H and ^{13}C NMR spectra of HL in Acetone-d$_6$ and CDCl$_3$ solution.
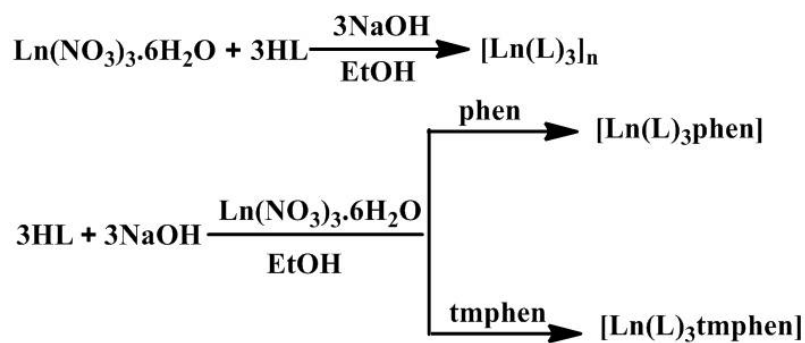
Scheme 2.2. Synthetic procedures for complexes 1-7**.**

[Eu(L)$_3$]$_n$ (1). Elemental analysis (%): calcd for C$_{69}$H$_{60}$N$_3$O$_9$Eu (1227.16): C, 67.52; H, 4.92; N, 3.42. Found: C, 67.78; H, 5.03; N, 3.71. IR (KBr) υ_{max}/cm^{-1}: 2929, 1605, 1594, 1422, 1252, 1173, 1020, 784 cm^{-1}. $m/z = 869.83$ (M - L)$^+$.

[Gd(L)$_3$]$_n$ (2). Elemental analysis (%): calcd for C$_{69}$H$_{60}$N$_3$O$_9$Gd (1232.45): C, 67.23; H, 4.90; N, 3.40. Found: C, 67.15; H, 5.23; N, 3.67. IR (KBr) υ_{max}/cm^{-1}: 2940, 1605, 1589, 1416, 1327, 1252, 1174, 1048, 786. *m/z* = 873.50 (M - L)$^+$.

[Tb(L)$_3$]$_n$ (3). Elemental analysis (%): calcd for C$_{69}$H$_{60}$N$_3$O$_9$Tb (1234.13): C, 67.15; H, 4.90; N, 3.40. Found: C, 67.45; H, 5.17; N, 3.56. IR (KBr) υ_{max}/cm^{-1} 2922, 1605, 1588, 1414, 1327, 1251, 1176, 1151, 786. *m/z* = 921.49 (M - L+ CO$_2$+1)$^+$.

Syntheses of Ln(L)$_3$(phen) and Ln(L)$_3$(tmphen) [Ln = Eu^{3+} and Tb^{3+}] complexes.

An ethanolic solution of Ln(NO$_3$)$_3\cdot$6H$_2$O (0.25 mmol) and the corresponding neutral donor (0.25 mmol) [1,10-phenanthroline for 4 and 6 and 3,4,7,8-tetramethyl-1,10-phenanthroline for 5 and 7, respectively) were added to an aqueous solution of HL (0.75 mmol) in the presence of NaOH (0.75 mmol). The immediate formation of a precipitate was followed by stirring the reaction mixture at room temperature for 10 h. The resulting precipitate was then filtered, washed sequentially with deionized water and ethanol, dried and stored in a desiccator.

Eu(L)$_3$(phen) (4). Elemental analysis (%): calcd for C$_{81}$H$_{68}$EuN$_5$O$_9$ (1407.42): C, 69.13; H, 4.87; N, 4.98; found C, 69.24; H, 4.92; N, 5.02. IR (KBr) υ_{max}: 2935, 1615, 1607, 1567, 1526, 1453, 1424, 1344, 1326, 1250, 1173, 1152, 1102, 851 cm^{-1}. *m/z* = 1050.24 (M - L)$^+$.

Eu(L)$_3$(tmphen) (5). Elemental analysis (%): calcd for C$_{85}$H$_{76}$EuN$_5$O$_9$ (1463.48): C, 69.76; H, 5.23; N, 4.79; found C, 69.81; H, 5.28; N, 4.83. IR (KBr) υ_{max}: 2929, 1604, 1558, 1526, 1452, 1416, 1325, 1249, 1172, 1149, 1012, 859, 784 cm^{-1}. *m/z* = 1106.11 (M - L)$^+$.

Tb(L)$_3$(phen) (6). Elemental analysis (%): calcd for C$_{81}$H$_{68}$TbN$_5$O$_9$ (1413.42): C, 68.78; H, 4.85; N, 4.95; found C, 68.64; H, 4.83; N, 5.03. IR (KBr) υ_{max}: 2937, 1619, 1602, 1568, 1525, 1453, 1424, 1326, 1250, 1173, 851 cm^{-1}. *m/z* = 1056.24 (M - L)$^+$.

Tb(L)$_3$(tmphen) (7). Elemental analysis (%): calcd for C$_{85}$H$_{76}$TbN$_5$O$_9$ (1470.46): C, 69.43; H, 5.21; N, 4.76; found C, 69.18; H, 5.27; N, 5.03. IR (KBr) υ_{max}: 2928, 1606, 1563, 1527, 1453, 1421, 1325, 1245, 1172, 1050, 1022, 861, 785 cm^{-1}. *m/z* = 1112.02 (M - L)$^+$.

2.4. Results and Discussion

Synthesis and Characterization of Ligand and Ln^{3+} Complexes 1-7.

In order to overcome the inherently weak absorption cross sections of the Eu^{3+} and Tb^{3+} ions and thereby enhance the luminescence efficiencies of the lanthanide complexes, a new antenna molecule was necessary. Accordingly, the new ligand 4-[4-(9H-carbazol-9-yl)butoxy]benzoic acid with appended functional peripheries of the carbazole chromophore was designed and synthesized. The overall synthesis procedure is outlined in Scheme 2.1. The ligand was obtained in an overall yield of 80-85% in three steps starting from 4-hydroxybenzoic acid. The newly designed ligand was characterized by ^{1}H NMR, ^{13}C NMR, mass spectroscopy (FAB-MS) and elemental analysis. The details of the syntheses of the new lanthanide complexes are summarized in the Experimental Section. The elemental analysis data for the seven complexes revealed that in each case the Ln^{3+} ion had reacted with the corresponding benzoic acid ligand in a metal-to-ligand mole ratio of 1:3. Moreover, complexes 4-7 also incorporate one molecule of a bidentate nitrogen donor ligand. In order to investigate the mode of coordination of the 4-[4-(9H-carbazol-9-yl)butoxy]benzoate ligand to the Ln^{3+} ions, the infrared spectra of the complexes were compared with that of the free ligand. The $\nu_{C=O}$ (–COOH) stretching frequency of the free ligand at 1696 cm^{-1} is absent in the IR spectra of complexes 1-7, whereas the characteristic peaks for ν_{as} (C=O) and ν_s (C=O) are observed at 1594–1525 cm^{-1} and 1453–1414 cm^{-1}, respectively. The foregoing frequencies imply that the oxygen atoms of the carboxylate groups are coordinated to the Ln^{3+} ion. Furthermore, compounds 1, 2, and 3 exhibit differences of 172, 173, and 174 cm^{-1}, respectively, between ν_{as} (C=O) and ν_s (C=O) ($\Delta\nu$). These values strongly suggest that the carboxylate groups are coordinated to the metal ions in a bidentate bridging mode [Deacon and Phillips 1980; Doeuff *et al.* 1987; Zhu *et al.* 2002; Djerdj *et al.* 2009]. Conversely, complexes 4-7, exhibit an analogous difference of $\Delta\nu$ (ν_{as} (C=O) – ν_s (C=O)) in the range of 101–115 cm^{-1}, thus indicating that the carboxylate groups are coordinated to the Ln^{3+} ions in bidentate chelating modes [Deacon and Phillips 1980; Nakamato *et al.* 1986; Kazuo 1986; Emeleus and Sharpe *et al.* 1977; Yu *et al.* 2004; Jaun *et al.* 2006; Huang *et al.* 2007]. The bands at 1644 and 1608 cm^{-1}, which

are assigned to the ν(C=N) stretching frequencies of the free phen and tmphen ligands, respectively, also shift to the lower wavenumbers 1619–1604 cm^{-1} in the cases of complexes 4-7, thus suggesting that the nitrogen atoms of the phen and tmphen ligands are also coordinated to the Ln^{3+} ion [Ye *et al.* 2010]. The absence of a broad-band absorption at 3200-3500 cm^{-1} confirms that complexes 1-7 are devoid of water molecules [Eliseeva *et al.* 2011].

Thermogravimetric analysis (TGA) experiments were conducted in order to determine the thermal stabilities of complexes 1-7 under a nitrogen atmosphere in the temperature range 30–1000°C (Figures 2.2 and 2.3). The TGA plots reveal high thermal stabilities for complexes 1-3 with no loss of mass being observed below 380°C. This result is consistent with the FT-IR data and confirms the absence of water molecules in the coordination spheres of the lanthanide ions.
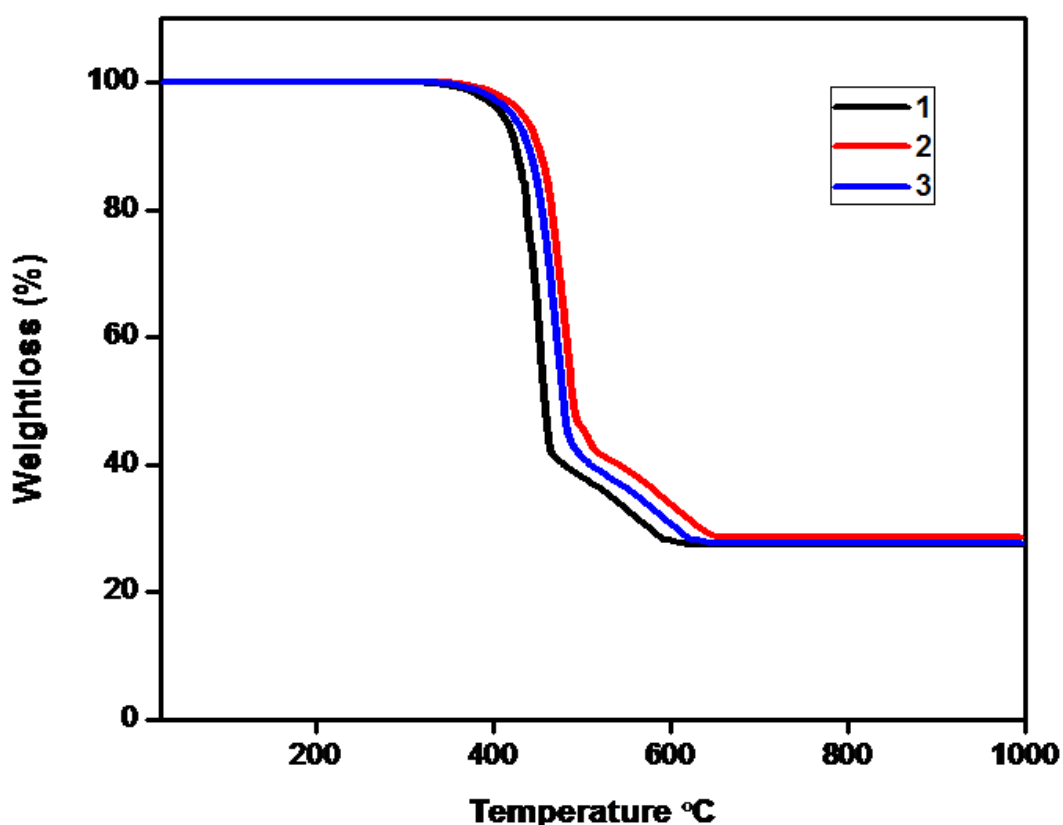
Figure 2.2. Thermo gravimetric curves for complexes 1-3.
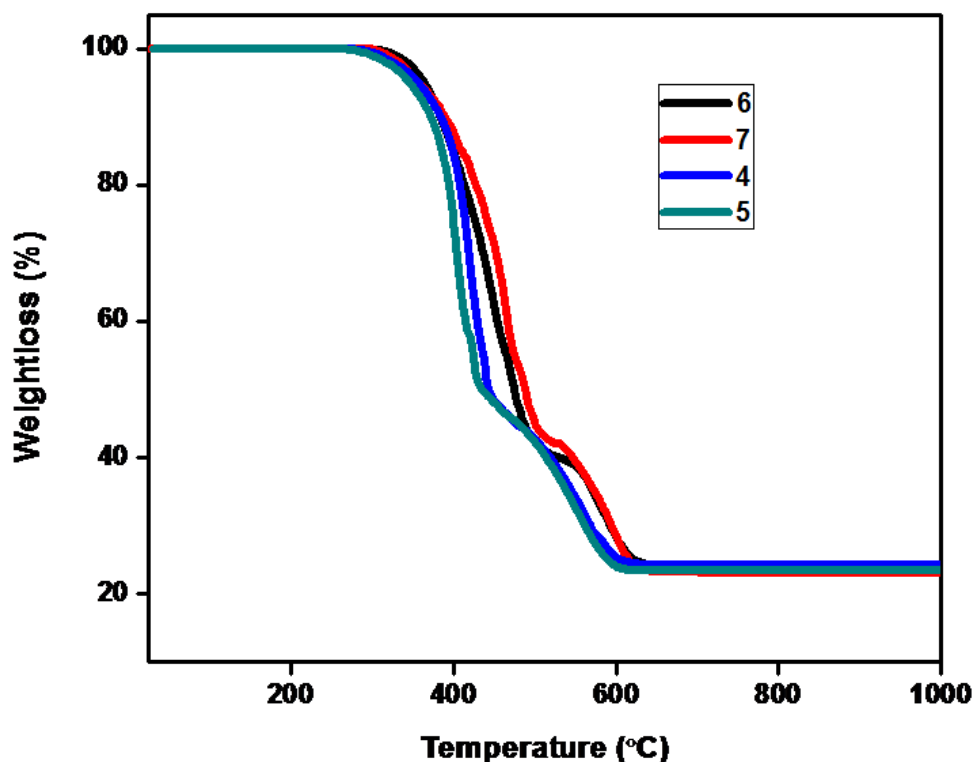
Figure 2.3. Thermo gravimetric curves for complexes 4-7.

At higher temperatures (380 to 640°C), the single weight loss is attributed to the decomposition of complexes 1-3 and the formation of lanthanide oxide. Contrastingly, for complexes 4-7 (Figure 2.3), there are two primary successive mass loss stages. The first stage takes place between 280 to 450°C (for 4 and 5) and 280 to 500°C (for 6 and 7), with a change of mass that is consistent with the loss of phen (from 4 and 6) or tmphen (from 5 and 7) ligands along with two of the 4-[4-(9H-carbazol-9-yl)butoxy]benzoate groups. The second mass loss occurs in the temperature range of 500–620°C, and corresponds to the elimination of a 4-[4-(9H-carbazol-9-yl)butoxy]benzoate thus resulting in a residual mass corresponding to that of lanthanide oxide.

X-ray Structural Characterization.

The similar X-ray powder diffraction patterns of complexes 1-3 imply that these compounds are isostructural (Figure 2.4). Analysis of the single-crystal X-ray diffraction data for compound 3 reveals that it forms a solvent-free, infinite one-dimensional (1-D) coordination polymer of formula $[Tb(L)_3]_n$. A perspective view

of 3 is presented in Figure 2.5. The data collection parameters along with selected bond lengths and angles are listed in Tables 2.1 and 2.2, respectively. Compound 3 crystallizes in the rhombohedral space group *R*-3. The Tb^{3+} metal centers are coordinated to six carboxylate oxygen atoms in an octahedral geometry. Perhaps the most noteworthy structural feature of 3 is the sole presence of a bidentate carboxylate bridging mode and the absence of more complex connectivities that are generally encountered in several lanthanide carboxylate coordination polymers. Moreover, the coordination number of six for compound 3 is unusually low for a terbium ion [Guseinova *et al.* 1968; Kistaiah *et al.* 1981; Furmanova *et al.* 1984; Lill and Cahill 2006; Li *et al.* 2005; Chen *et al.* 2007; Fomina *et al.* 2012]. Similar structural features have been previously observed for Tb^{3+}-1,3,5-cyclohexanetricarboxylates [Lill and Cahill 2006].
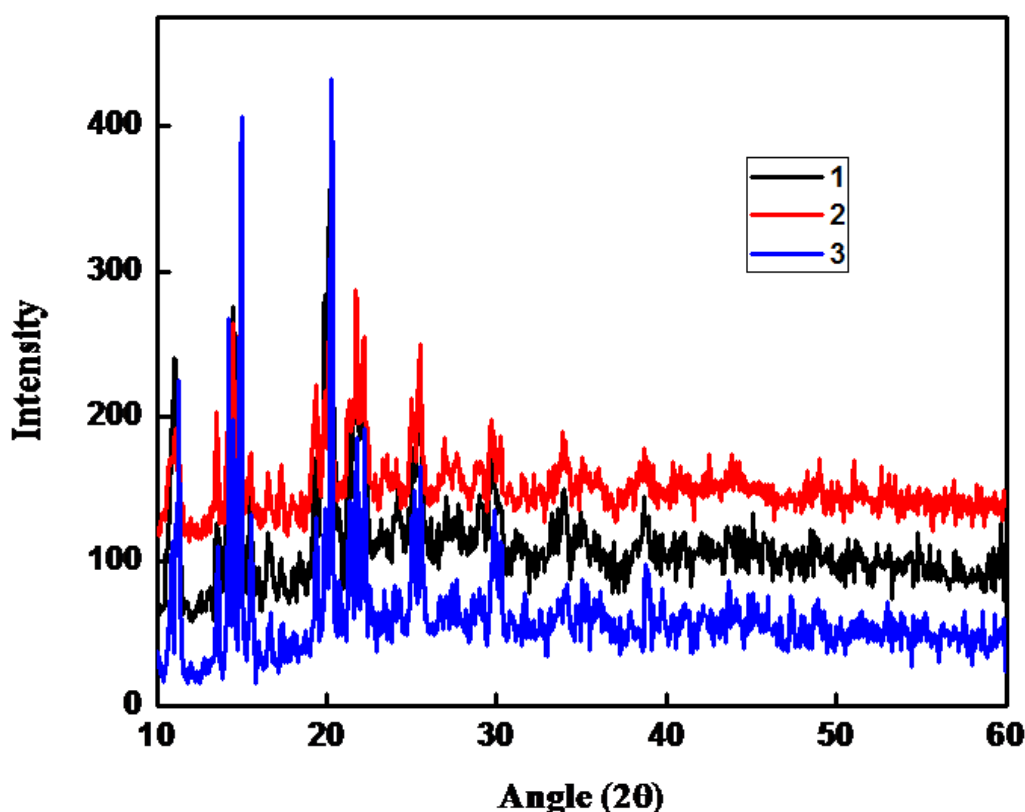
Figure 2.4. XRD pattern for complexes 1, 2 and 3.
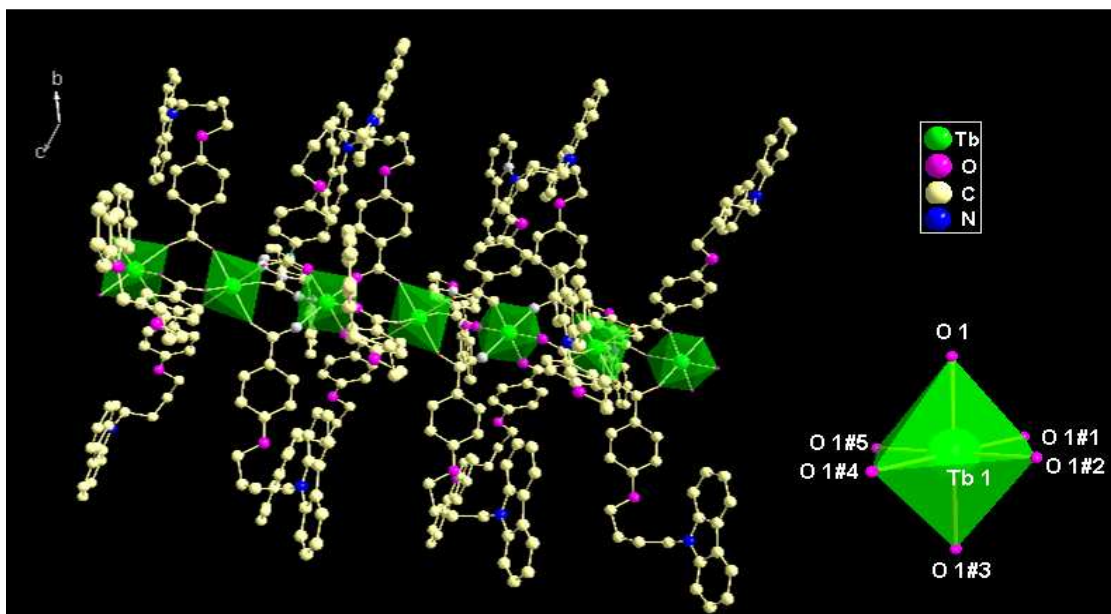
Figure 2.5. The 1D coordination polymer chain and coordination environment of the Tb^{3+} ions in complex 3 with atom-labelling scheme. All hydrogen atoms were omitted for clarity.

A search of the Cambridge Structural Database reveals that approximately 155 structures have been reported in which the lanthanide center has a coordination number of six. The majority of these structures are polymeric. However, a few of them are oligomeric, molecular species. Typically these complexes are formed in non-aqueous media and involve sterically demanding ligands. The incorporation of a bulky carbazolylbutyl group in the *p*-hydroxy benzoate ligand appears to be responsible for the exclusion of solvent from this structure and the introduction of steric crowding within the immediate coordination environment [Rao *et al.* 2004; Cotton 2006; Lill and Cahill 2006; Bußkamp *et al.* 2007; Fomina *et al.* 2012]. The Tb1−Tb2−Tb1 bond angle of 180° indicates that the carboxylate ligand, which is linked in a one-dimensional array, can be best described as a linear chain. The interatomic Tb…Tb distance is 4.768 Å and the Tb-O bond lengths of the bidentate bridging carboxylate group of 2.247(4) and 2.256(3) Å are comparable with those of reported values [Teotonio *et al.* 2005; Bußkamp *et al.* 2007].

A detailed analysis of the packing diagram of 3 reveals that the coordination polymers are connected by means of C-H-π interactions between the benzoate moiety of one ligand and the carbazole moiety of an adjacent ligand (Figure 2.6),

thus resulting in the generation of an infinite two-dimensional supramolecular structure.

Table 2.1. Crystal Data Collection and Structure Refinement Parameters for complex 3

Parameters	3
empirical formula	$C_{69}H_{60}N_3O_9Tb$
Fw	1234.18
crystal system	Rhombohedral
space group	R-3
cryst size (mm^3)	$0.20 \times 0.05 \times 0.04$
Temperature	153(2)
a/Å	18.865(2)
b/Å	18.865(2)
c/Å	18.865(2)
α (deg)	117.220
β (deg)	117.220
γ (deg)	117.220
V / Å^3	2855.9(6)
Z	2
ρ_{calcd}/g cm^{-3}	1.435
μ/mm^{-1}	1.301
$F(000)$	1264
R1 [$I > 2\sigma(I)$]	0.0431
wR2 [$I > 2\sigma(I)$]	0.0673
R1 (all data)	0.0951
wR2 (all data)	0.0796
GOF	1.055

UV–vis Spectra.

The UV-Vis absorption spectra of the free ligands and those of the corresponding lanthanide complexes were recorded in N,N-dimethylacetamide (DMA) solution ($c = 2\times10^{-5}$ M), the results of which are presented in Figures 2.7 and 2.8, respectively. The five peaks at 254, 264, 293, 334 and 345 nm are assigned to the π–π* transitions of the carbazole moiety of the ligand [Zheng *et al.* 2008; Nie *et al.* 2007; Ambili Raj *et al.* 2010]. In comparison with the spectrum of the free ligand HL, the absorption bands of the corresponding lanthanide complexes are red shifted. The spectral

shapes for the complexes in DMA solution are similar to those of the free ligand, thus indicating that coordination to the lanthanide ion does not significantly influence the energy of the singlet state of the carboxylate ligand [Shi *et al.* 2005].

Table 2.2. Selected bond lengths and bond angles for the complex 3

	3
Tb1 –O1	2.247(4)
Tb2 –O2	2.256(3)
Tb(1)-O(1)#1	2.247(4)
Tb(1)-O(1)#2	2.247(4)
Tb(1)-O(1)#3	2.247(4)
Tb(1)-O(1)#4	2.247(4)
Tb(1)-O(1)#5	2.247(4)
Tb(2)-O(2)#2	2.256(3)
Tb(2)-O(2)#6	2.256(3)
Tb(2)-O(2)#5	2.256(3)
Tb(2)-O(2)#7	2.256(3)
Tb(2)-O(2)#8	2.256(3)
O1– Tb1 –O1#1	91.00(16)
O1#1– Tb1 –O1#2	91.00(16)
O1#2– Tb1 –O1#3	91.00(16)
O1#3– Tb1 –O1#4	89.00(16)
O1#4– Tb1 –O1#5	91.00(16)
O1#5– Tb1 –O1	89.00(16)
O2– Tb2 –O2#2	91.30(16)
O2#2– Tb2 –O2#5	91.30(16)
O2#5– Tb2 –O2#8	88.70(16)
O2#8– Tb2 –O2#7	88.70(16)
O2#7– Tb2 –O2#6	91.30(16)
O2#6– Tb2 –O2	88.70(16)
Tb2– Tb1 –Tb2	180.00

In the cases of complexes 4-7, the electronic transitions of the carboxylate, phen and tmphen units are overlapped and exhibit much more intense carbazole features [Nie *et al.* 2007]. Moreover, the molar absorption coefficient at 267 nm (for 4-7) increases considerably with the incorporation of the bidentate nitrogen donor [Ascencio *et al.* 2010]. Furthermore, the large molar absorption coefficient (ε) for the ligand 4-[4-(9H-carbazol-9-yl)butoxy]benzoic acid (1.57×10^{4} L mol^{-1} cm^{-1}) implies that the carboxylic acid ligand is a strong chromophore. The molar

absorption coefficient values for compounds 1-7 appear at λ_{max} 4.71×10^4, 4.99×10^4, 4.96×10^4, 4.92×10^4, 4.89×10^4, 4.77×10^4, and 4.80×10^4 L mol^{-1} cm^{-1}, respectively, the magnitudes of which are approximately three times higher than those for the free ligand, thus further confirming the presence of three ligated carboxylate moieties in each complex.
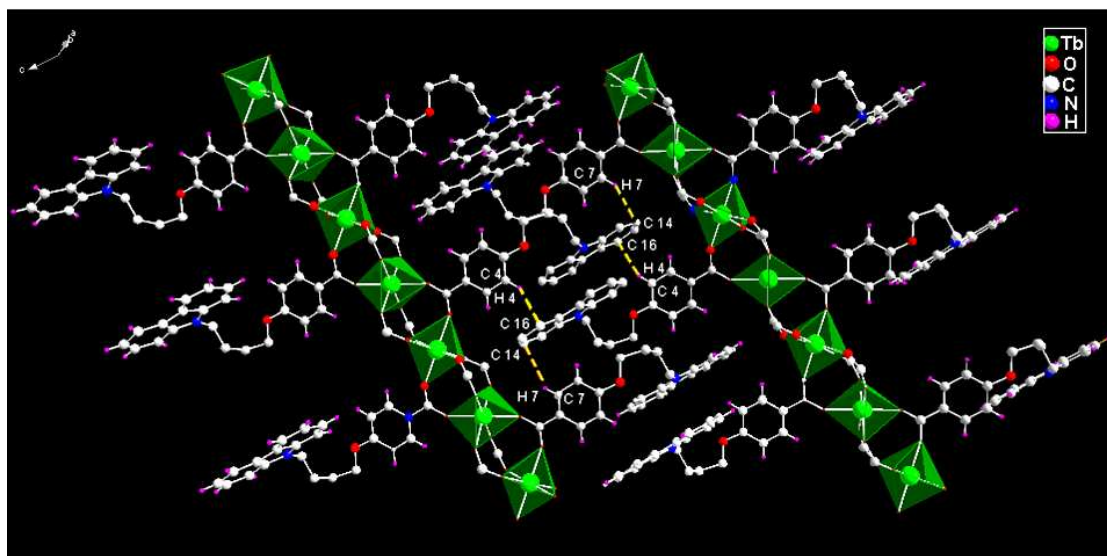
Figure 2.6. The molecular array formed by the CH•••π interactions involving C4–H4•••C16 (D−A=3.575 Å, H−A=2.795 Å and angle 142.10˚) and C7–H7•••C14 (D−A=3.586 Å, H−A=2.799 Å and angle 142.99˚) when viewed along the direction of the b axis (some of the ligand atoms were omitted for clarity).

PL Properties of Complexes.

In order to elucidate the energy migration pathways for complexes 1-7, it was necessary to determine the singlet and triplet energy levels of the ligand. These were estimated by reference to the wavelengths of the UV-vis absorbance edges and the lower wavelength emission edges of the corresponding phosphorescence spectra of Gd^{3+} complexes, respectively. Since the lowest excited energy level of Gd^{3+} ($^6P_{7/2}$) is too high to accept energy transfer from the ligands, the triplet state energy levels of the ligands are not significantly affected by complexation to the Gd^{3+} ion [Xu *et al.* 2006]. In order to determine the triplet energy level ($^3\pi\pi^*$) of the ligand, the phosphorescence spectrum of the compound [Gd(L)$_3$] was measured in DMA

solution at 77 K (Figure 2.9), revealing a triplet state energy level at 23923 cm^{-1}. Thus the triplet energy level of the newly designed carboxylic acid lies above the lowest excited resonance level of both Eu^{3+} ($^5D_0$ = 17300 cm^{-1}) and the $^5D_4$ level of Tb^{3+} (20500 cm^{-1}), thus demonstrating the sensitization efficacy of the ligand [Latva *et al.* 1997]. The triplet energy level of tmphen is found to be 21834 cm^{-1} (Figure 2.10).
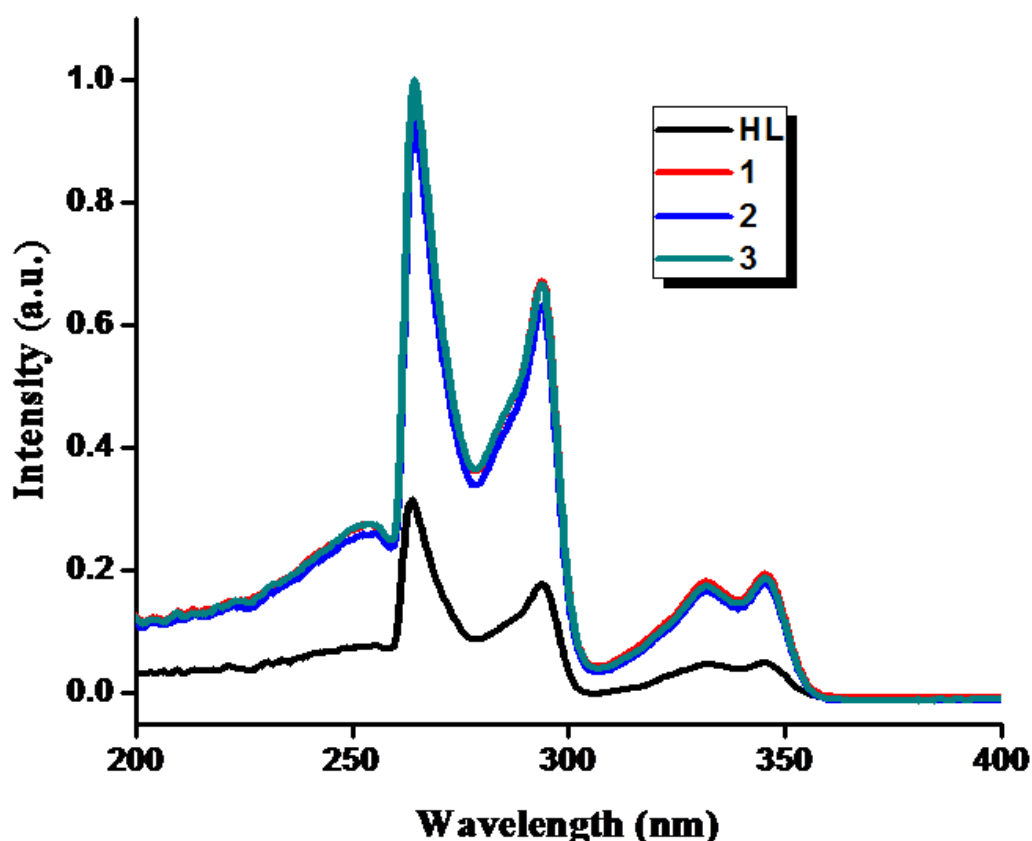
Figure 2.7. UV-visible absorption spectra of ligand HL and complexes 1-3 in DMA solution (c = 2 × 10^{-5} M).

The singlet and triplet energy levels for phen (31,000 and 22,100 cm^{-1}) were obtained from the reported literature values [Yu and Su 2003; Li *et al.* 2012]. The singlet ($^1\pi\pi^*$) energy levels of HL and tmphen were determined by referring to the UV-vis upper absorption edges of the corresponding Gd^{3+} complexes. The values were found to be 28089 cm^{-1} and 32786 cm^{-1}, respectively. According to Reinhoudt's empirical rule, the intersystem crossing process becomes effective

when $\Delta E = (^1\pi\pi^* - ^3\pi\pi^*)$ is at least 5000 cm^{-1} [Steemers *et al.* 1995]. Thus the present value of 4166 cm^{-1} suggests that the system has the capability for intersystem crossing from the singlet to the triplet level.
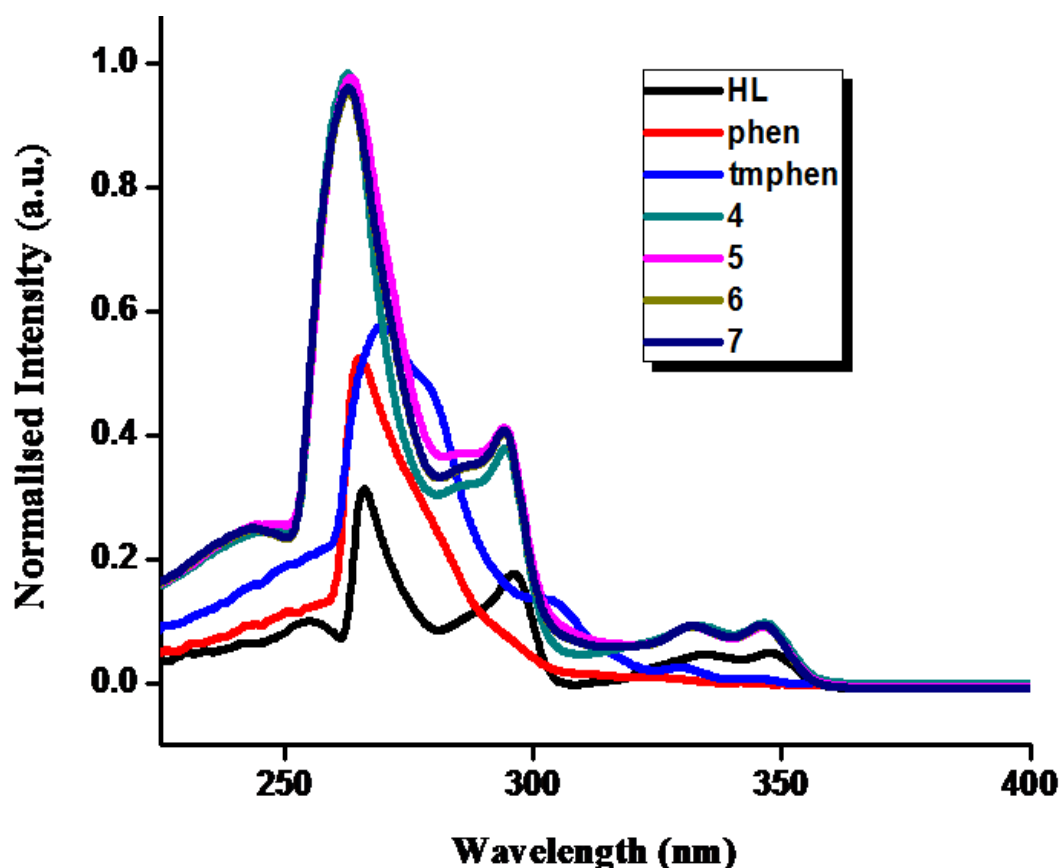
Figure 2.8. UV-Visible absorption spectra of ligand HL, phen, tmphen and complexes 4-7 in DMA solution (c = 2×10^{-5} M).

The excitation spectra of complexes 1, 4 and 5 were obtained by monitoring the $^5D_0 \rightarrow ^7F_2$ transition of Eu^{3+} and the results are displayed in Figures 2.11 and 2.12, respectively. The excitation spectrum of complex 1 features a broad band spanning the 330–370 nm region with a maximum at approximately 355 nm. This spectrum also features several narrow bands that arise from the intraconfigurational transitions from the $^7F_0$ ground state to the following levels (in nm): $^5H_4$ (374), $^5L_6$ (394), $^5D_3$ (414), $^5D_2$ (464), $^5D_1$ (532) and $^5D_0$ (578) [Teotonio *et al.* 2005; Shyni *et al.* 2007; Raphael *et al.* 2008; Biju *et al.* 2009; Ambili Raj *et al.* 2009; Sivakumar *et al.* 2011].

The intraconfigurational transitions exhibit a higher intensity than that of the ligand band, thus indicating that the indirect excitation is less efficient than the direct excitation. This phenomenon is further evidenced by the residual emission observed from the ligand that is apparent in the emission spectrum of complex 1 [Stanley *et al.* 2010; Ramya *et al.* 2010; Sivakumar *et al.* 2012]. On the other hand, the excitation spectra of the Eu^{3+} complexes 4 and 5 consist of broad bands in the range of 250 to 450 nm and are attributed to the ligand centered singlet–singlet transitions. In addition to this band, narrow bands arising from 4f–4f transitions from the ground state $^7F_0$ level to the $^5L_6$ (394 nm), $^5D_3$ (414 nm), and $^5D_2$ (464 nm) excited levels are also observed. The relative intensity of the broad band is higher than that arising from the Eu^{3+} ion, thus indicating that the indirect excitation processes is more efficient for these complexes [Teotonio *et al.* 2004]. The room temperature emission spectra of the Eu^{3+} complexes 1, 4 and 5 excited at 355 nm are displayed in Figures 2.11 and 2.12, respectively. The emission data exhibit intense narrow bands from the $^5D_0 \rightarrow {}^7F_J$ transitions (where J = 0–4) which are dominated by the hypersensitive $^5D_0 \rightarrow {}^7F_2$ transition at 612 nm. The intensity of the $^5D_0 \rightarrow {}^7F_2$ electric dipole
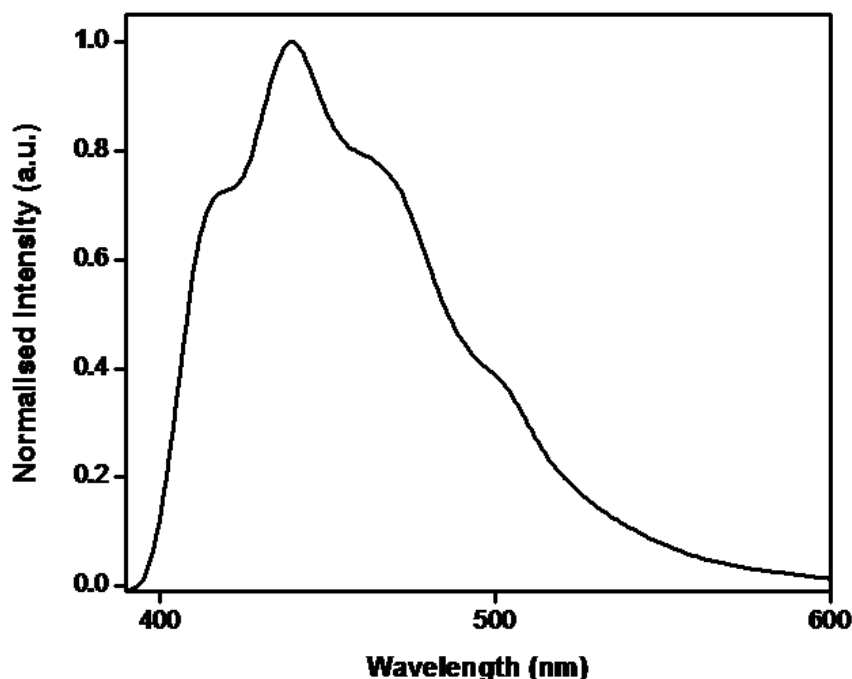
Figure 2.9. Phosphorescence spectrum of $[Gd(L)_3]_n$ at 77 K.

47
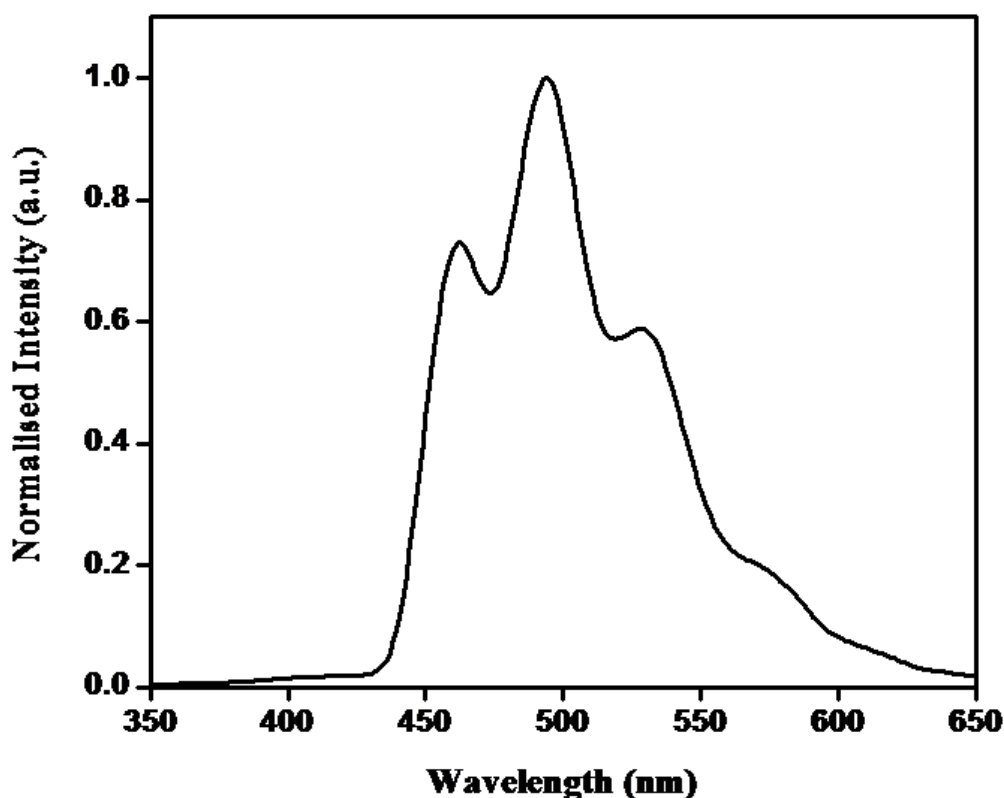
Figure 2.10. Phosphorescence spectrum of $[Gd(tmphen)(NO_3)_3]$ at 77 K.

transition is dependent on the degree of asymmetry in the environment of the Eu^{3+} ion, whereas the $^5D_0 \rightarrow {}^7F_1$ magnetic dipole transition is unrelated to the site asymmetry. The intensity of the emission band at 612 nm ($^5D_0 \rightarrow {}^7F_2$) is greater than those of the others, indicating that there is no inversion center at the site of the Eu^{3+} ion [Ye *et al.* 2010; Eliseeva *et al.* 2011]. Furthermore, the absence of ligand emission indicates that the ligand triplet state plays an important role in the luminescence sensitization of the Eu^{3+} ion in complexes 4 and 5.

The excitation and emission spectra of terbium complexes **3, 6** and 7 in the solid state at room temperature are depicted in Figures 2.13 and 2.14, respectively. The excitation spectra for all of the complexes were recorded by monitoring the strongest emission band of the Tb^{3+} cation. Each complex exhibits a broad band between 250 and 450 nm with an excitation maximum at approximately 355 nm which is assigned to the $\pi-\pi^*$ electronic transition of the ligand [Li *et al.* 2012]. The

characteristic sharp lines of the Tb^{3+} energy level structure, which are attributable to transitions between the $^7F_5$ and the $^5L_6$, $^5G_6$, $^5L_{10}$ and $^5L_9$ levels, were absent in these spectra, thus proving that luminescence sensitization proceeds via ligand excitation rather than by direct excitation of the Tb^{3+} ion absorption levels. The emission spectra for complexes 3, 6 and 7 exhibit green luminescence and exhibit typical emission bands at 491, 545, 585 and 622 nm, which are assigned to $^5D_4 \rightarrow {}^7F_J$ (J = 6−3) transitions [Ye *et al.* 2010; Eliseeva *et al.* 2011]. The dominant band of these emissions is attributed to the hypersensitive transition $^5D_4 \rightarrow {}^7F_5$ of the Tb^{3+} ions, while the more intense luminescent band corresponds to the $^5D_4 \rightarrow {}^7F_6$ transition and the two less intense bands are assigned to the $^5D_4 \rightarrow {}^7F_4$ and $^5D_4 \rightarrow {}^7F_3$ transitions, respectively.   It is worth noting that in the cases of complexes 6 and 7 there is no apparent residual ligand-based emission in the 350–450 nm region, thus
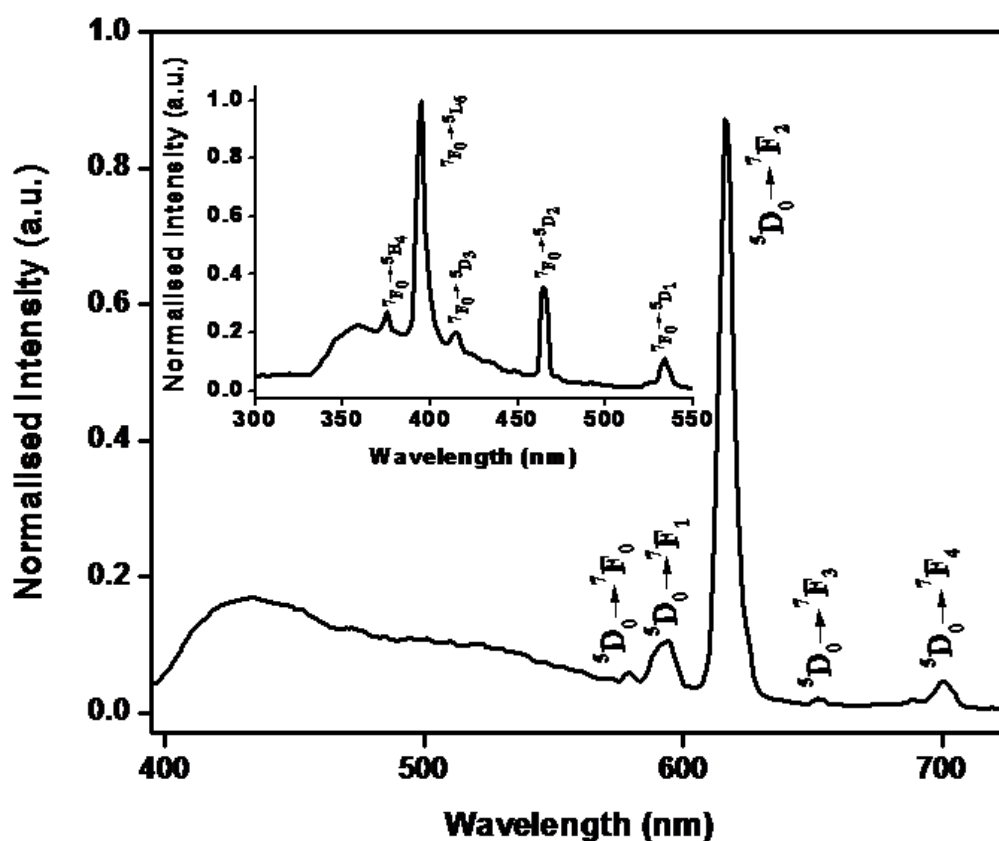
Figure 2.11. Room temperature emission spectra of complex 1, inset shows the excitation spectra of complex 1 (λ_{ex}= 355 nm).

49

implying an efficient energy transfer from the ligand excited states to the terbium f-excited states [Zhang *et al.* 2012]. However, in the case of complex 3, a residual emission due to the ligand was detected in the 350-450 nm region, thus indicating that this indirect excitation processes is not as efficient in the case of complex 3.
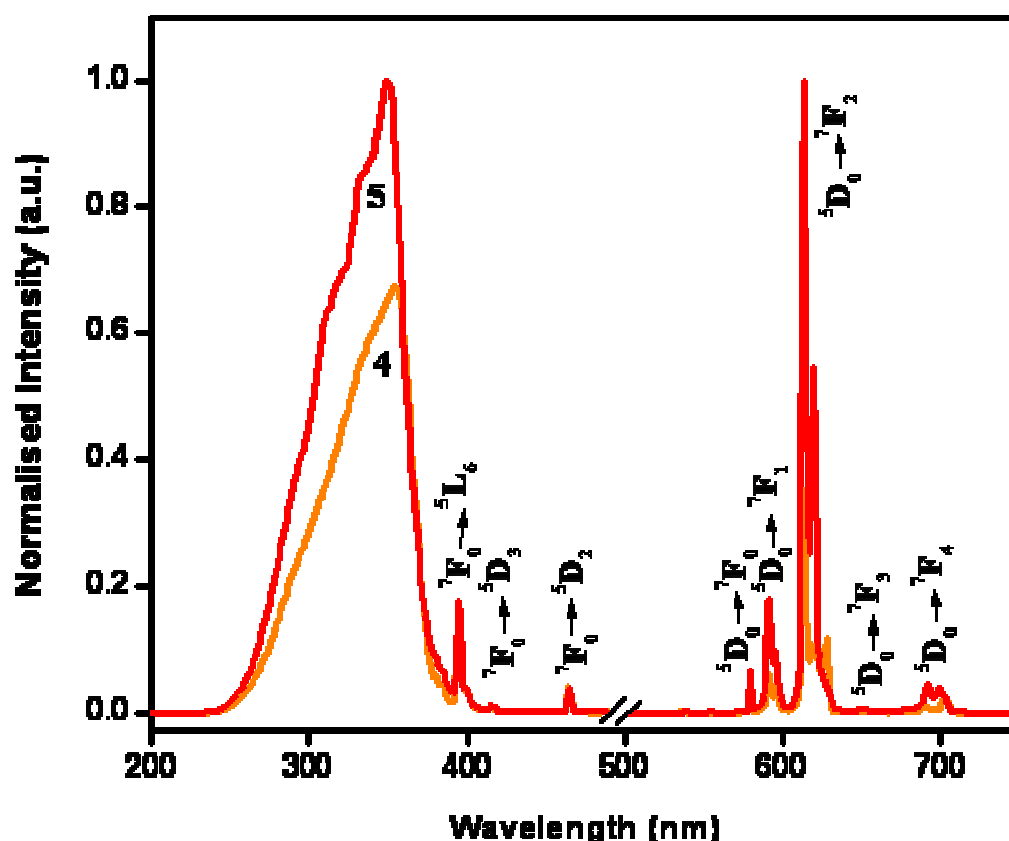
Figure 2.12. Room temperature excitation and emission spectra of complexes 4 and 5 (λ_{ex}= 355 nm).

The excited state lifetime values (τ_{obs}) for $^5D_0$ (Eu^{3+}) and $^5D_4$ (Tb^{3+}) were measured at both ambient (298 K) and low temperatures (77 K) for the Ln^{3+} complexes 1 and 3-7, by monitoring the more intense lines of the $^5D_0 \rightarrow ^7F_2$ and $^5D_4 \rightarrow ^7F_5$ transitions (Figures 2.15 and 2.16). The pertinent values are summarized in Table 2.3. The measured luminescence decays of these complexes can be described by monoexponential kinetics, which suggests that in these complexes only one species exists in the excited state. In combination with the data from the

photoluminescence intensities, the excited state lifetime values show a correlation between enhanced luminescence intensities and longer lifetime values (Table 2.3). The somewhat shorter lifetimes observed for complexes 1 and 3 in comparison with those for complexes 4-7 may be due to the existence of dominant nonradiative decay channels associated with the metal-to-metal energy transfer processes that are characteristic of polymeric complexes. Furthermore, the lifetime values for the terbium compounds at 295 K are marginally lower than the corresponding values at 77 K, thus reflecting the presence of weak, thermally activated deactivation processes in the investigated systems.
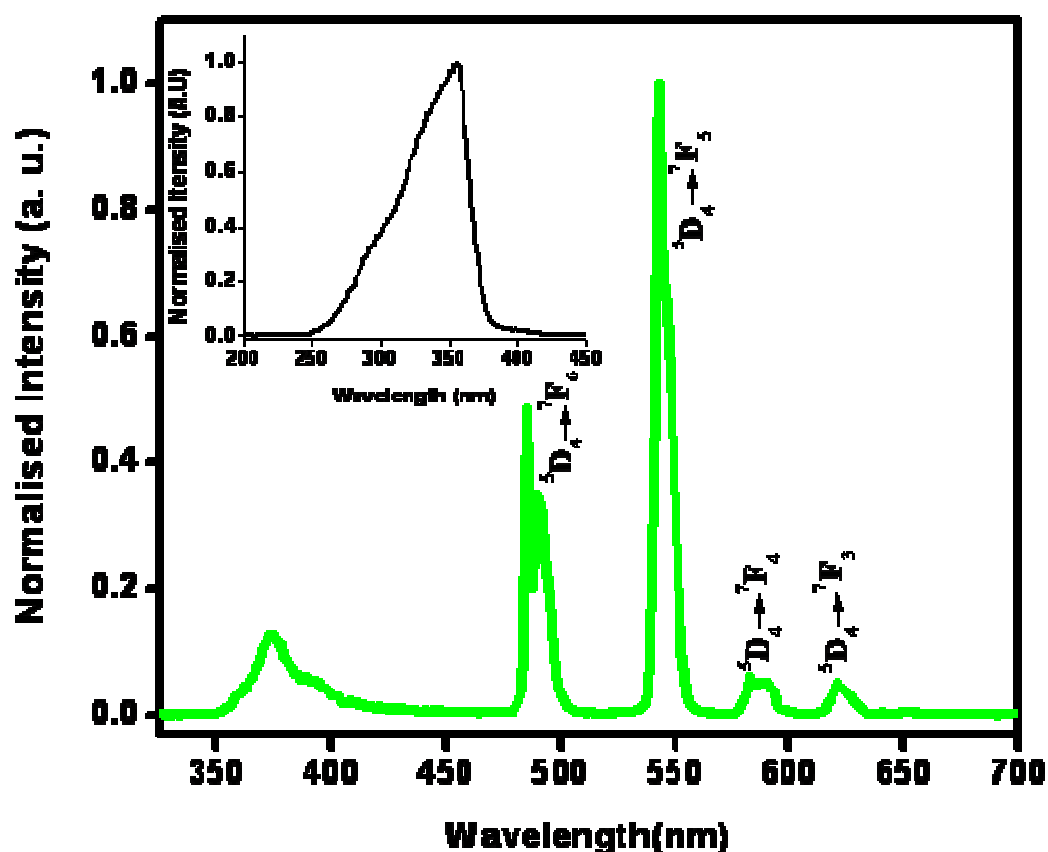
Figure 2.13. Room temperature emission spectra of complex 3, inset shows the excitation spectra of complex 3 (λ_{ex} = 355 nm).

Quantum yields and sensitisation efficiency. The photoluminescence quantum yield ($\Phi_{overall}$) is an important parameter for evaluation of the efficiencies of the emission processes in luminescent materials. The overall luminescence quantum

51

yield ($\Phi_{overall}$) can be determined experimentally by excitation of the ligand. However, this approach does not provide information regarding the independent efficiency of ligand sensitization (Φ_{sens}) or that of the lanthanide centered luminescence (Φ_{Ln}). In fact, it is a product of the ligand sensitization efficiency and the intrinsic quantum yield of the lanthanide luminescence as shown in equation (1):

$$\Phi_{sens} = \frac{\Phi_{overall}}{\Phi_{Ln}} \qquad (1)$$

The intrinsic quantum yields of europium could not be determined experimentally upon direct f–f excitation because of the very weak absorption intensity. However, these quantum yields can be estimated by using equation (2) after calculation of the radiative lifetime (τ_{rad}) [equation (3)]:

$$\Phi_{Ln} = \left(\frac{A_{RAD}}{A_{RAD} + A_{NR}}\right) = \frac{\tau_{obs}}{\tau_{RAD}} \qquad (2)$$

$$A_{RAD} = \frac{1}{\tau_{RAD}} = A_{MD,0}\, n^3 \left(\frac{I_{TOT}}{I_{MD}}\right) \qquad (3)$$

where $A_{MD,0} = 14.65$ s^{-1} represents the spontaneous emission probability of the magnetic dipole $^5D_0 \rightarrow {}^7F_1$ transition, n is the refractive index of the medium, I_{TOT} is the total integrated emission of the $^5D_0 \rightarrow {}^7F_J$ transitions, and I_{MD} represents the integrated emission of the $^5D_0 \rightarrow {}^7F_1$ transition. A_{RAD} and A_{NR} are radiative and non-radiative decay rates, respectively. The intrinsic quantum yield for Tb^{3+} (Φ_{Tb}) was estimated according to equation 4 with the assumption that the decay process at 77 K in a deuterated solvent is purely radiative [Xiao and Selvin 2001].

$$\Phi_{Tb} = \tau_{obs\,(298\,K)}\,/\,\tau_{obs\,(77\,K)} \qquad (4)$$

Table 2.3 summarizes the $\Phi_{overall}$, Φ_{Ln}, Φ_{sen}, radiative (A_{RAD}) and nonradiative (A_{NR}) decay rates. It is evident from this table that the $\Phi_{overall}$ for the europium oordination polymer is lower than that of the terbium analogue, which may be due in part to the larger energy gap ($\Delta E = {}^3\pi\pi^* - {}^5D_0 = 6673$ cm^{-1}) between the excited state level of

the Eu^{3+} cation and the triplet energy level of the ligand. On the other hand, due to the smaller energy gap between the $^5D_4$ excited state level of the Tb^{3+} cation and the triplet state of the ligand ($\Delta E = {}^3\pi\pi^* - {}^5D_4 = 3423$ cm^{-1}) complex 3 shows an improved quantum yield. However, the overall quantum yields for complexes 1 and 3 were found to be somewhat deficient due to the dominant nonradiative decay channels associated with the metal-to-metal energy transfer pathways in these polymeric species. However, incorporation of the bidentate nitrogen donors phen or tmphen breaks the coordination polymer into discreet monomeric complexes while simultaneously serving to enhance the overall quantum yields of complexes 4-7. Finally, the presence of tmphen in the cases of complexes 5 and 7 results in superior quantum yields relative to those of the phen based complexes and can be explained on the basis of the improved efficiency in energy transfer from the tmphen to the primary ligand.
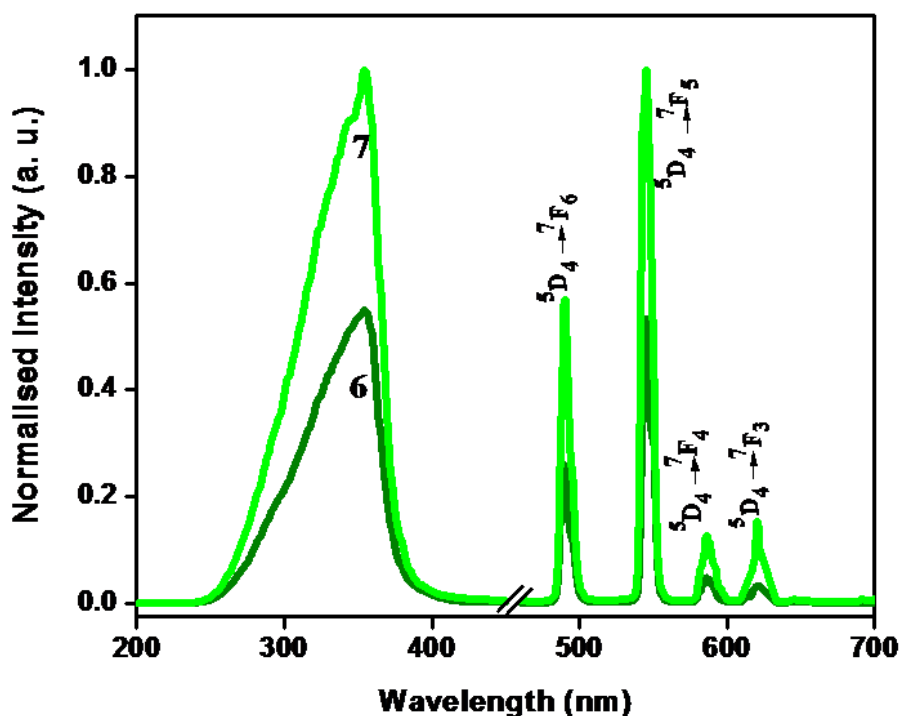
Figure 2.14. Room temperature excitation and emission spectra of complexes 6 and 7 ($\lambda_{ex} = 355$ nm).
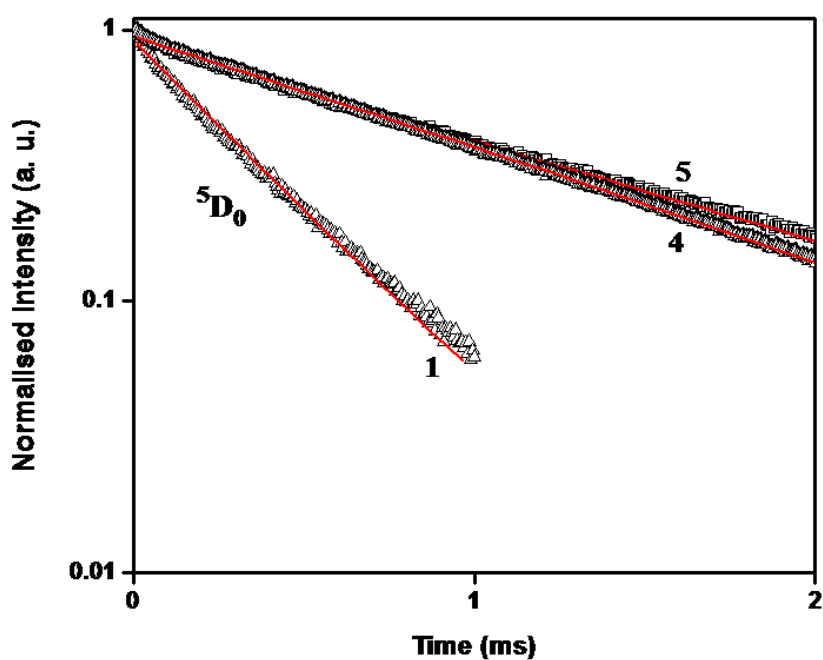
Figure 2.15. Experimental luminescence decay profiles for complexes 1, 4 and 5 monitored around 612 nm and excited at their maximum emission wave lengths.
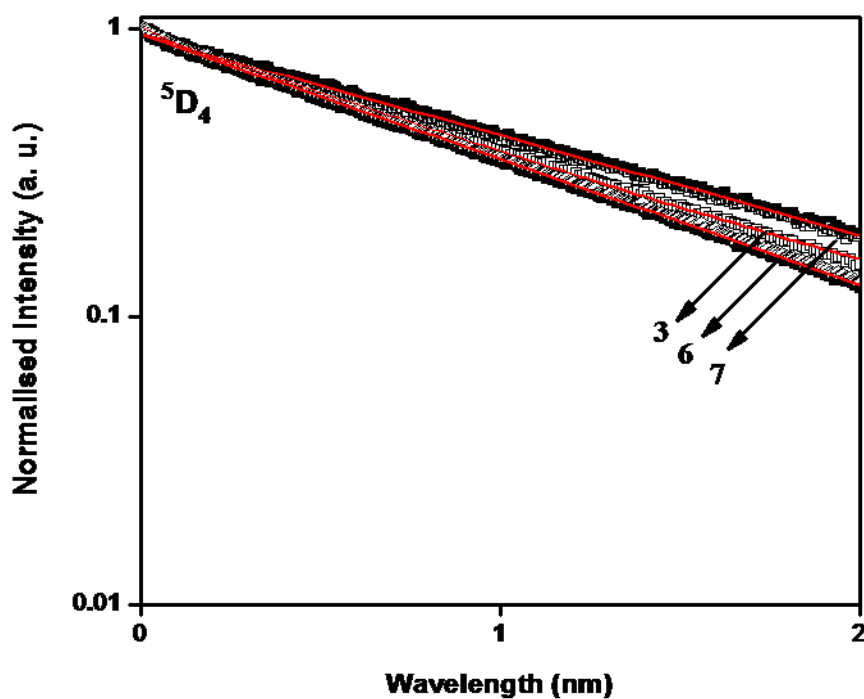
Figure 2.16. Experimental luminescence decay profiles for complexes 3, 6 and 7 monitored around 545 nm and excited at their maximum emission wave lengths.

Table 2.3. Radiative (A_{RAD}) and nonradiative (A_{NR}) decay rates, $^5D_0/^5D_4$ lifetimes (τ_{obs}), radiative lifetimes (τ_{RAD}), intrinsic quantum yields (Φ_{Ln}), energy transfer efficiencies (Φ_{sen}) and overall quantum yields ($\Phi_{overall}$) for complexes 1-7

Comp-ound	A_{RAD}/s^{-1}	A_{NR}/s^{-1}	$\tau_{obs}/\mu s$	$\tau_{RAD}/\mu s$	Φ_{Ln} (%)	Φ_{sen} (%)	$\Phi_{overall}$ (%)
1	496	2414	344 ± 10	2016 ± 20	17	0.64	0.11 ± 0.01^b
4	375	536	1098 ± 10	2666 ± 20	41	24	10.00 ± 1^a
							9.65 ± 0.9^b
5	362	488	1176 ± 10	2762 ± 20	43	49	19.10 ± 1^a
							21.00 ± 2^b
3			986 ± 10	1175 ± 10^c	62	2.32	2.00 ± 0.2^a
							1.45 ± 0.1^b
6			1006 ± 10	1225 ± 10^c	82	19	14.07 ± 1^a
							16.00 ± 1^b
7			1262 ± 10	1387 ± 10^c	88	37	33.30 ± 3^a
							32.42 ± 3^b

[a]Absolute quantum yield; [b]Relative quantum yield; [c] 77 K.

2.5. Conclusions

In summary, a unique, green luminescent solvent-free terbium coordination polymer based on the new 4-[4-(9H-carbazol-9-yl)butoxy]benzoate ligand has been synthesized and structurally authenticated by single-crystal X-ray diffraction. The polymer exhibits an unusually low coordination number for a terbium cation (CN = 6). While the reason for this rare coordination environment is unclear, it is possibly related to the steric influence that results from the bulky nature of the ligand species. Photophysical investigations revealed that the presence of bidentate nitrogen donor ligands significantly enhances the quantum yields of both the Eu^{3+} and Tb^{3+} benzoate complexes. This observation can be explained on the basis of additional energy transfer from the ancillary ligand to the carboxylate ligand in the ternary complexes 4-7, which in turn enhances the overall sensitization efficiency of the complex molecule. This result may be further explained on the basis of the minimization of nonradiative decay rates in monomeric complexes in comparison with those of polymeric species (1 and 3).

Chapter 3

Synthesis, crystal structures and photophysical properties of homodinuclear lanthanide xanthene-9-carboxylates
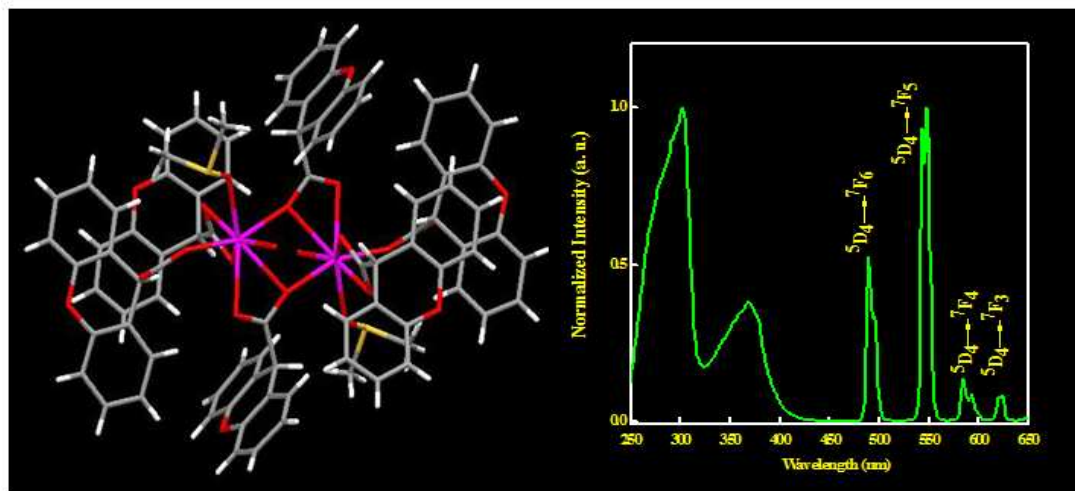
3.1. Abstract. Three new homodinuclear lanthanide(III) complexes of xanthene-9-carboxylic acid, $[Ln_2(XA)_6(DMSO)_2(H_2O)_2]$ (Ln = Eu (1), Tb (2) and Gd (3); HXA = xanthene-9-carboxylic acid; DMSO = dimethylsulfoxide), have been synthesized, of which 1 and 2 were structurally characterized by single-crystal X-ray diffraction. These compounds crystallize in the monoclinic space group $P2_1/n$ with a = 17.849(4) Å, b = 9.6537(19) Å, c = 23.127(5) Å, β = 109.06(3)°, and V = 3766.5(13) Å^3 for 1 and a = 17.809(4) Å, b = 9.6548(19) Å, c = 23.075(5) Å, β = 108.97(3)°, and V = 3752.1(13) Å^3 for 2. The crystal structures of 1 and 2 consist of homodinuclear species that are bridged by two oxygen atoms from two carboxylate ligands. The two lanthanide ions are related by a center of inversion. Each lanthanide ion is coordinated by eight oxygen atoms in an overall distorted square-prismatic geometry. Six of the oxygen atoms are furnished by the carboxylate moieties, and the remaining two oxygen atoms are provided by water and DMSO molecules. The photophysical properties of these complexes in the solid state at room temperature have been investigated. The quantum yields were found to be 0.06 ± 0.01 and $7.30 \pm 0.73\%$ for 1 and 2, respectively.

3.2. Introduction

Due to the Laporte forbidden character and intra-configurational nature of the 4*f* transitions, luminescence from lanthanide cations is typically highly monochromatic, exhibits long-lived excited state lifetimes when compared to organic compounds, and is usually insensitive to quenching by molecular oxygen, making these metal ions ideal for many applications in multidisciplinary fields such as materials for telecommunications, lighting devices, and luminescent probes for bio-analyses and live cell imaging and sensing [Kido and Okamoto 2002; de Bettencourt-Dias 2007; Brunet *et al.* 2007; Bünzli 2010]. However, the spin- and parity forbidden nature of the f-f transitions prevent direct excitation of lanthanide luminescence, these metal ions require sensitization by suitable organic chromophores [Lehn *et al.* 1990]. Accordingly, it is necessary to employ organic ligands to function as antennas by absorbing light and transferring this energy to the excited states of the central lanthanide ions [Lehn *et al.* 1990; Sabbatini *et al.*1993]. The excited lanthanide ions then undergo radiative transitions to lower energy states which results in the characteristic multiple narrow band emissions. Since the emission intensity (brightness) and the colour of the lanthanide emission both depend on the type of sensitizer employed, new sensitizing chromophores are highly sought after. As a consequence, a number of chromophoric antenna ligands have now been developed in an effort to achieve brighter Ln^{3+} luminescence. In this regard, the *β*-diketonate [Binnemans 2009; Ambili Raj *et al.* 2009; [a]Biju *et al.* 2009; Biju *et al.* 2009; Divya *et al.* 2010; Divya *et al.* 2011] and aromatic carboxylate ligands [Ramya *et al.* 2010; Sivakumar *et al.* 2010; Sivakumar *et al.* 2011] have received the most attention.

Recently, aromatic carboxylate coordination complexes that exhibit unique photophysical properties and intriguing structural features have attracted considerable interest [Eddaoudi *et al.* 2001; Pan *et al.* 2004; Teotonio *et al.* 2004; Bünzli *et al.* 2007]. For example, a series of benzoic acid derivatives [Santos *et al.* 2003; Zhang *et al.* 2003; Li *et al.* 2005; de Bettencourt-Dias and Viswanathan 2006; Fiedler *et al.* 2007; Bußkamp *et al.* 2007; Ramya *et al.* 2010; Sivakumar *et al.* 2010; Sivakumar *et al.* 2011; Lucky *et al.* 2011] and pyridine based carboxylate ligands [Chatterton *et al.* 2005; Chen and Fukuzumi 2009; Chen *et al.* 2009; de Faria *et al.*

2011] have been evaluated as possible sensitizers for europium(III) and terbium(III) luminescence.

Xanthenes are important classes of compounds that find use as dyes, fluorescent materials for visualization and laser technologies due to their useful spectroscopic properties [John *et al.* 2006; Chen *et al.* 2012]. In comparison with the aromatic carboxylic acids mentioned above, the use of xanthene-based carboxylic acids as photosensitizers for lanthanide ions are scarce.
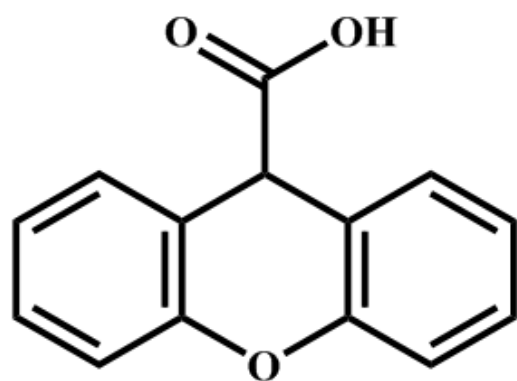
xanthene-9-carboxylic acid

Given the important potential applications of lanthanide carboxylates and the fascinating properties of these ligands, we were prompted to prepare a new series of lanthanide complexes featuring the xanthene-9-carboxylate ligand. Herein, the syntheses, characterization and photophysical properties of the homodinuclear xanthene-9-carboxylate complexes of Eu^{3+}, Tb^{3+}, and Gd^{3+} have been described.

3.3. Experimental Section

Materials and Instrumentation.

The commercially available chemicals Eu(III) nitrate hexahydrate (Acros Organics; purity 99.9%); Gd(III) nitrate hexahydrate (Acros Organics; purity 99.9%); Tb(III) nitrate hexahydrate (Acros Organics; purity 99.9%); and xanthene-9-carboxylic acid (Aldrich; purity 98%) were used without further purification. All of the other chemicals used were of analytical reagent grade. The other characterization techniques employed in the present work are as same as that described in chapter 2.

Synthesis of Homodinuclear Complexes.

An aqueous solution of $Ln(NO_3)_3 \cdot 6H_2O$ (0.5 mmol) (Ln = Eu, Tb, or Gd) was added to a solution of xanthene-9-carboxylic acid (1.5 mmol) in water in the presence of NaOH (1.5 mmol). Precipitation took place immediately, and each reaction mixture was stirred subsequently for 10 h at room temperature [Zhang *et al.* 2006] (Scheme 3.1). The product was filtered, washed with water, dried, and stored in a desiccator. The resulting complexes were then purified by recrystallization from a dimethylsulfoxide/tetrahydrofuran solvent mixture. Single crystals were obtained from a dimethylsulfoxide/tetrahydrofuran solvent mixture after storage for three weeks at ambient temperature.
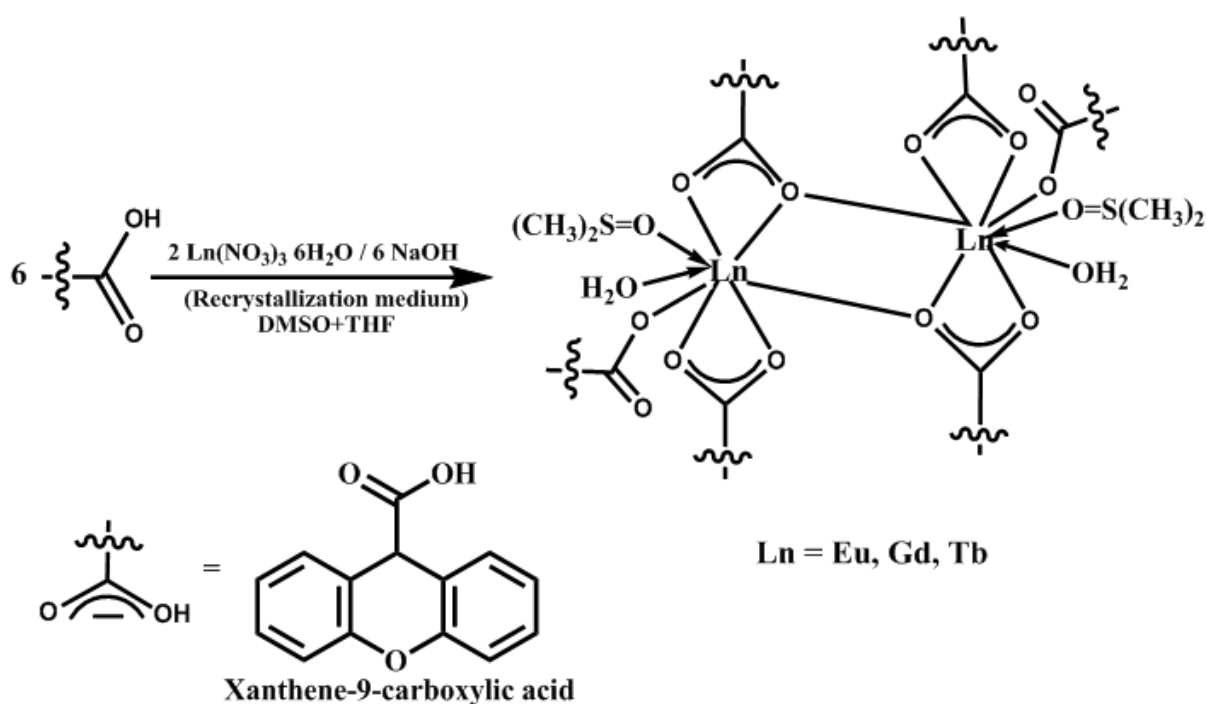
Scheme 3.1. Synthetic Route to the Homobimetallic Lanthanide Complexes.

$Eu_2(XA)_6(DMSO)_2(H_2O)_2$ (1). Elemental analysis (%): Calcd for $C_{88}H_{70}Eu_2O_{22}S_2$ (1847.56): C, 57.20; H, 3.81; S, 3.47. Found: C, 57.11; H, 3.67; S, 3.32. IR (KBr) v_{max}: 3434, 1602, 1572, 1541, 1479, 1454, 1391, 1259, 1116, 1040, 949, 749 cm^{-1}.

Tb$_2$(XA)$_6$(DMSO)$_2$(H$_2$O)$_2$ (2). Elemental analysis (%): Calcd for C$_{88}$H$_{70}$Tb$_2$O$_{22}$S$_2$ (1861.48): C, 56.78; H, 3.79; S, 3.44. Found: C, 56.66; H, 3.88; S, 3.35. IR (KBr) ν_{max}: 3351, 1602, 1572, 1542, 1483, 1453, 1405, 1260, 1034, 949, 748 cm^{-1}.

Gd$_2$(XA)$_6$(DMSO)$_2$(H$_2$O)$_2$ (3). Elemental analysis (%): Calcd for C$_{88}$H$_{70}$Gd$_2$O$_{22}$S$_2$ (1858.02): C, 56.88; H, 3.79; S, 3.45. Found: C, 56.47; H, 3.41; S, 3.41. IR (KBr) ν_{max}: 3395, 1603, 1571, 1545, 1485, 1453, 1387, 1319, 1261, 1119, 1038, 874, 749 cm^{-1}.

3.4. Results and Discussion

Synthesis and Characterization of Complexes 1-3.
The synthetic procedure for Ln^{3+} complexes 1-3 is summarized in Scheme 3.1. The elemental analysis data for 1-3 reveal that each Ln^{3+} ion has reacted with HXA in a metal-to-ligand mole ratio of 1:3. The carbonyl stretching frequencies for 1-3 appear at lower energies than that for HXA (1688 cm^{-1}), indicating that the carbonyl oxygen atoms are coordinated to the Ln^{3+} ion in each case. Furthermore, the IR spectra of 1-3 show three different values for the carbonyl stretching frequency (for 1: 1602, 1572, 1541 cm^{-1}; 2: 1602, 1572, 1542 cm^{-1}; 3: 1603, 1571, 1545 cm^{-1}) due to the fact that the xanthene-9-carboxylate ligands exhibit three different coordination modes (vide infra) [Deacon and Phillips 1980; Sivakumar *et al.* 2010; Ramya *et al.* 2010]. The broad IR band that is apparent in the 3000-3500 cm^{-1} region for 1-3 is indicative of the presence of coordinated water molecules in these complexes. Likewise, the peaks detected in the ~1030-1040 cm^{-1} region imply the presence of coordinated DMSO molecules in these complexes. These peaks are red-shifted with respect to that of unligated DMSO (1047 cm^{-1}) [Sivakumar *et al.* 2010]. It is clear from the thermogravimetric analysis data that 1-3 (Figure 3.1) undergo a mass loss of 11% (Calcd: 10.3%) up to 275 °C, which corresponds to the elimination of the coordinated solvent molecules. Further decomposition takes place in two steps, the first of these occurring between 275 and 350 °C (59% mass loss for 1, 60% for 2, and 57% for 3) and the second between 350 and 600 °C (10% mass loss for 1, 9% for 2, and 12% for 3), leaving a residue of approximately 20% for 1-3, which corresponds to the lanthanide oxides.

X-ray Structural Characterization.

The structures of $Eu_2(XA)_6(DMSO)_2(H_2O)_2$ (1) and $Tb_2(XA)_6(DMSO)_2(H_2O)_2$ (2) were determined by single-crystal X-ray diffraction. Details of the crystal data and data collection parameters are given in Table 3.1, and selected bond lengths and bond angles are listed in Table 3.2. Complexes 1 and 2 are isostructural and crystallize in the monoclinic space group $P2_1/n$. Each complex molecule is dimeric, containing two Ln^{3+} ions, surrounded by six xanthene-9-carboxylate ligands. The dimeric structure features an inversion center of symmetry indicating that the Ln(1) and Ln(1_3) centers are in equivalent chemical environments. The Ln–Ln distances are 4.108 Å (1) and 4.076 Å (2). A comparison with structures that are available in the CSD [Cambridge Structural Database, version 5.27] reveals that this distance falls within the range of 3.785-4.532 Å that has been observed for Ln^{3+} complexes that feature the bridging bidentate coordination mode.
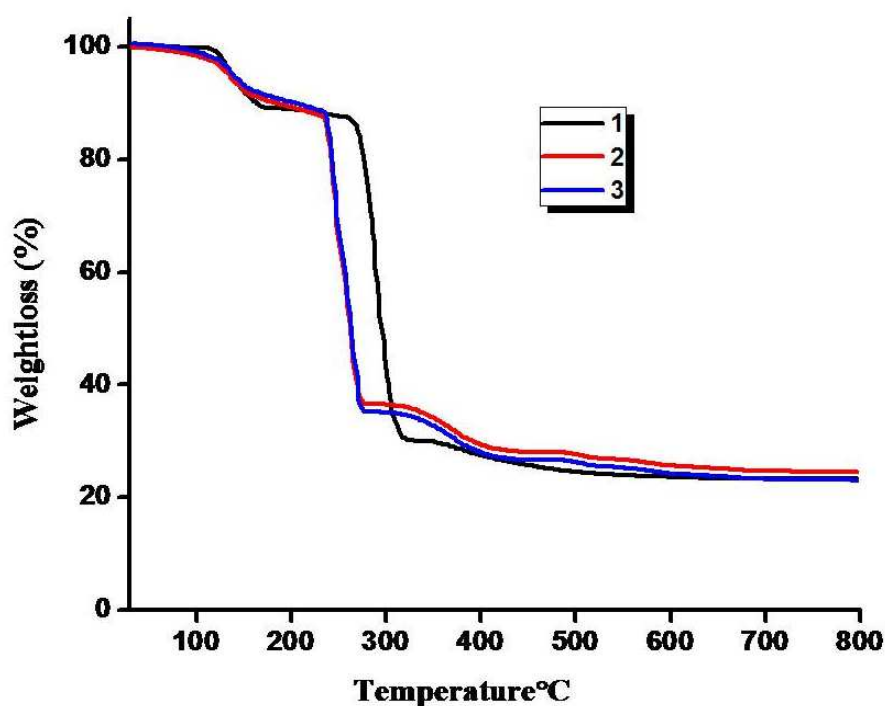
Figure 3.1. Thermo gravimetric curves for the Ln^{3+} complexes 1-3.

The ligands show three different coordination modes to the Ln ions: bidentate chelating, tridentate chelating bridging, and monodentate, thus corroborating the IR data. The asymmetric unit and coordination environments of 1 and 2 are shown in

Figures 3.2-3.5. The atoms O(1) and O(2) belong to the carboxylate ligand, which binds in a bidentate fashion to the Eu(1) ion. One carboxylate group bridges the two Eu ions in a triply coordinated manner. The other carboxylate group, O(3), binds in a monodentate mode. Different types of binding modes for the HXA ligand observed in Eu and Tb complexes 1 and 2 are shown in Figure 3.6. The coordination sphere of the metal ion is completed by water and DMSO molecules bonding via O(6) and O(9), producing a coordination number of eight at the Eu^{3+} center. The coordination polyhedra can be described as distorted square antiprisms of approximately C_{2v} symmetry in which six oxygen atoms belong to the three xanthene-9-carboxylate moieties and two oxygen atoms are provided by one water and one DMSO molecule. In 1, the Eu–O bond lengths range from 2.249 to 2.609 Å, and in 2 the Tb–O bond lengths are in the range 2.242 to 2.591 Å, which fall in the expected range for this type of complex [Zhang *et al.* 2003; Sivakumar *et al.* 2010].

Table 3.1. Crystal Data, Collection, and Structure Refinement Parameters for 1 and 2

Parameters	1	2
empirical formula	$C_{44}H_{33}EuO_{11}S$	$C_{44}H_{33}TbO_{11}S$
fw	921.72	928.68
cryst syst	monoclinic	monoclinic
space group	$P2_1/n$	$P2_1/n$
cryst size (mm^3)	$0.20 \times 0.15 \times 0.15$	$0.25 \times 0.25 \times 0.15$
temperature (K)	153(2)	153(2)
a (Å)	17.849(4)	17.809(4)
b (Å)	9.6537(19)	9.6548(19)
c (Å)	23.127(5)	23.075(5)
α (deg)	90	90
β (deg)	109.06(3)	108.97(3)
γ (deg)	90	90
V ($Å^3$)	3766.5(13)	3752.1(13)
Z	4	2
ρ_{calcd} (g cm^{-3})	1.625	1.644
μ (mm^{-1})	1.786	2.006
$F(000)$	1856	1864
R1 [$I > 2\sigma(I)$]	0.0437	0.0457
wR2 [$I > 2\sigma(I)$]	0.0900	0.1005
R1 (all data)	0.0949	0.0965
wR2 (all data)	0.1215	0.1317
GOF	1.034	1.022

Table 3.2. Selected Bond Lengths and Bond Angles for 1 and 2

	1		2
Eu1-Eu1_3[a]	4.1081(8)	Tb1-Tb1_3[a]	4.076(1)
Eu1-O1	2.531(3)	Tb1-O1	2.522(7)
Eu1-O2	2.424(3)	Tb1-O2	2.409(7)
Eu1-O3	2.249(3)	Tb1-O5	2.591(6)
Eu1-O5	2.379(3)	Tb1-O4	2.462(6)
Eu1-O5#1	2.609(3)	Tb1-O5#1	2.357(6)
Eu1-O6	2.402(3)	Tb1-O7	2.242(6)
Eu1-O7	2.475(3)	Tb1-O10	2.352(6)
Eu1-O9	2.367(3)	Tb1-O11	2.388(7)
O3-Eu1-O9	78.60(12)	O7-Tb1-O10	78.4(2)
O9-Eu1-O6	78.25(12)	O10-Tb1-O11	78.3(2)
O6-Eu1-O5#1	71.47(11)	O11-Tb1-O5#	82.6(2)
O5-Eu1-O5#1	69.20(12)	O5-Tb1-O5#	69.1(2)
O5-Eu1-O7	120.26(11)	O5-Tb1-O4	51.56(19)
O7-Eu1-O2	77.03(12)	O4-Tb1-O2	76.9(2)
O2-Eu1-O1	52.26(11)	O2-Tb1-O1	52.4(2)
O1-Eu1-O3	84.95(12)	O1-Tb1-O7	84.6(2)

[a] Eu1 and Eu1_3 and Tb1 and Tb1_3 are symmetrical metal atoms.

The longest Eu–O bonds involve the oxygen atoms of one of the triply coordinated ligands [Eu(1)–O(5) = 2.609 Å, Eu(1)–O(7) = 2.475 Å] and the shortest such bond is associated with the monodentate carboxylate ligand [Eu(1)–O(3) = 2.249 Å]. On the other hand, the Eu–O distances of the coordinated water and DMSO molecules [Eu(1)–O(6) = 2.402 Å and Eu(1)–O(9) = 2.367 Å, respectively] are shorter than those of the bidentate and tridentate xanthates. It is interesting to note that, due to the coordination of H_2O and DMSO molecules, one of the terminal carboxylate groups on each Ln center ligates in a monodentate fashion. Similar trends in bond lengths and intermetallic distances have been reported by Viswanathan and de Bettencourt-Dias for dimeric Eu^{3+} and Tb^{3+} complexes of thiophenyl-derivatized nitrobenzoate ligands [de Bettencourt Dias and Viswanathan 2006; Bußkamp *et al.* 2007; Sivakumar *et al.* 2010].
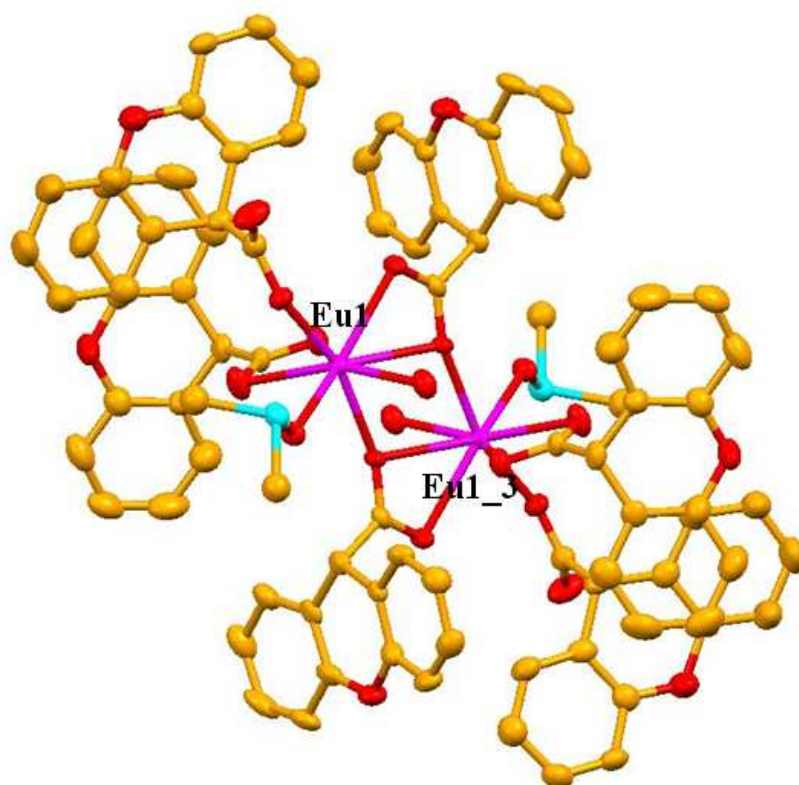
Figure 3.2. Asymmetric unit of complex 1. All of the hydrogen atoms were omitted for clarity.
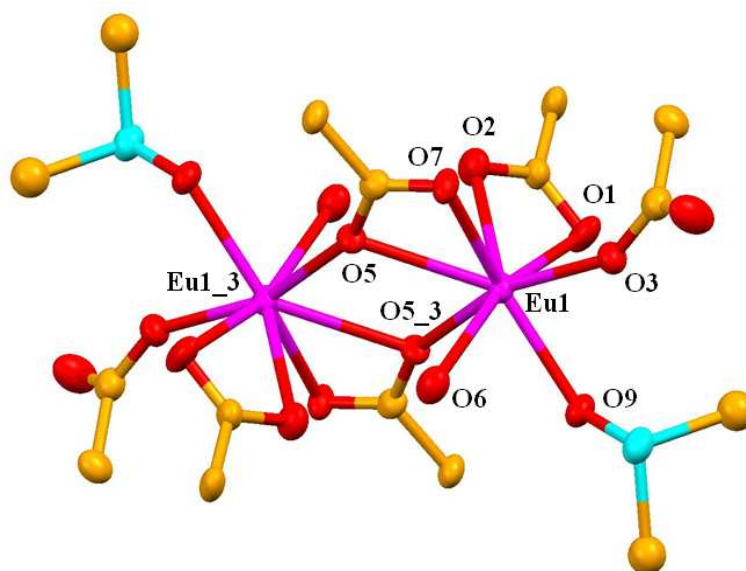
Figure 3.3. Coordination environment of the Eu^{3+} ions in 1 with partial atom-labeling scheme. All of the hydrogen atoms were omitted for clarity. Eu1 and Eu1_3 are symmetrical metal atoms.
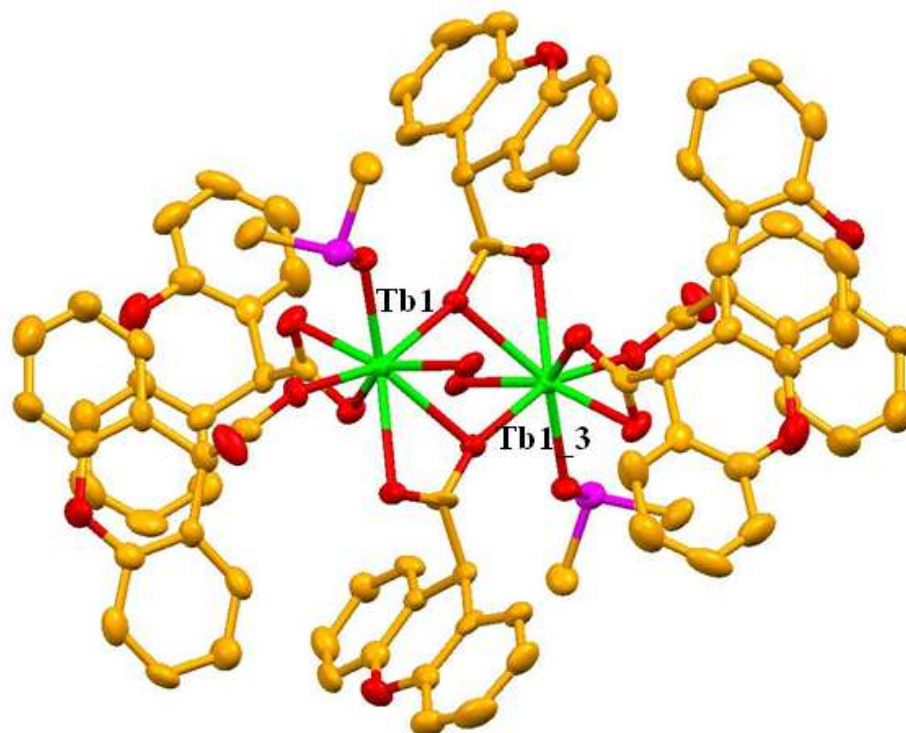
Figure 3.4. Asymmetric unit of complex 2. All of the hydrogen atoms were omitted for clarity.
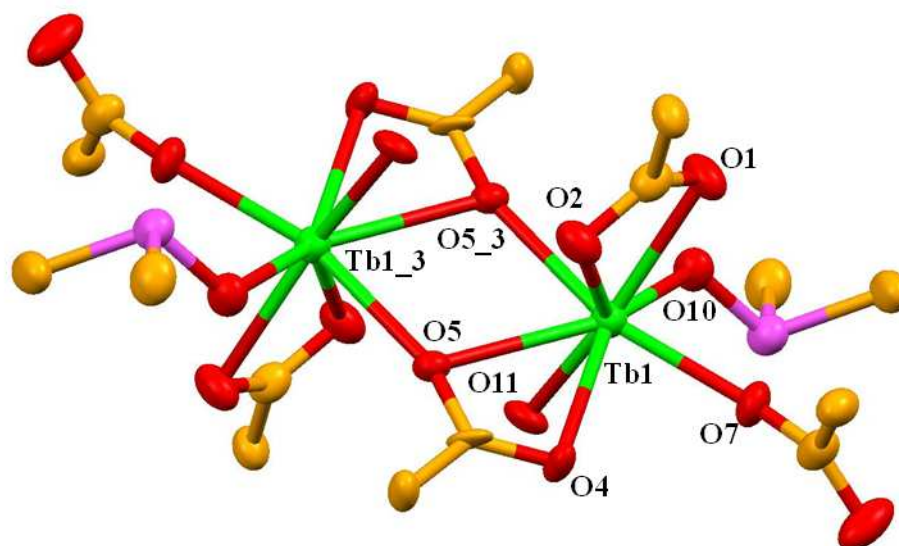
Figure 3.5. Coordination environment of the Tb^{3+} ions in 2 with partial atom-labeling scheme. All of the hydrogen atoms were omitted for clarity. Tb1 and Tb1_3 are symmetrical metal atoms.
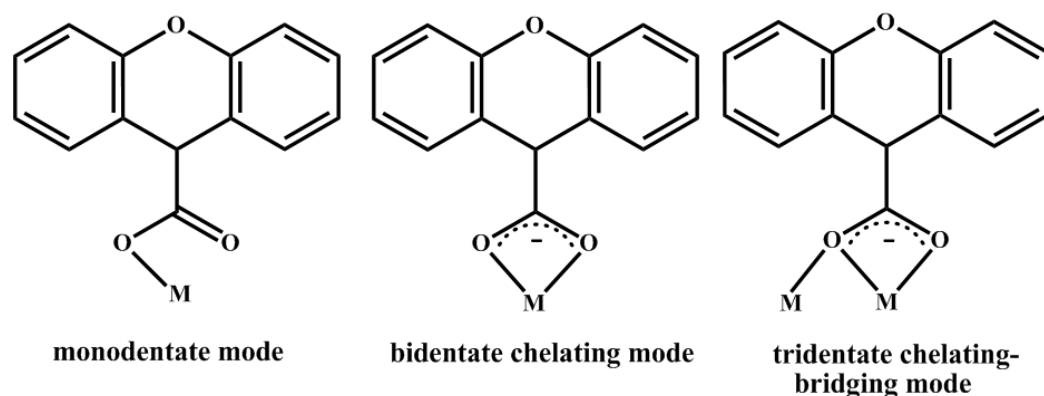
Figure 3.6. Different types of binding modes for the HXA ligand observed in Eu^{3+} and Tb^{3+} complexes 1 and 2.

UV–vis Spectra.

The UV–vis absorption spectra of the free ligand HXA and the corresponding xanthate Ln^{3+} complexes were measured in DMSO solution ($c = 1\times10^{-5}$ M), and are displayed in Figure 3.7. The absorption maxima for 1 (290 nm), 2 (290 nm), and 3 (289 nm), which are attributable to singlet–singlet $^1\pi-\pi^*$ absorptions of the aromatic rings, are slightly red-shifted with respect to that of the free ligand HXA ($\lambda_{max} = 287$ nm). The shapes of the spectral bands for the complexes are similar to that of the free ligand, suggesting that the coordination of the Ln^{3+} ion does not have a significant influence on the $^1\pi-\pi^*$ transition. However, a small red shift observed in the absorption maximum of each complex is a consequence of the enlargement of the conjugate structure of the ligands after coordination to the lanthanide ion. The molar absorption coefficient values (ε) for 1–3 at λ_{max} are 1.67×10^4, 1.74×10^4, and 1.69×10^4 L mol^{-1} cm^{-1}, respectively, which are about six times than that of HXA (2.85×10^3 L mol^{-1} cm^{-1} at 287 nm), indicating the presence of six xanthate ligands per homodinuclear lanthanide complex. Furthermore, the large molar absorption coefficient for HXA indicates that the carboxylic acid ligand has a strong ability to absorb light.

PL Properties of Complexes 1 and 2.

The normalized steady-state excitation and emission spectrum of homodinuclear europium complex 1 (in the solid state) at room temperature is shown in Figure 3.8. The excitation spectrum of 1 exhibits a series of sharp lines characteristic of the Eu^{3+} energy-level structure, and can be assigned to transitions between the $^7F_{0,1}$ and $^5L_6$, $^5D_{3,2,1}$ levels [Dieke 1968; Carnall 1987; Steemers *et al.* 1995; Pavithran *et al.* 2005; Pavithran *et al.* 2006; Biju *et al.* 2006; Aebischer *et al.* 2009].
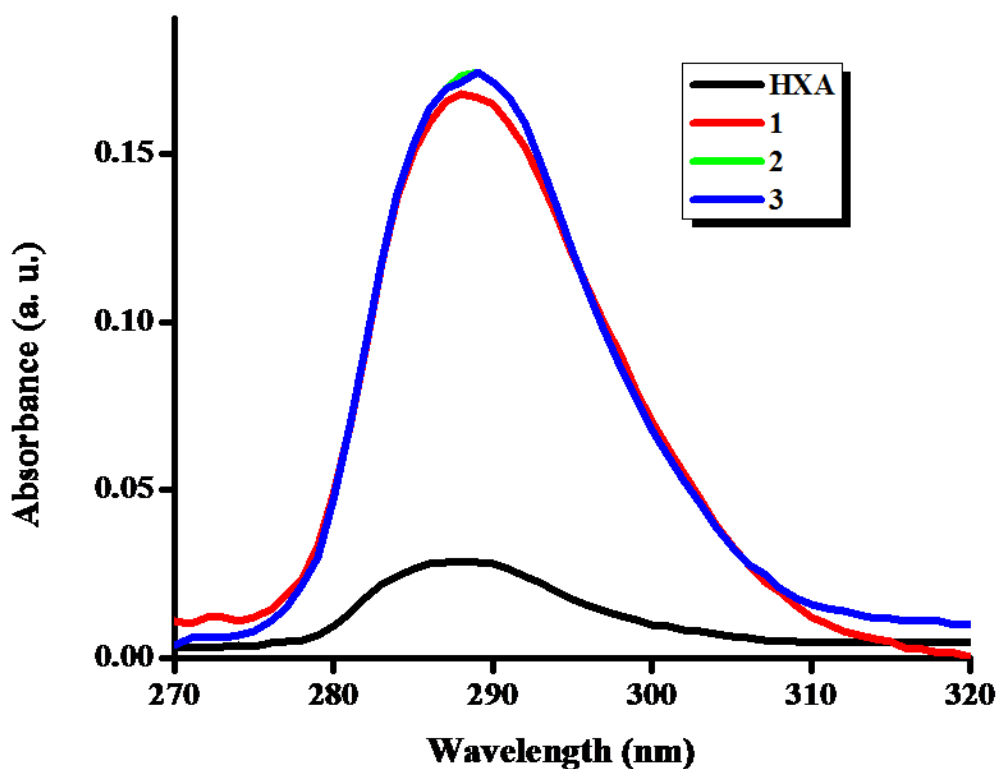
Figure 3.7. UV–visible absorption spectra of xanthene-9-carboxylic acid (HXA) and 1-3 in DMSO solution ($c = 1 \times 10^{-5}$ M).

A weak, broad band between 250 and 450 nm is also evident. This transition is less intense than the 4f absorption of the europium ion, which proves that luminescence sensitization via excitation of the ligand is not efficient in 1. The ambient temperature emission spectrum of 1 ($\lambda_{ex} = 362$ nm) displays characteristically sharp peaks in the 575–725 nm region, which are associated with the $^5D_0 \rightarrow {}^7F_{0-4}$ transitions of the Eu^{3+} ion [Carnall 1987; Dieke 1968; Pavithran *et al.* 2005; Biju *et al.* 2006]. The five peaks that are anticipated for the $^5D_0 \rightarrow {}^7F_{0-4}$ transitions are well resolved,

and the hypersensitive $^5D_0 \rightarrow ^7F_2$ transition is very intense, pointing to a highly polarisable chemical environment around the Eu^{3+} ion. The presence of only one line for the $^5D_0 \rightarrow ^7F_0$ transition strongly indicates the existence of only one coordination site for the Eu^{3+} cations, as this transition occurs between nondegenerated levels.
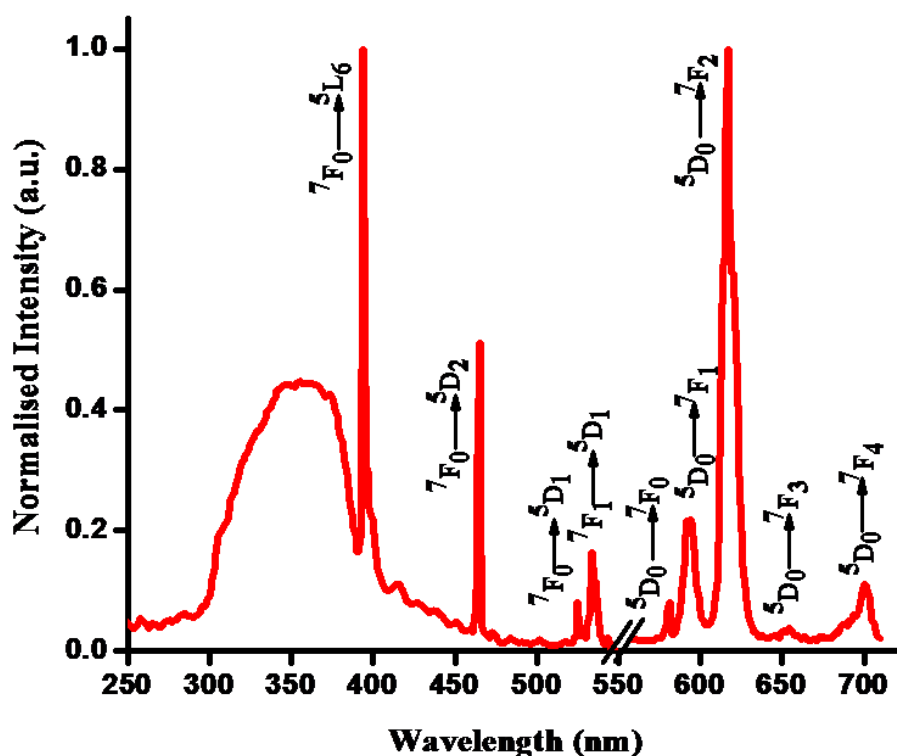
Figure 3.8. Room-temperature (300K) excitation and emission spectra for 1 ($\lambda_{ex}=$ 362 nm) with emissions monitored at approximately 613 nm.

The excitation spectrum of terbium complex 2, monitored around the peak of the intense $^5D_4 \rightarrow ^7F_5$ transition of the Tb^{3+} ion, exhibits a broad band between 250 and 450 nm with a maximum at approximately 302 and a shoulder at 360 nm (Figure 3.9). The peak at 302 nm can be assigned to the $^1\pi-\pi^*$ transition of the aromatic ring, and the shoulder at 360 nm is attributable to the $^1\pi-\pi^*$ transition of the carbonyl group of the HXA ligand. The room-temperature normalized emission spectra of terbium complex 2 exhibit the characteristic emission bands for Tb^{3+} (λ_{ex} = 302 nm) centered at 490, 545, 585, and 620 nm, which result from deactivation of the $^5D_4$ excited state to the corresponding ground state ^7F_J (J = 6, 5, 4, 3) of the Tb^{3+}

ion (Figure 3.9). The most- intense emission is centered at 545 nm and corresponds to the hypersensitive transition $^5D_4 \rightarrow ^7F_5$ [Dieke 1968; Carnall 1987; Biju *et al.* 2009; Remya *et al.* 2008; Sivakumar *et al.* 2010; Ramya *et al.* 2010].
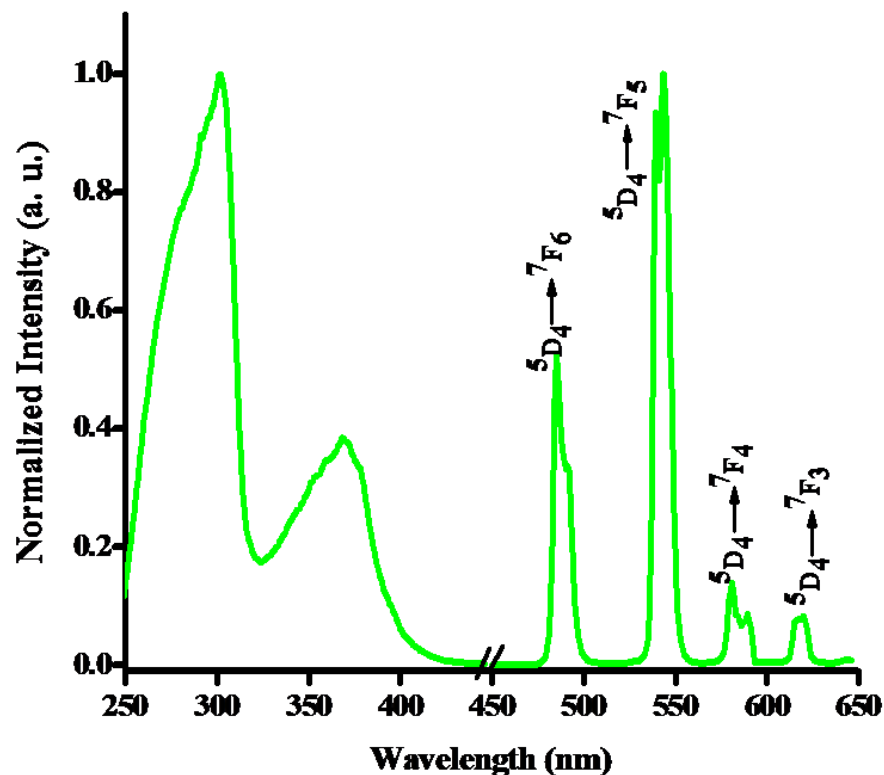
Figure 3.9. Room-temperature (300 K) excitation and emission spectra for 2 (λ_{ex} = 302 nm) with emissions monitored at approximately 545 nm.

The overall quantum yield ($\Phi_{overall}$) for a lanthanide complex treats the system as a black box in which the internal process is not explicitly considered. Given that the complex absorbs a photon (i.e., the antenna is excited), the overall quantum yield can be defined as [Xiao and Selvin 2001; Charbonniere *et al.* 2004; Quici *et al.* 2005]

$$\Phi_{overall} = \Phi_{transfer}\Phi_{Ln} \qquad (2)$$

Here, $\Phi_{transfer}$ is the efficiency of energy transfer from the ligand to Ln^{3+}, and Φ_{Ln} represents the intrinsic quantum yield of the lanthanide ion. The overall quantum

yields ($\Phi_{overall}$) for lanthanide complexes 1 and 2 were found to be 0.06 ± 0.01 and $7.30 \pm 0.73\%$, respectively. The lifetime value for the $^5D_4$ level of 2 ($\tau = 1.11 \pm 0.01$ ms) was determined from the luminescence decay profile at room temperature by fitting with a monoexponential curve. A typical decay profile for 2 is shown in Figure 3.10. On the other hand, a shorter lifetime was observed for 1 ($\tau = <10~\mu$s). The observed quantum yield and lifetime values, especially those for the homodinuclear terbium complex, were found to be promising, as compared to those reported recently for a homodinuclear terbium complex of nitrobenzoic acid ($\Phi = 3.14~\%$ and $\tau = 666.7 \pm 28.5~\mu$s in methanol solution) [de Bettencourt-Dias and Viswanathan 2006] and a homodinuclear terbium complex of thiophene carboxylic acid ($\tau = 230~\mu$s in solid state) [Teotonio *et al.* 2004].
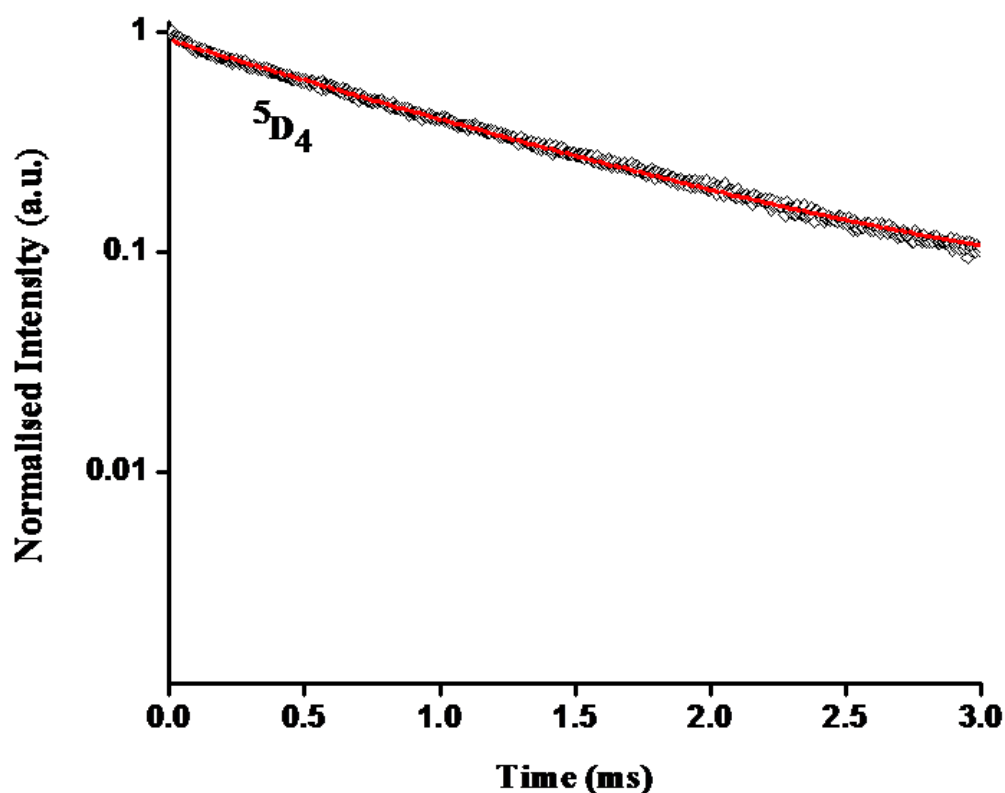
Figure 3.10. Luminescence decay profile of 2 excited at 302 nm and monitored at approximately 545 nm. The straight lines are the best fits ($r^2 = 0.99$) considering single-exponential behaviour.

Energy Transfer between the Ligand and Ln^{3+}.

To demonstrate the energy transfer process, the phosphorescence spectrum of Gd$_2$(XA)$_6$(DMSO)$_2$(H$_2$O)$_2$ was measured for the triplet energy-level data of HXA. From the phosphorescence spectra (Figure 3.11), the triplet energy level ($^3\pi\pi*$) of Gd$_2$(XA)$_6$(DMSO)$_2$(H$_2$O)$_2$, which corresponds to its lower wavelength emission edge, is 25839 cm^{-1} (387 nm). Because the lowest excited state, $^6P_{7/2}$, of Gd^{3+} is too high to accept energy from the ligand, the data obtained from the phosphorescence spectra actually reveal the triplet energy level of HXA in lanthanide complexes [Li *et al.* 2005; Xin *et al.* 2004]. The singlet state energy ($^1\pi\pi*$) level of HXA is estimated by referencing its upper absorbance edge, which is 32573 cm^{-1} (307 nm).
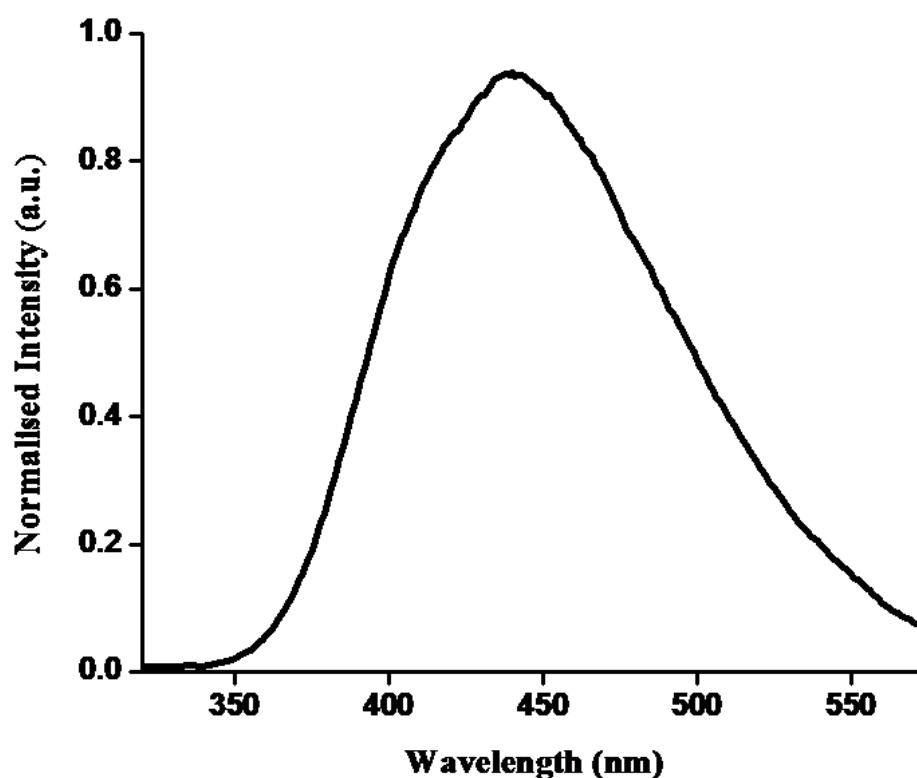
Figure 3.11. Phosphorescence spectrum of Gd$_2$(XA)$_6$·2DMSO·2H$_2$O at 77 K.

In general, the sensitization pathway in luminescent europium complexes consists of excitation of the ligands into their excited singlet states, subsequent intersystem crossing of the ligands to their triplet states, and energy transfer from the triplet state

to the ^5D_J manifold of the Eu^{3+} ions, followed by internal conversion to the emitting $^5D_0$ state. Finally, the Eu^{3+} ion emits when a transition to the ground state occurs [Pavithran *et al.* 2005; Li *et al.* 2005; Pavithran *et al.* 2006]. Moreover, electron transition from the higher excited states, such as $^5D_3$ (24800 cm^{-1}), $^5D_2$ (21200 cm^{-1}), and $^5D_1$ (19000 cm^{-1}), to $^5D_0$ (17500 cm^{-1}) becomes feasible by internal conversion, and most of the photophysical processes take place in this orbital. Consequently, most europium complexes give rise to typical emission bands at ~581, 593, 614, 654, and 702 nm, corresponding to the deactivation of the $^5D_0$ excited state to the ^7F_J ground states ($J = 0–4$). In a similar way, the 4f electrons of the Tb^{3+} ion are excited to the ^5D_J ion manifold from the ground state. Finally, the Tb^{3+} ion emits when the 4f electrons undergo a transition from the excited-state of $^5D_4$ to the ^7F_J ground states ($J = 6–3$). The energy level diagram based on the present results and the possible energy transfer pathways for the lanthanide homodinuclear complexes are shown in Figure 3.12.
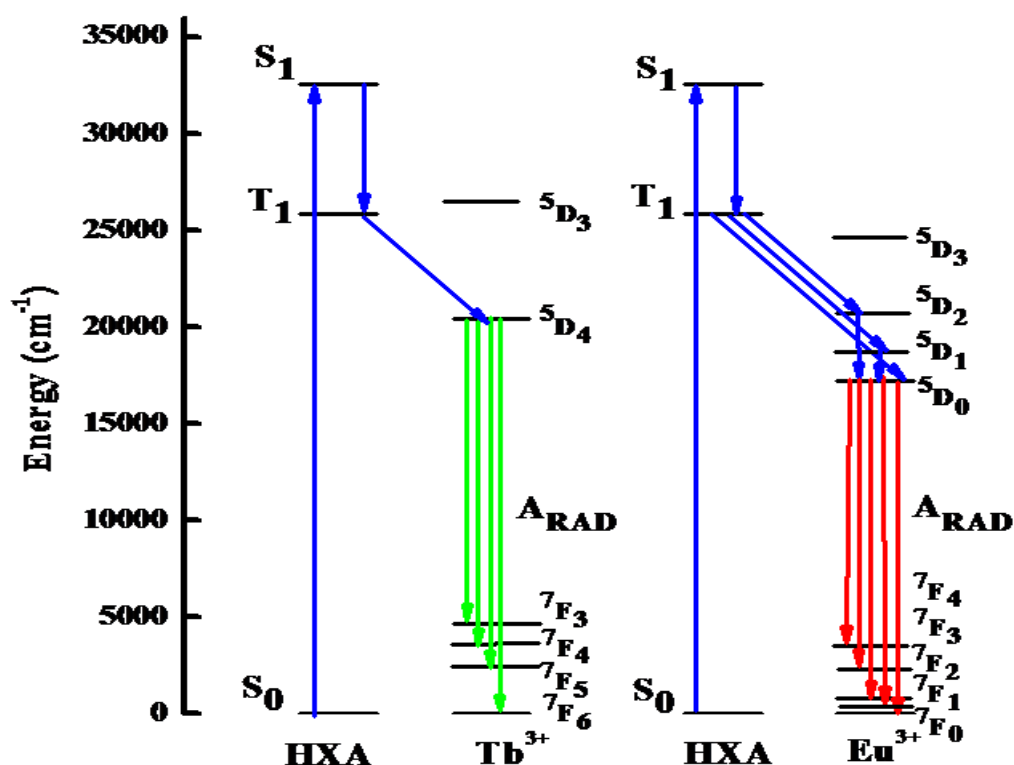
Figure 3.12. Schematic energy level diagrams and energy transfer processes for 1 and 2. S_1 represents the first excited singlet state and T_1 represents the first excited triplet state.

The gap between the $^3\pi\pi^*$ and $^1\pi\pi^*$ states ($\Delta E = {}^1\pi\pi^* - {}^3\pi\pi^* = 6734$ cm^{-1}) of xanthene-9-carboxylic acid is favorable for a relatively efficient intersystem crossing process [Steemers *et al.* 1995; Bünzli and Piguet 2001]. Latva's empirical rule [Latva *et al.* 1997] states that an optimal ligand-to-metal energy transfer process for Ln^{3+} needs ΔE ($^3\pi\pi^* - {}^5D_J$) = 2500–4000 cm^{-1} for Eu^{3+} and 2500-4500 cm^{-1} for Tb^{3+}. The triplet energy level of xanthene-9-carboxylic acid (25839 cm^{-1}) is higher than the $^5D_0$ level of Eu^{3+} (17250 cm^{-1}) and the $^5D_4$ level of Tb^{3+} (20400 cm^{-1}). This therefore supports the observation of stronger sensitization of the terbium complexes than the europium complexes because of the smaller overlap between the ligand triplet and europium ion excited states.

3.5. Conclusions

A series of new lanthanide complexes (Eu^{3+}, Tb^{3+}, and Gd^{3+}) of xanthene-9-carboxylic acid have been synthesized, two of which were structurally characterized. The X-ray crystal structures indicate that the Eu^{3+} and Tb^{3+} complexes are dimeric and bridged by two carboxylate ions. The coordination polyhedra can be described as distorted square antiprisms of approximately C_{2V} symmetry in which six oxygen atoms belong to the three xanthene-9-carboxylate moieties, and two oxygen atoms are provided by one water and one DMSO molecule. Interestingly, three different carboxylate coordination modes were evident at each Ln^{3+} ion. Relatively short Ln$\cdots$Ln distances were observed in these complexes due to the presence of triply coordinated carboxylates as bridging entities. Luminescence studies demonstrated that the xanthene-9-carboxylate ligand exhibits a good antennae effect with respect to the Tb^{3+} ion due to efficient intersystem crossing (ΔE ($^1\pi\pi^* - {}^3\pi\pi^*$) = 6734 cm^{-1}) and ligand-to-metal energy transfer. The triplet state of the xanthene-9-carboxylate ligand is located at ~25839 cm^{-1}, which results in a sizable sensitization of the Tb^{3+}-centered luminescence (quantum yield 7.30 ± 0.73%; lifetime 1.11 ± 0.01 ms), whereas the luminescence of Eu^{3+} is only poorly sensitized (quantum yield 0.06 ± 0.01%; lifetime <10 μs). Thus, the present results demonstrate that the xanthene-9-carboxylic acid complex of Tb^{3+} may find potential applications as a light conversion molecular device in many photonic applications.

Chapter 4

2-Thiopheneacetato-based one-dimensional coordination polymer of Tb^{3+}: Enhancement of terbium-centered luminescence in the presence of bidentate nitrogen donor ligands
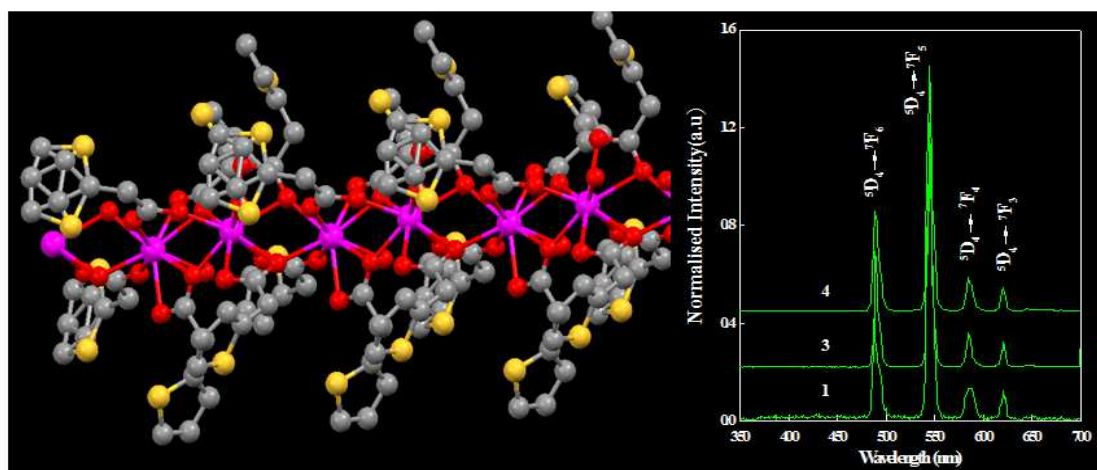
4.1. Abstract. Four new lanthanide(III) complexes of 2-thiopheneacetic acid (HTPAC), [Tb(TPAC)$_3$·H$_2$O]$_n$ (1), [Gd(TPAC)$_3$·H$_2$O]$_n$ (2), [Tb(TPAC)$_3$(phen)]$_2$ (3) and [Tb(TPAC)$_3$(bath)]$_2$ (4) (phen = 1,10-phenanthroline; bath = bathophenanthroline) have been synthesized and characterized by various spectroscopic techniques. The X-ray structure of 1 reveals that each Tb^{3+} ion is connected to two neighboring ions by six thiopheneacetic acid ligands via the carboxylate groups to form an infinite one-dimensional coordination polymer. The unit cell contains only one independent crystallographic site for the Tb ions. The carboxylate groups of the six molecules of the thiopheneacetate ligands are coordinated in both bidentate bridging and tridentate chelate-bridging modes. Each Tb^{3+} ion is coordinated by nine oxygen atoms in an overall distorted tricapped trigonal-prismatic geometry. Eight of the oxygen atoms are furnished by the carboxylate moieties, and the remaining oxygen atom is provided by the water molecule. The photophysical properties of these complexes in the solid state at room temperature have been investigated. The quantum yields of 3 (4.43 ± 0.44%) and 4 (9.06 ± 0.90%) were found to be significantly enhanced by the presence of the bidentate nitrogen donor ligands in comparison with that of 1 (0.07 ± 0.01%) due to effective energy transfer from the secondary ligands.

4.2. Introduction

The choice of ligand for the so-called "antenna effect" plays a key role in constructing efficient luminescent lanthanide complexes. Two important requirements to be considered in selecting an "antenna" ligand are the strength of binding to the lanthanide metal and the ultraviolet (UV) absorption properties of the ligand. Among a host of organic ligands, carboxylate ligands are hard Lewis bases and are known to bind to Ln^{3+} ions strongly [Lehn *et al.* 1990; Sabbatini *et al.* 1993]. Moreover, such carboxylate groups absorb UV radiation strongly and the absorbed energy is transferred efficiently to the lanthanide metal center. The enhanced stability is of obvious practical importance in terms of device performance [Eddaoudi *et al.* 2001; Pan *et al.* 2004; Chen *et al.* 2007; Sivakumar *et al.* 2010].

In particular, ligands containing five-membered heterocycles, such as the anions 2-thiophene carboxylate (TPC), 2-thiophene acetate (TPAC) and 2-furane carboxylate (FUR), are excellent complexing agents, presenting three possible sites of coordination to metal ions, one from the S (TPC and TPAC) or O (FUR) of the heterocyclic group and two from the carboxylate group [Zhang *et al.* 2002; Zhang *et al.* 2003; Teotonio *et al.* 2004; Chen *et al.* 2004; Teotonio *et al.* 2005]. However, owing to the hard acid behaviour of the Ln^{3+} ions, there is a strong affinity of these metal ions for hard base, negatively charged carboxylate oxygen donors. In most Ln^{3+}-coordination compounds reported with TPC and FUR, the carboxylate groups are involved in the metal–ligand bonding by chelating and bridging coordination modes, forming dinuclear, polymeric or network structures [Teotonio *et al.* 2005].

It has been recognized that thiophene-derivatization in nitrobenzoic and isophthalic acids exhibited enhanced terbium-centered luminescence as compared to unsubstituted ligands [de Bettencourt-Dias 2005; Viswanathan and de Bettencourt-Dias 2006]. A preliminary study by Malta and co-workers [Teotonio *et al.* 2005] demonstrated that thiophene acetic acid (HTPAC) can be used as a potential sensitizer for lanthanide emissions. However, to the best of our knowledge, systematic investigations of the luminescent properties of terbium thiophene acetate complexes in the presence of bidentate nitrogen donors and the structural characterization of such complexes by single-crystal X-ray diffraction have not been

reported previously. This has prompted us to synthesize a series of terbium complexes featuring the thiophene acetic acid ligand. This chapter discloses the syntheses, characterization and photophysical properties of three terbium thiophene acetate complexes that also involve the coordination of bidentate nitrogen donors. The Tb^{3+}-thiophene acetate aqua complex was structurally characterized by single-crystal X-ray diffraction.
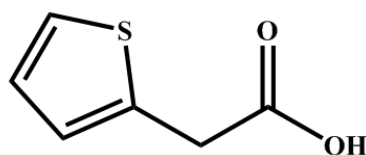
2-thiophene acetic acid

4.3. Experimental section

Materials and Instrumentation.

The commercially available chemicals terbium(III) nitrate hexahydrate (Acros Organics; purity 99.9%); gadolinium(III) nitrate (Acros Organics; purity 99.9%); 2-thiopheneacetic acid (Aldrich; purity 98%); 1,10-phenanthroline monohydrate (Merck; purity 99.5%); 4,7-diphenyl-1,10-phenanthroline (Aldrich; purity 97%); were used without further purification. All the other chemicals used were of analytical reagent grade. The mass spectra were recorded on a JEOL JSM 600 fast atom bombardment (FAB) high resolution mass spectrometer (FAB-MS). The other spectroscopic techniques employed for the characterization of the complexes 1-4 are same as that described in the previous chapter.

Syntheses of Complexes 1 and **2.**

An ethanolic solution of Ln(NO$_3$)$_3$·6H$_2$O (0.5 mmol) (Ln = Tb or Gd) was added to a solution of HTPAC (1.5 mmol) in ethanol in presence of NaOH (1.5 mmol). The resulting reaction mixture was stirred for 24 h at room temperature (Scheme 4.1). After one week colorless crystals of X-ray diffraction quality were obtained.

[Tb(TPAC)₃·H₂O]ₙ (1): Elemental analysis (%): Calcd for $C_{18}H_{17}O_7S_3Tb$ (600.45): C, 36.00; H, 2.85; S, 15.98. Found: C, 36.24; H, 2.79; S, 15.84. IR (KBr): ν_{max} = 3451, 1630, 1554, 1412, 1384, 1274, 1252, 1127, 1034, 945, 700 cm⁻¹.

[Gd(TPAC)₃·H₂O]ₙ (2): Elemental analysis (%): Calcd for $C_{18}H_{17}GdO_7S_3$ (598.76): C, 36.10; H, 2.86; S, 16.06. Found: C, 36.42; H, 2.66; S, 15.84. IR (KBr): ν_{max} = 3412, 1607, 1557, 1486, 1426, 1381, 1281, 1105, 696 cm⁻¹.
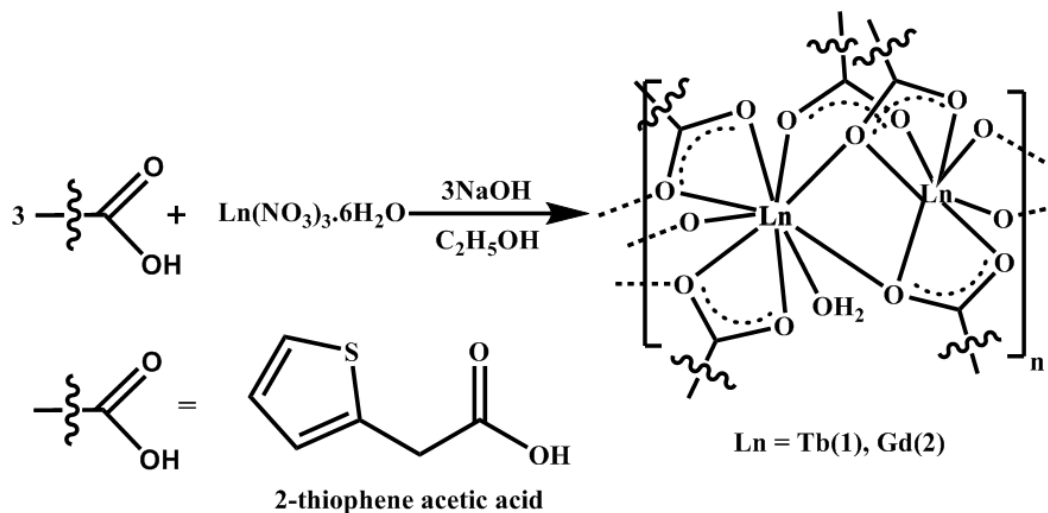
Scheme 4.1. Synthetic Route to the Lanthanide Complexes 1 and 2.

Syntheses of Complexes 3 and 4.

An ethanolic solution of $Tb(NO_3)_3\cdot6H_2O$ (0.25 mmol) and 1,10-phenanthroline or bathophenanthroline (0.25 mmol) were added to an aqueous solution of HTPAC (0.75 mmol) in the presence of NaOH (0.75 mmol). Precipitation takes place immediately and the reaction mixture was stirred at room temperature for 10 h (Scheme 4.2). The solid produced was isolated by filtration, washed with water, followed by ethanol, then dried and stored in a desiccator.

Tb₂(TPAC)₆(phen)₂ (3): Elemental analysis (%): Calcd for $C_{60}H_{46}N_4O_{12}S_6Tb_2$ (1524.01): C, 47.24; H, 3.03; N, 3.67; S, 12.61. Found: C, 46.92; H, 2.95; N, 3.78; S, 12.58. IR (KBr): ν_{max} = 3411, 1610, 1591, 1563, 1517, 1427, 1401, 1348, 1276, 1247, 1103, 923, 848 cm⁻¹. m/z = 1524.01 (M⁺).

Tb$_2$(TPAC)$_6$(bath)$_2$ (4): Elemental analysis (%): Calcd for C$_{84}$H$_{62}$N$_4$O$_{12}$S$_6$Tb$_2$ (1829.68): C, 55.14; H, 3.41; N, 3.06; S, 10.51. Found: C, 54.83; H, 3.27; N, 3.01; S, 10.58. IR (KBr): ν_{max} = 3435, 1619, 1560, 1520, 1492, 1428, 1393, 1357, 1279, 1180, 1091, 935, 853 cm^{-1}. *m/z* = 1829.96 [M$^+$]. Unfortunately, all efforts to grow single crystals of complexes 2-4 were unsuccessful.
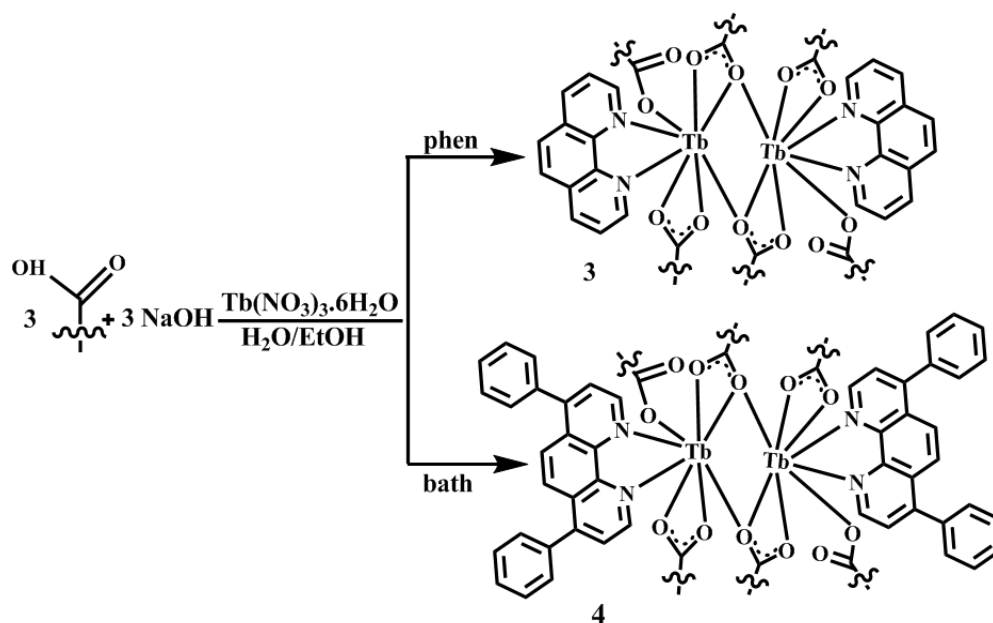
Scheme 4.2. Synthetic Route to the Lanthanide Complexes 3 and 4.

4.4. Results and Discussion

Synthesis and Characterization of Complexes 1-4.

The synthetic procedures for Ln^{3+} complexes 1-4 are summarized in Schemes 4.1 and 4.2. The elemental analysis and spectroscopic data for 1 and 2 indicate that Ln^{3+} ion has reacted with HTPAC in a metal-to-ligand mol ratio of 1:3. On the other hand, the microanalyses and FAB-MS studies of the compounds 3 and 4 revealed that Tb^{3+} ion has reacted with HTPAC in a metal-to-ligand mol ratio of 2:6 along with two molecules of the bidentate nitrogen ligand. Similar binuclear terbium carboxylate complexes, namely [Tb(2-FBA)$_3$·2,2'-bpy]$_2$ and [Tb(2-FBA)$_3$·phen]$_2$ (2-FBA = 2-fluorobenzoate), which also feature bidentate nitrogen donors have been reported elsewhere and characterized by means of single-crystal X-ray analysis [Li

et al. 2005]. In order to investigate the coordination modes of the HTPAC anion to the Ln^{3+} ion, the IR spectra of 1-4 were compared with that of the HTPAC ligand. The FT-IR spectrum of the HTPAC ligand evidences two intense bands at approximately 1450 and 1704 cm^{-1}, which are attributable to the symmetric $\upsilon_s(C=O)$ and *anti*-symmetric $\upsilon_{as}(C=O)$ vibration modes, respectively. In the cases of the IR spectra of 1-4, both of these C=O vibrational modes are shifted to lower wave numbers and split into two peaks (1384, 1412 cm^{-1} and 1554, 1630 cm^{-1} in 1; 1381, 1426 cm^{-1} and 1557, 1607 cm^{-1} in 2; 1384, 1427 cm^{-1} and 1563, 1610 cm^{-1} in 3; 1393, 1428 cm^{-1} and 1560, 1619 cm^{-1} in 4), thus indicating coordination of the carbonyl oxygen to the Ln^{3+} cations. Furthermore, the IR spectra of these complexes exhibit a separation of the asymmetric and symmetric stretching vibrations ($\Delta\upsilon_{(C=O)}$ = $\upsilon_{as} - \upsilon_s$) at approximately 240 and 142 cm^{-1} for 1, 226 and 131 cm^{-1} for 2, 226 and 136 cm^{-1} for 3, 226 and 132 cm^{-1} for 4, which implies coordination of the carboxylate group to the Ln^{3+} cation in a bidentate bridging and chelate mode in each case [Yong *et al.* 2005; de Bettencourt-Dias and Viswanathan 2006; Viswanathan and de Bettencourt-Dias 2006]. The IR spectra of 1 and 2 also exhibit a broad band at approximately 3451 and 3412 cm^{-1}, which is characteristic of an O–H stretching vibration $\upsilon(O–H)$, and thus suggestive of the presence of a coordinated water molecule in both complexes. Moreover, the red shifts observed for the C=N stretching frequencies of the nitrogen donors in the complexes 3 and 4 (1591 cm^{-1} in 3 and 1590 cm^{-1} in 4) in comparison with those of the free ligands phen (1613 cm^{-1}) and bath (1608 cm^{-1}) imply coordination of these ligands to the Tb^{3+} cation in each case.

The thermal decomposition behaviour of the complexes 1-4 was investigated by means of TGA. Although no attempt has been made to identify the intermediate products formed during the thermal analysis, it is clear that the first step in the thermograms of complexes 1 and 2 (Figures 4.1 and 4.2) corresponds to the loss of a coordinated water molecule in the temperature range 30–200°C. Subsequent thermal decomposition takes place in two steps, and leaves a residue of approximately 60% of the initial mass for 1 and 2, which corresponds to the formation of the corresponding lanthanide oxides. In contrast, complexes 3 and 4 are stable up to 260 and 275°C, respectively. Both complexes undergo decomposition in two steps, and leave a residue that corresponds to terbium oxide (36% for 3 and 31% for 4).
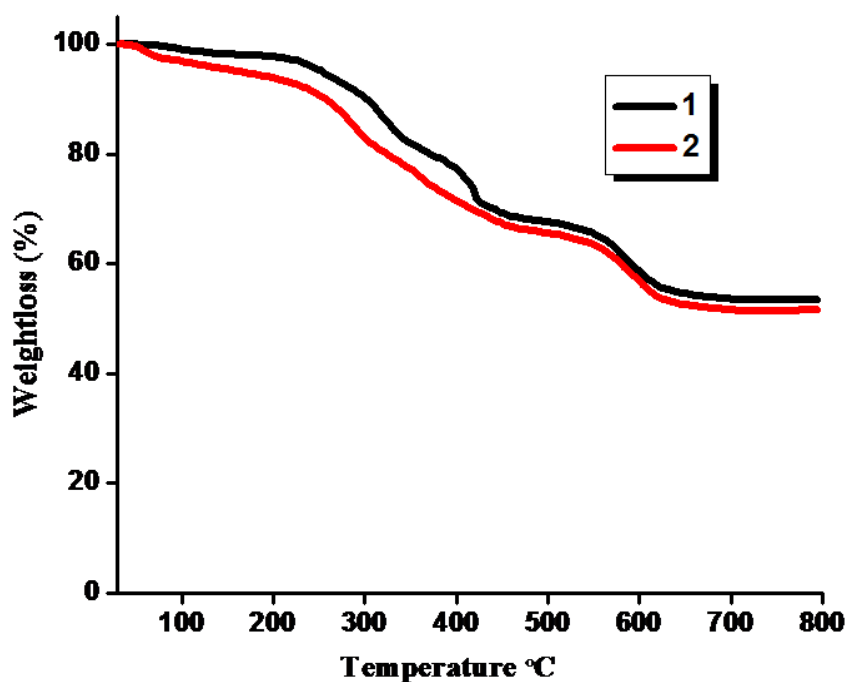
Figure 4.1. Thermo gravimetric curves for the Ln^{3+} complexes 1 and 2.
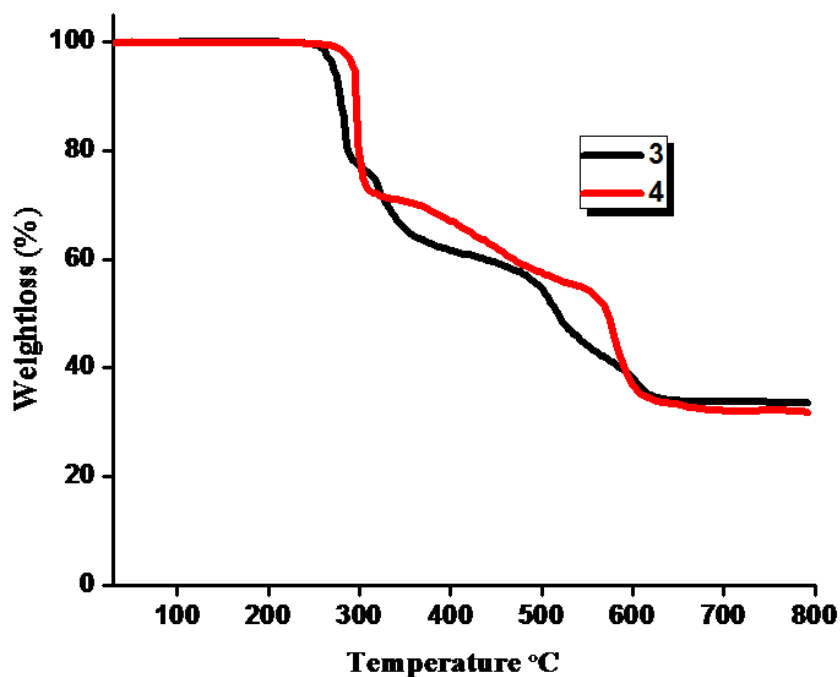
Figure 4.2. Thermo gravimetric curves for the Ln^{3+} complexes 3 and 4.

The X-ray powder diffraction patterns of complexes 1 and 2 are similar, indicating they are isostructural (Figure 4.3). Similarly, from the XRD patterns of

complexes 3 and 4 (Figure 4.4), one can conclude that they are isostructural and crystalline.
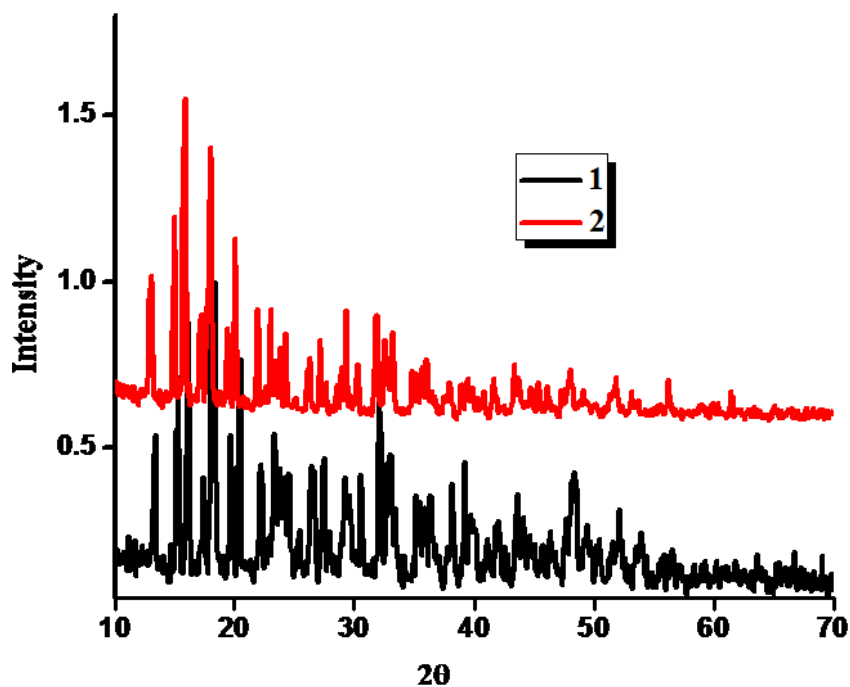
Figure 4.3. XRD pattern of complexes 1 and 2.
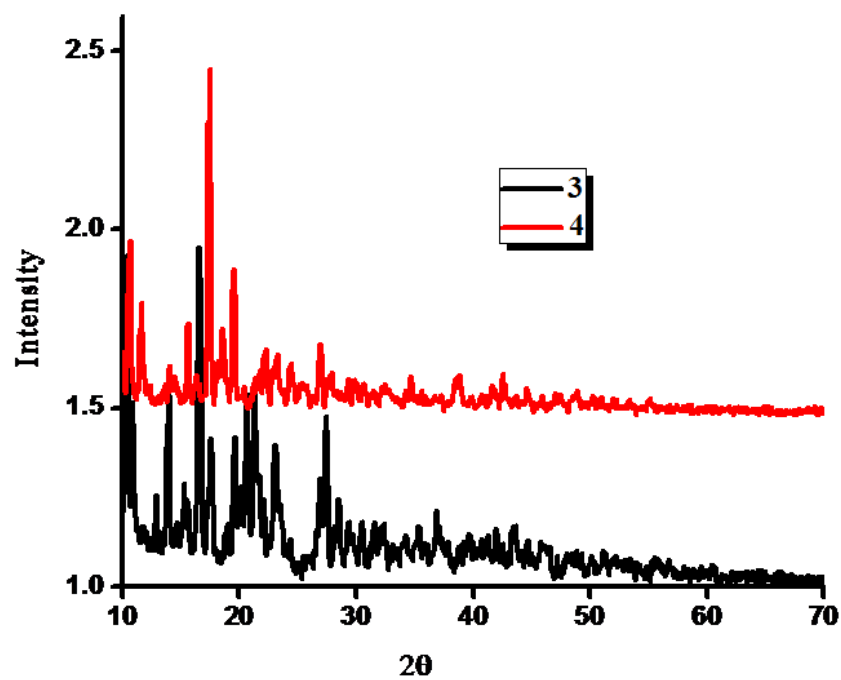
Figure 4.4. XRD pattern of complexes 3 and 4.

X-ray Crystal Structure of [Tb(TPAC)$_3$·H$_2$O]$_n$ (1).

The polymeric structure of complex 1 is illustrated in Figures 4.5 and 4.6, and the details of the crystal data and data collection parameters are given in Table 4.1. A selection of pertinent bond lengths and bond angles is presented in Table 4.2. Compound 1 crystallizes in the orthorhombic space group *Pnma* with a = 7.835(10) Å, b = 19.378(10) Å, c = 13.539(10) Å, $\alpha = \beta = \gamma = 90°$ and V = 2055.6(3) Å^3. The unit cell features only one crystallographically independent site for the Tb cations and is labeled as Tb1. Interestingly, other polymeric thiophene acetate complexes of Ce^{3+}, Pr^{3+}, Nd^{3+}, Sm^{3+} and Eu^{3+} feature two independent Ln^{3+} complexes [Wang *et al.* 2004]. The X-ray structure of 1 reveals that each Tb^{3+} ion is connected to two neighboring cations by six carboxylate ligands to form an infinite one-dimensional chain along the *a* axis. Some of the HTPAC ligands are disordered, which has been treated in the normal fashion. The carboxylate groups of the six molecules of thiophene acetate exhibit bidentate bridging and tridentate chelating-bridging modes, which corroborates well with the IR spectroscopic data. Two of the six carboxylate groups simultaneously bridge the two Tb^{3+} ions, while the other four carboxylate groups are chelated to two Tb^{3+} ions and simultaneously bridge two Tb^{3+} ions. Each Tb^{3+} is further surrounded by one H$_2$O molecule to form an overall nine coordinate array around the metal. As shown in Figure 4.6., the coordination polyhedron of Tb1 is a distorted tricapped-trigonal prism. The intra-chain Tb1···Tb1^a distance of 4.048 Å, is smaller than the Ln···Ln distances reported for lanthanide thiopheneacetate complexes (4.274–4.311 Å for Ce^{3+}, 4.274–4.312 Å for Nd^{3+} and 4.159–4.261 Å for Eu^{3+}) [Chen *et al.* 2004; Teotonio *et al.* 2005]. This trend can be explained on the basis of the lanthanide contraction. Since the Tb1^a–Tb1–Tb1^a angle is 150.86° it can be regarded as representing a linear chain along the *a* axis. The Tb–O (CO) bond lengths of the bidentate bridging carboxylate groups [2.292(10)–2.406(10) Å] are smaller than those of the tridentate chelating-bridging moieties [2.453(8)–2.502(7) Å]. On the other hand, the Tb–O distance of the coordinated water molecule [2.430(13) Å] is shorter than those of the tridentate bridging ligand and longer than those of bidentate bridging ligand. Similar trends in bond lengths have been reported elsewhere [Chen *et al.* 2004; Teotonio *et al.* 2005] for polymeric thiophene acetate complexes of Ce^{3+}, Pr^{3+}, Nd^{3+}, Sm^{3+} and Eu^{3+}.

Table 4.1. Crystal Data, Collection, and Structure Refinement Parameters for complex 1

Parameters	1
empirical formula	$C_{18}H_{17}O_7S_3Tb$
fw	600.42
crystal system	orthorhombic
space group	*Pnma*
cryst size (mm^3)	0.10 x 0.15 x 0.10
temperature	153(2)
a (Å)	7.835(10)
b (Å)	19.378(10)
c (Å)	13.539(10)
α (deg)	90
β (deg)	90
γ (deg)	90
V ($Å^3$)	2055.6(3)
Z	4
ρ_{calcd} (g cm^{-3})	1.940
μ (mm^{-1})	3.783
$F(000)$	1176
R1 [$I > 2\sigma(I)$]	0.0724
wR2 [$I > 2\sigma(I)$]	0.1410
R1 (all data)	0.1281
wR2 (all data)	0.1552
GOF	1.24
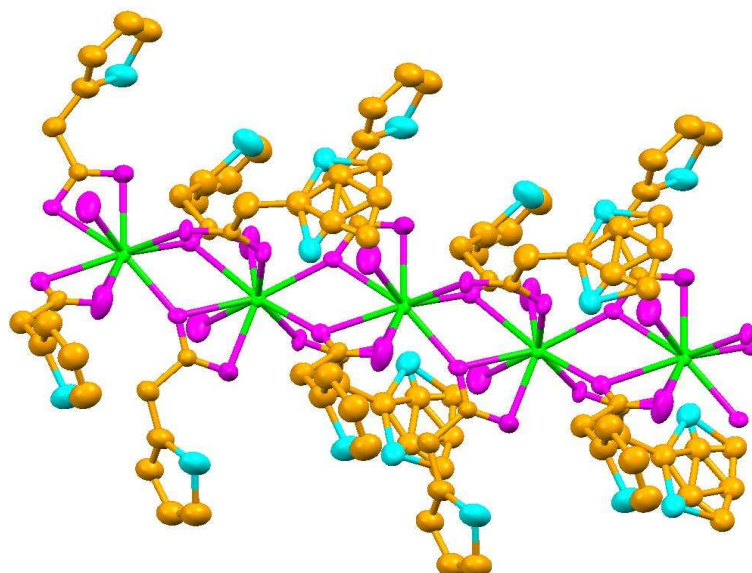
Figure 4.5. Polymeric structure of the complex 1. Thermal ellipsoids were drawn at the 30% probability level and H atoms were omitted for clarity.

Table 4.2. Selected Bond Lengths and Bond angles for 1

	1
Tb1–O3	2.292(10)
Tb1–O1^a	2.369(7)
Tb1–O1'	2.369(7)
Tb1–O4^a	2.406(10)
Tb1–O5	2.430(13)
Tb1–O2	2.453(8)
Tb1–O1	2.502(7)
Tb1–O2$^{"}$	2.453(8)
Tb–O1$^{"}$	2.502(7)
Tb1–Tb1^a	4.048
O2–Tb1–O1	52.0(2)
O5–Tb1–O1	68.7(3)
O4^a–Tb1–O5	141.6(4)
O4^a–Tb1–O1$^{"}$	79.0(2)
O2$^{"}$–Tb1–O1$^{"}$	52.0(2)
O1^a–Tb1–O2$^{"}$	71.4(2)
O3–Tb1–O1'	75.9(3)
O3–Tb1–O1^a	75.9(3)
Tb1^a–Tb1–Tb1^a	150.86°
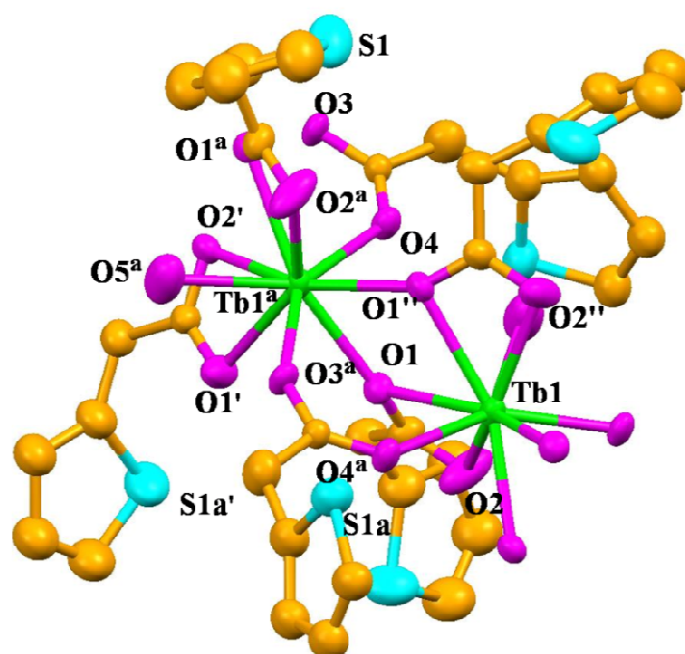
Figure 4.6. Coordination environment of the Tb^{3+} ions in this complex with atom-labeling scheme. All hydrogen atoms were omitted for clarity.

UV-vis Spectra.

The UV-vis absorption spectra of the free ligand HTPAC and the corresponding thiophene acetate lanthanide complexes were measured in DMSO solution ($c = 2\times10^{-5}$ M), and are displayed in Figures 4.7 and 4.8. The absorption spectra of the neutral donors (phen, bath) are shown in Figure 4.9. The absorption maxima for 1 (287 nm), 2 (287 nm), 3 (286 nm), and 4 (286 nm) which are attributable to singlet–singlet $^1\pi$–π^* absorptions of the aromatic rings, are slightly red-shifted with respect to that of the free ligand HTPAC ($\lambda_{max} = 276$ nm). The spectral contours for the complexes are similar to that of the free ligand, suggesting that the coordination of Ln^{3+} ion does not have a significant influence on the $^1\pi$–π^* transition. However, a small red-shift observed in the absorption band of each complex is a consequence of the enlargement of the conjugate structure of the ligand following coordination to the metal ion. The molar absorption coefficient values (ε) for 1 and 2 at λ_{max} are 1.64×10^4 and 1.72×10^4 L mol^{-1} cm^{-1}, respectively, and thus approximately three times larger than that of the free ligand HTPAC (6.44×10^3 at 276 nm), are indicative of the presence of three HTPAC ligands in both complexes. In contrast, the molar absorption coefficient values for complexes 3 and 4 (3.64×10^4 and 3.72×10^4 Lmol^{-1}cm^{-1}), are six times larger than that for HTPAC, implying the presence of six thiophene acetate ligands. Furthermore, the large molar absorption coefficient for HTPAC indicates that the carboxylic acid ligand has a strong ability to absorb light.

PL Properties of Complexes 1-4.

The photophysical properties of the HTPAC donor states in the Tb^{3+} complexes have been investigated on the basis of the phosphorescence spectrum of the $[Gd(TPAC)_3 \cdot H_2O]_n$ (2) complex. Because there is a large energy gap (ca. 32000 cm^{-1}) between the $^8S_{7/2}$ ground state and the first $^6P_{7/2}$ excited state of the Gd^{3+} ion, it cannot accept any energy from the first excited triplet state of the ligand via intramolecular ligand-to-metal energy transfer. Thus the phosphorescence spectra of complex 2 actually reveals the triplet energy level ($^3\pi\pi^*$) of HTPAC in the Tb^{3+} complexes. The excitation spectrum of the complex 2 exhibits a broad band between 250 and 450 nm (Figure 4.10), with a maximum around 330 nm which may be attributed to the ligand-centered $S_0\rightarrow S_1$ (π,π^*) transition of the thiophene moiety. The phosphorescence spectrum of the complex 2 (Figure 4.11) also displays a broad

band between 350 and 650 nm with a maximum around 550 nm when excited in the $S_0 \rightarrow S_1$ transition (330 nm). On the basis of the phosphorescence spectrum of complex 2, the triplet energy level of HTPAC corresponds to the lower emission edge wavelength and appear at 22321 cm^{-1} (448 nm). The singlet energy level ($^1\pi\pi^*$) of HTPAC can be estimated by referencing its higher absorption edge, which appear at 31250 cm^{-1} (320 nm). It is interesting to note that the triplet energy level of HTPAC is above the energy of the main emitting level of $^5D_4$ of Tb^{3+}, indicating that the HTPAC ligand can act as an antenna to photosensitize the Tb^{3+} ion.
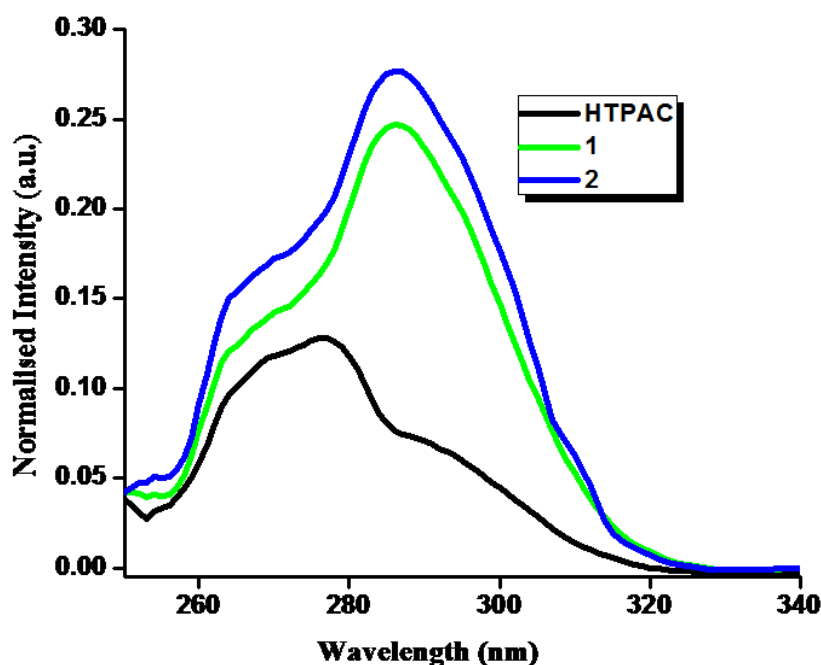
Figure 4.7. UV-visible absorption spectra of 2-thiophene acetic acid (HTPAC) and complexes 1 and 2 in DMSO (c = 2×10^{-5} M).

The normalized excitation spectra for the Tb^{3+} complexes, which were recorded at 303 K, and monitored around the intense $^5D_4 \rightarrow ^7F_5$ transition of the Tb^{3+} ion, are shown in Figure 4.12. The excitation spectra for all three complexes exhibit a broad band between 250 and 450 nm, which is attributable to the ligand centered $S_0 \rightarrow S_1$ (π,π^*) transition of the aromatic thiophene moiety [Teotonio *et al.* 2005]. The excitation spectrum of 1 also exhibits a series of sharp bands arising from 4f–4f transitions from the ground state $^7F_5$ level to the $^5L_6$ (341), $^5L_9$ (351), $^5L_{10}$ (369), $^5G_6$

(378), $^5D_3$ (380) and $^5D_4$ (488) excited. However, these transitions are less intense than that of the broad band attributable to the ligand levels, which proves that luminescence sensitization via ligand excitation, is more efficient than the direct excitation of the Tb^{3+} ion absorption levels. Interestingly, in the excitation spectra of complexes 3 and 4 the intensity of the absorption band at 340 nm due to the $^7F_5 \rightarrow {}^5L_6$ 4f–4f transitions (inset of Figure 4.12) is considerably less than that of the free ligand. Thus, the luminescence sensitization via excitation of the ligand is more effective than direct excitation of the Tb^{3+} ion in these particular complexes.

The emission spectra of the complexes 1, 3 and 4 (λ_{ex} = 290, 330 and 330 nm, respectively) exhibit the characteristically narrow band emissions for Tb^{3+} and correspond to the $^5D_4-{}^7F_J$ (J = 6–3) transitions (Figure 4.13). The most intense emission which is centered at 545 nm corresponds to the $^5D_4 \rightarrow {}^7F_5$ transition and is responsible for the brilliant green emission color of these complexes [Binnemans 2005; Biju *et al.* 2006; Pavithran *et al.* 2006]. Furthermore, the fact that the ligand emission in the region 250–450 nm could not be detected in the emission spectra of these complexes indicates that efficient energy transfer between the ligand excited states and the emissive level of the Tb^{3+} ion.
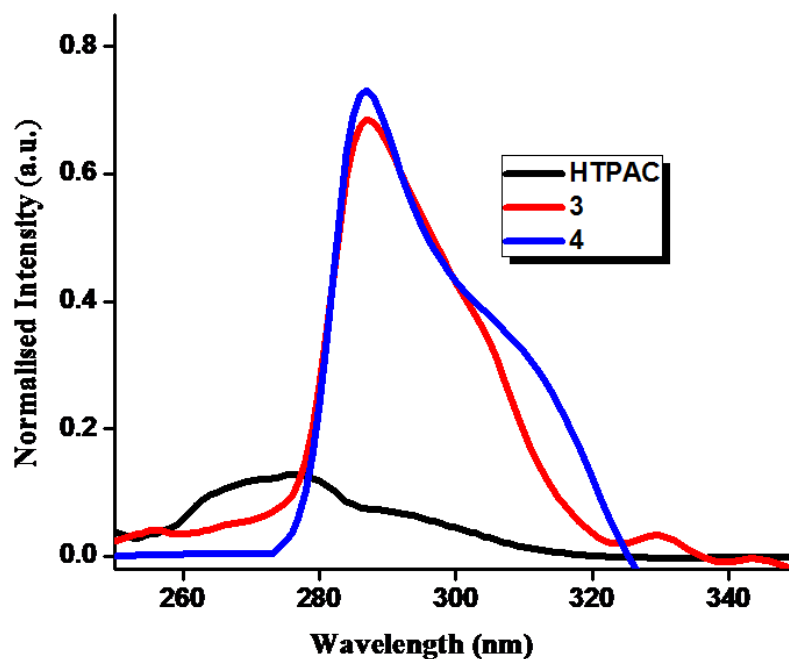
Figure 4.8. UV-visible absorption spectra of 2-thiophene acetic acid (HTPAC) and complexes 3 and 4 in DMSO (c = 2 × 10^{-5} M).
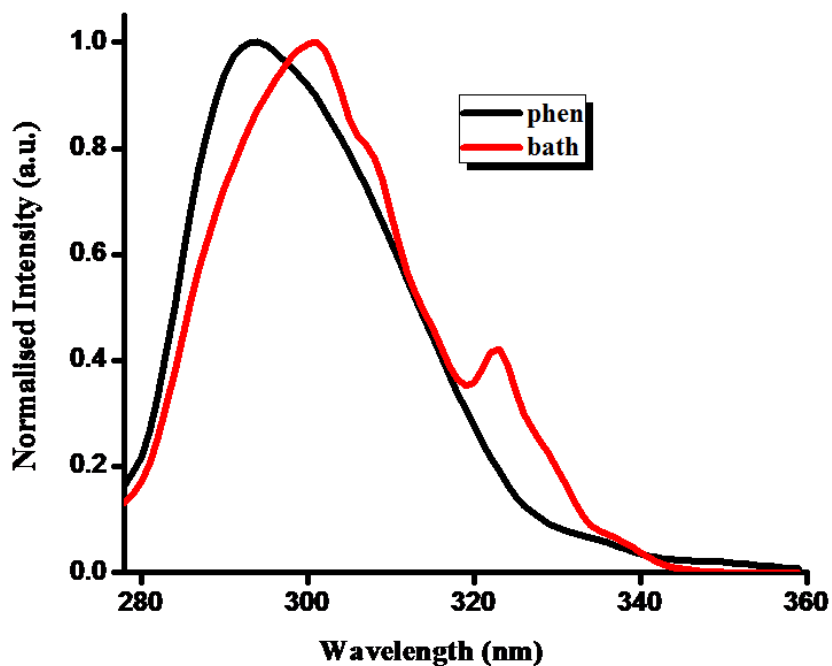
Figure 4.9. UV-visible absorption spectra of neutral ligands in DMSO (c = 2 × 10^{-5} M).
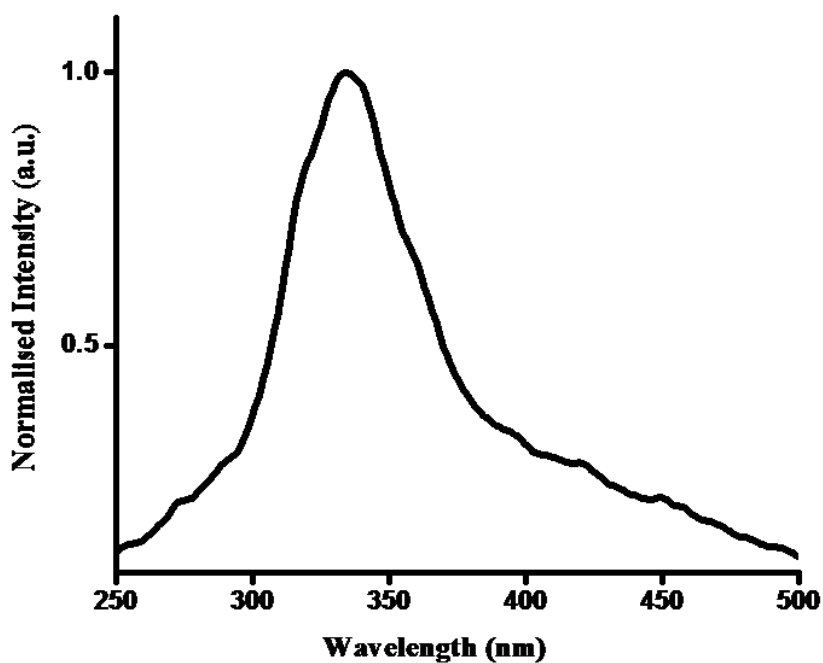
Figure 4.10. Excitation spectra of complex [Gd(TPAC)$_3$·H$_2$O]$_n$ at 77 K.
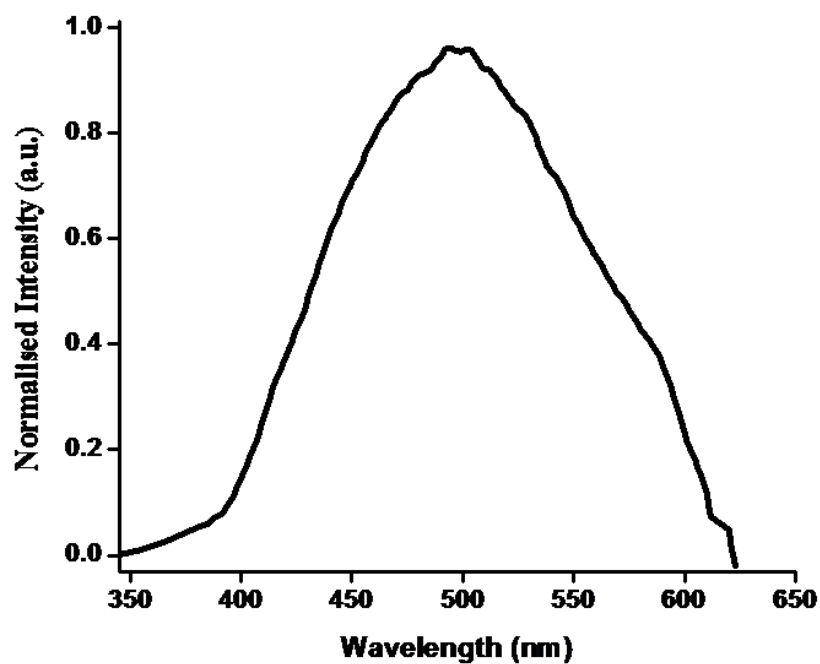
Figure 4.11. Phosphorescence spectra of [Gd(TPAC)$_3$·H$_2$O]$_n$ at 77 K.
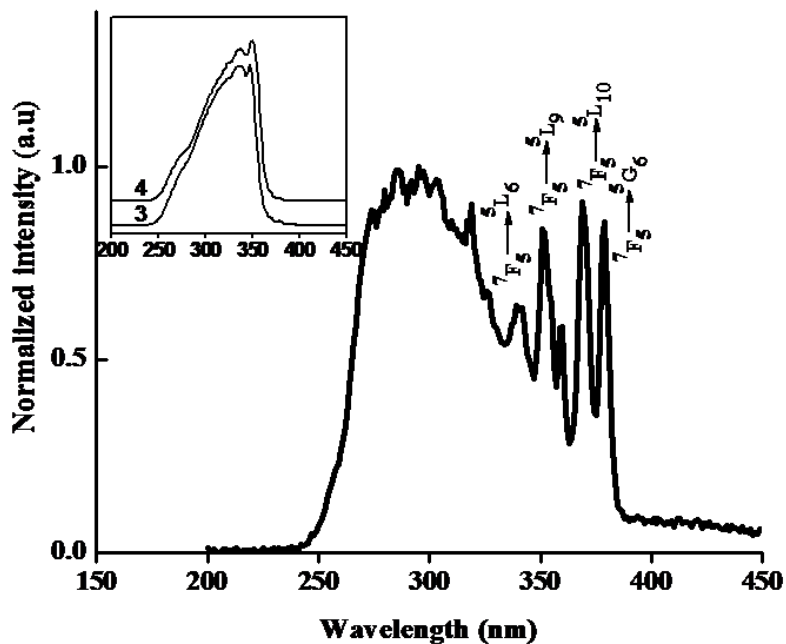
Figure 4.12. Room temperature excitation spectra of complex 1; the inset shows the room temperature excitation spectra of complexes 3 and 4.

The overall quantum yield ($\Phi_{overall}$) for a lanthanide complex treats the system as a "black box" in which the internal process is not considered explicitly. Given that the complex absorbs a photon (i.e. the antenna is excited), the overall quantum yield can be defined as shown [Xiao and Selvin 2001; Charbonniere *et al.* 2004; Quici *et al.* 2005]. $\Phi_{transfer}$ is the efficiency of energy transfer from the ligand to Tb^{3+} and Φ_{Tb}, represents the intrinsic quantum yield for the lanthanide cation. The overall quantum yields ($\Phi_{overall}$) for 1, 3 and 4 were found to be 0.07 ± 0.01, 4.43 ± 0.44 and $9.06 \pm 0.90\%$, respectively.

$$\Phi_{overall} = \Phi_{transfer}\Phi_{Tb}$$
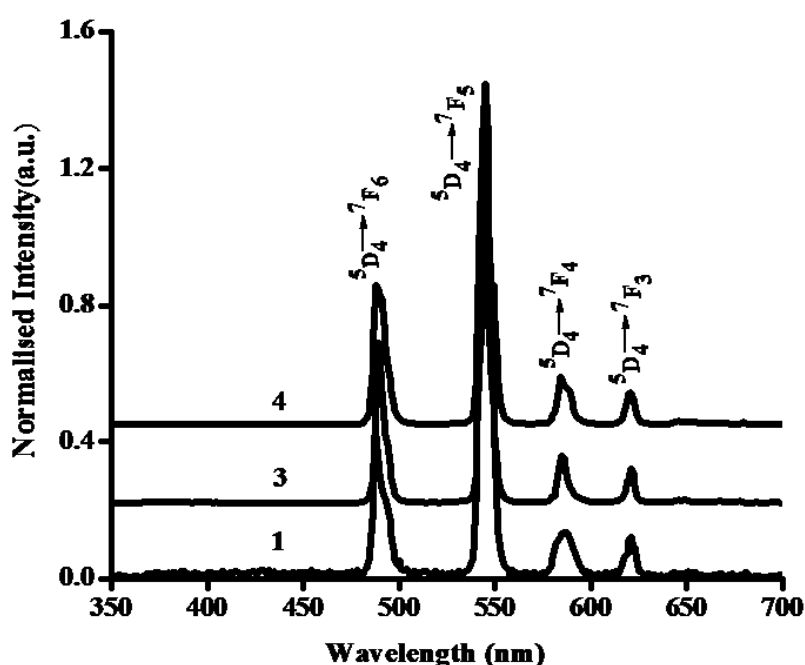
Figure 4.13. Room temperature emission spectra of complexes 1, 3 and 4.

It is clear that 1, which has water molecules in the one dimensional coordination sphere exhibits a lower quantum yield. This is due to the presence of O–H oscillators in this system, which effectively quenches the luminescence of the Tb^{3+} cation. Furthermore, the energy transfer between the lanthanide ions themselves is a nonradiative process and would account for the decrease in the terbium cation emission intensity, particularly when the metal ion concentration is high [Li *et al.* 2001]. In contrast, 3 and 4 exhibit high quantum yields, which may be due to the formation of dinuclear complexes. Additionally, the bidentate nitrogen donor

98

present in the coordination sphere of these complexes may also cause energy transfer to the neighboring HTPAC ligand. Following this, the HTPAC ligand subsequently transfers energy to the Tb^{3+} cation via the usual triplet pathway thus explaining the increased luminescence intensity in the present study. Of 3 and 4, the latter exhibits a particularly high quantum yield due to the extended conjugation induced by the introduction of two phenyl groups in the 4' and 7' positions of the phenanthroline ligand.

The $^5D_4$ lifetime values ($\tau_{obsd.}$) were determined from the luminescent decay profiles for 1, 3 and 4 at room temperature by fitting the data with a mono exponential curve. This analysis indicated the presence of single chemical environment around the emitting Tb^{3+} cation. Typical decay profiles for 1, 3 and 4 are shown in Figures 4.14 and 4.15. The somewhat shorter lifetime observed for complex 1 than for complexes 3 and 4 ($\tau = 1.05 \pm 0.01$ ms for 1; 1.35 ± 0.01 ms for 3 and 1.73 ± 0.01 ms for 4) may be due to the dominant nonradiative decay channels associated with vibronic coupling due to the presence of water molecules, as has been well documented in the case of several hydrated terbium complexes. On the other hand, longer lifetime values were observed for complexes 3 and 4 due to the absence of nonradiative decay pathways. The observed quantum yields and lifetime values, especially those for 4, are promising when compared with the recently reported 5-(thiophen-3-yl)isophthalate–terbium complex ($\Phi = 7.46\%$ and $\tau = 213.9$ μs in aqueous solution) [de Bettencourt-Dias 2005], terbium-thiophenyl-derivatized nitrobenzoate complexes ($\Phi = 4.7$–9.8% and $\tau = 208$–725 μs in methanol solution) [Viswanathan and de Bettencourt-Dias 2006] and the terbium complex of thiophene carboxyli cacid ($\tau = 230$ μs in solid state) [Eddaoudi *et al.* 2001; Pan *et al.* 2004; Teotonio *et al.* 2004; Bünzli *et al.* 2007].

Energy Transfer between Ligands and Tb^{3+}.

In general, the sensitization pathway in luminescent terbium complexes consists of excitation of the coordinated ligands into their excited states, subsequent intersystem crossing of the ligands to their triplet states, and energy transfer from the triplet state of the ligand to the ^5D_J manifold of the Tb^{3+} cation. This is followed by internal conversion to the emitting $^5D_4$ state, and finally the Tb^{3+} cation emits radiation. Therefore, the energy level match between the triplet states of the ligands
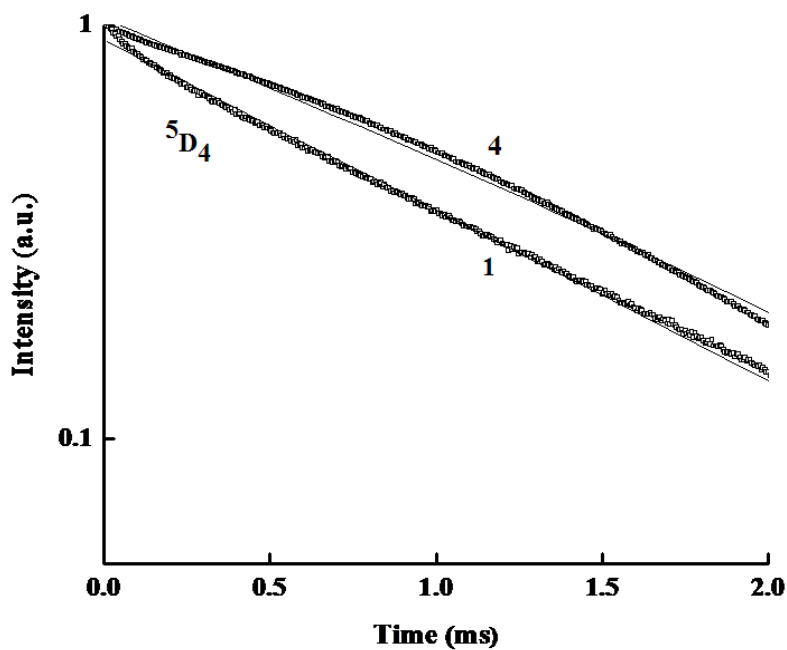
Figure 4.14. Experimental luminescence decay profiles of complexes 1 and 4 monitored around 545 nm and excited at their maximum emission wave lengths.
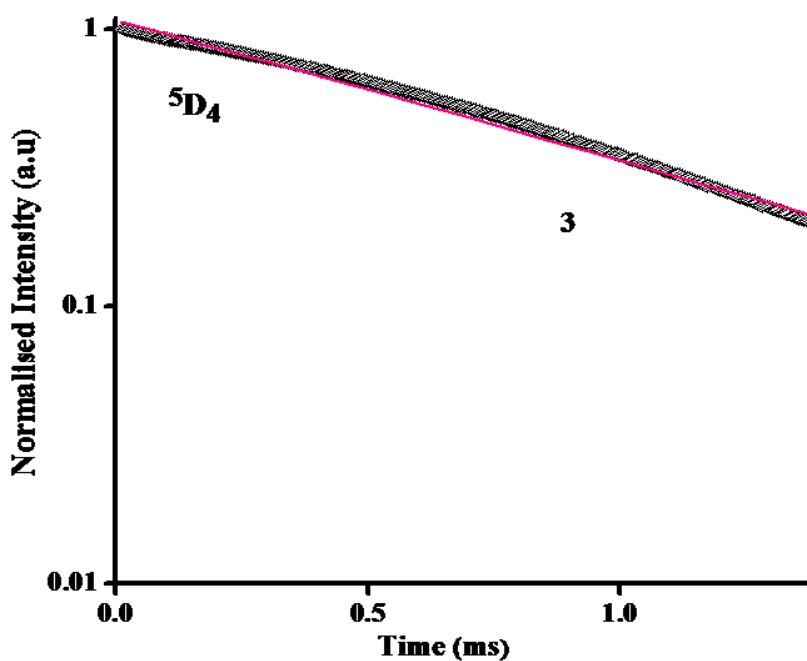
Figure 4.15. Experimental luminescence decay profiles of complex 3 monitored around 545 nm and excited at their maximum emission wave lengths.

to the $^5D_4$ state of the Tb^{3+} cation is one of the key factors which govern the luminescence properties of terbium complexes. It is well known that in organolanthanide complexes neutral ligands often play a role in terms of absorbing and transporting energy to other ligands or to the central metal ion [Roesky and Andruh 2003]. It is clear from Figures 4.16 and 4.17, that there is a large area of overlap between the room-temperature emission spectrum of the bidentate nitrogen donor and the phosphorescence spectrum of $[Gd(TPAC)_3 \cdot H_2O]_n$ and hence any secondary ligand present in the coordination sphere of the 3 and 4 can efficiently transfer its absorbed energy to the triplet state of the HTPAC. Furthermore, the bidentate nitrogen donor ligand can also transfer energy to itself and thus undergo singlet-triplet excitation. A schematic energy level diagram based on the foregoing is presented in Figure 4.19.
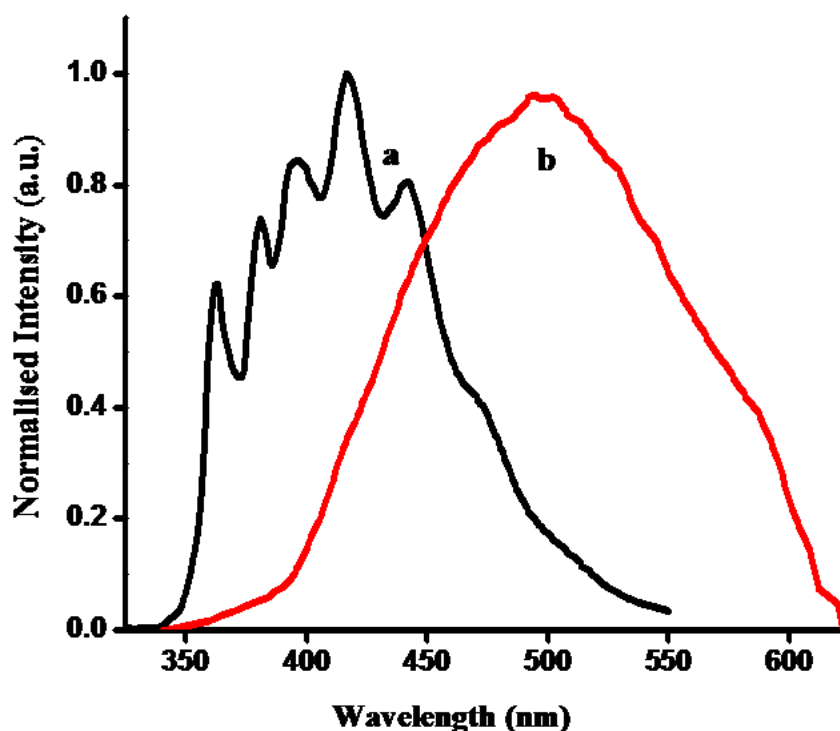
Figure 4.16. Emission spectra of phen (solid state) 303 K (a); and emission spectra of $[Gd(TPAC)_3 \cdot H_2O]_n$ 77 K ($CDCl_3$ solution, b).

101
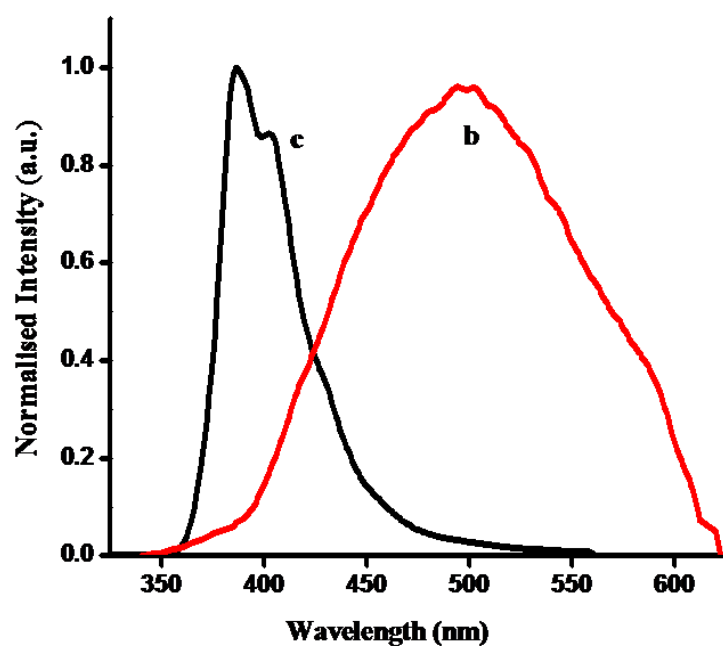
Figure 4.17. Emission spectra of bath (solid state) 303 K (c); and emission spectra of [Gd(TPAC)$_3$·H$_2$O]$_n$ 77K (CDCl$_3$ solution, b).
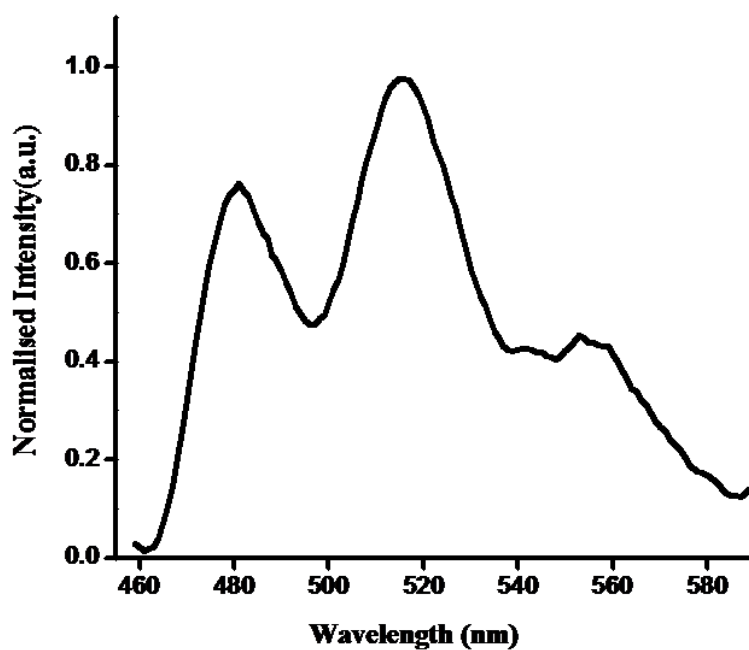
Figure 4.18. Phosphorescence spectra of Gd(bath)$_2$·(NO$_3$)$_3$ at 77 K.

In order to elucidate the energy transfer process, the phosphorescence spectra of the complexes [Gd(TPAC)$_3$·H$_2$O]$_n$ (Figure 4.11) and Gd(bath)$_2$(NO$_3$)$_3$ (Figure 4.18) were measured for the triplet energy levels of the ligands. On the basis of the

phosphorescence spectra, the triplet energy levels of $[Gd(TPAC)_3 \cdot H_2O]_n$ and $Gd(bath)_2(NO_3)_3$, correspond to their lower emission edge wavelengths and appear at 22321 cm^{-1} (448 nm) and 21000 cm^{-1} (476 nm), respectively. The singlet energy levels ($^1\pi\pi^*$) of HTPAC and bath can be estimated by referencing their higher absorption edges, which appear at 31250 cm^{-1} (320 nm) and 29000 cm^{-1} (344 nm), respectively. The singlet and triplet energy levels for phen (31000 and 22100 cm^{-1}) were taken from the literature [Yu and Su *et al.* 2003]. According to Reinhoudt's empirical rule [Steemers *et al.* 1995], the intersystem crossing process becomes effective when ΔE ($^1\pi\pi^* - {}^3\pi\pi^*$) is at least 5000 cm^{-1}. The energy gaps ΔE ($^1\pi\pi^* - {}^3\pi\pi^*$) for HTPAC, phen, bath are 8929, 8900 and 8000 cm^{-1}, respectively. Thus, the intersystem crossing processes are effective for all of the ligands. Latva's empirical rule [Latva *et al.* 1997] states that an optimal ligand-to-metal energy transfer process for Ln^{3+} needs ΔE ($^3\pi\pi^* - {}^5D_J$) = 2500–4500 cm^{-1} for Tb^{3+}. The energy gaps, ΔE ($^3\pi\pi^* - {}^5D_4$) are found to be 1821, 1500 and 500 cm^{-1} for HTPAC, phen and bath, respectively. Thus these energy gap values clearly indicate that a ligand-to-metal energy transfer process is effective in these systems. However, due to narrow energy gaps between $^3\pi\pi^*$ and the ^5D_J energy level of the Tb^{3+} ion, back transfer of energy may also take place.
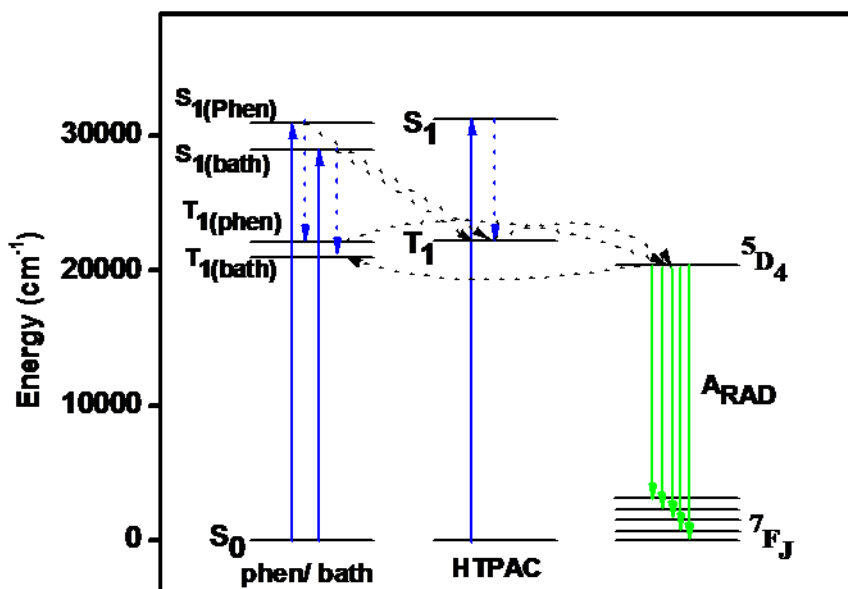
Figure 4.19. Schematic energy level diagrams and energy transfer processes for complexes 3 and 4. S_1 represents the first excited singlet state and T_1 represents the first excited triplet state.

4.5. Conclusions

Three new complexes of Tb^{3+} with 2-thiophene acetic acid, and in which 1,10-phenanthroline or bathophenanthroline serve as co-ligands have been synthesized and investigated on the basis of their photophysical properties. The Tb^{3+} complex 1 crystallizes in the orthorhombic space group *Pnma* with a = 7.835(10) Å, b = 19.378(10) Å, c = 13.539(10) Å, $\alpha = \beta = \gamma = 90°$ and V = 2055.6(3) Å^3. The unit cell contains only one crystallographically independent site for Tb^{3+} cations, contrary to those of previously reported Ce^{3+}, Pr^{3+}, Nd^{3+} and Eu^{3+} thiophene acetate coordination polymers. Relatively short Tb–Tb distances are evident in 1 which features a triply coordinated carboxylate as a bridging-bidentate ligand. Weak luminescence has been detected for the Tb^{3+} coordinated polymer due to the presence of a water molecule in the coordination sphere. This could also be due to the transfer of energy between the Ln^{3+} ions themselves which is a nonradiative process that becomes significant at high lanthanide concentrations. In the presence of bidentate nitrogen donor co-ligands, thermally stable binuclear complexes of the type $[Tb(TPAC)_3(phen)]_2$ or $[Tb(TPAC)_3(bath)]_2$ were produced. The overall quantum yields of these complexes were significantly enhanced by the displacement of coordinated water molecules from the coordination sphere of the thiophene acetate terbium complex by a highly conjugated bidentate nitrogen donor. Another factor contributing to the enhanced quantum yields might be the effective energy transfer of the secondary ligand to the triplet state of the primary ligand due to overlap of the singlet and triplet levels of the bidentate nitrogen ligand and primary ligand. Moreover, the observed quantum yields and lifetime values, especially those for 3 and 4, were found to be promising when compared with those reported recently for a terbium 5-(thiophen-3-yl)-isophthalate complex (Φ = 7.46% and τ = 213.9 µs in aqueous solution) [de Bettencourt-Dias 2005], a terbium-thiophenyl-derivatized nitrobenzoate complexes (Φ = 4.7–9.8% and τ = 208–725 µs in methanol solution) [Viswanathan and de Bettencourt-Dias 2006] and a terbium complex of thiophene carboxylic acid (τ = 230 µs in solid state) [Eddaoudi *et al.* 2001; Pan *et al.* 2004; Bünzli *et al.* 2007; Teotonio *et al.* 2004]. However, the luminescent efficiencies observed in the present systems are found to be inferior to the *p*-aminobenzoate

complexes of Tb^{3+} in the presence of bidentate nitrogen donor ($\Phi = 90\%$) [Fiedler *et al.* 2007].

List of Publications

LIST OF PUBLICATIONS

Publications from the thesis

1. **R. Shyni,** S. Biju, M. L. P. Reddy, Alan H. Cowley, and Michael Findlater, "Synthesis, Crystal Structures, and Photophysical Properties of Homodinuclear Lanthanide Xanthene-9-carboxylates," *Inorg. Chem.,* **2007**, 46, 11025-11030.

2. **Shyni Raphael,** M. L. P. Reddy**,** Alan H. Cowley, and Michael Findlater, "2-Thiopheneacetato-Based One-Dimensional Coordination Polymer of Tb3+: Enhancement of Terbium-Centered Luminescence in the Presence of Bidentate Nitrogen Donor Ligands,"*Eur. J. Inorg. Chem.,* **2008**, 4387–4394.

3. **Shyni Raphael**, M. L. P. Reddy, Kalyan V. Vasudevan and Alan H. Cowley, "Synthesis, crystal structure and photophysical properties of lanthanide coordination polymers of 4-[4-(9H-carbazol-9-yl)butoxy]benzoate: The effect of bidentate nitrogen donors on luminescence," Communicated to Dalton Transactions, **2012**.

Papers presented at National/International Conferences

1. Synthesis, Crystal Structures, and Photophysical Properties of Homodinuclear Lanthanide Xanthene-9-carboxylates- Poster presented in MTIC –XII, 2007, Chennai **2007**.

2. 2-Thiopheneacetato-Based One-Dimensional Coordination Polymer of Tb3+: Enhancement of Terbium-Centered Luminescence in the Presence of Bidentate Nitrogen Donor Ligands- Shyni Raphael, Poster presented in Indian Analytical Science Congress- 2008, Munnar **2008**.

References

References

Aebischer, A.; Gumy, F.; Bünzli, J.-C. G. "Intrinsic quantum yields and radiative lifetimes of lanthanide tris(dipicolinates)," *Phys. Chem. Chem. Phys.,* *11*, **2009**, 1346-1353.

[a]Alpha, B.; Balzani, V.; Lehn, J.-M.; Perathoner, S.; Sabbatini, N. "Luminescence probes: The Eu^{3+}- and Tb[3+]-cryptates of polypyridine macrobicyclic ligands," *Angew. Chem., Int. Ed. Engl.*, *26*, **1987**, 1266.

[b]Alpha, B.; Lehn, J.-M.; Mathis, G. "Energy transfer luminescence of europium(III) and terbium(III) cryptates of macrobicyclic polypyridine ligands," *Angew. Chem., Int. Ed. Engl. 26*, **1987**, 266.

Ambili Raj, D. B.; Biju, S.; Reddy, M. L. P. "4,4,5,5,5-Pentafluoro-1-(9H-fluoren-2-yl)-1,3-pentanedione complex of Eu^{3+} with 4,5-bis(diphenylphosphino)-9,9-dimethylxanthene oxide as a promising light-conversion molecular device," *Dalton Trans.*, *36*, **2009**, 7519-7528.

Ambili Raj, D. B.; Francis, B.; Reddy, M. L. P.; Butorac, R. R.; Lynch, V. M.; Cowley, A. H. "Highly luminescent poly(methyl methacrylate)-incorporated europium complex supported by a carbazole-based fuorinated *β*-diketonate ligand and a 4,5-bis(diphenylphosphino)-9,9-dimethylxanthene oxide co-ligand," *Inorg. Chem.*, *49*, **2010**, 9055-9063.

Ascencio, M. C.; Miranda, E. K. G.; Cruz, F. R.; Sandoval, O. J.; Sandoval, S. J. J.; Olivares, R. C.; Jancik, V.; Toscano, R. A.; Montalvo, V. G. "Lanthanide(III) complexes with 4,5-bis(diphenylphosphinoyl)-1,2,3-triazolate and the use of 1,10-phenanthroline as auxiliary ligand," *Inorg. Chem.*, *49*, **2010**, 4109-4116.

Bai, Y. Y.; Yan, B.; Chen, Z. X. "A strong luminescent quaternary dimeric complex [Tb(BAA)$_2$(Phen)(NO$_3$)]$_2$: Hydrothermal synthesis, structure, and photophysics," *Russ. J. Coord. Chem., 31,* **2005***, 445-451.

113

References

Barja, B.; Baggio, R.; Garland, M. T.; Aramendia, P. F.; Pena, O.; Perec, M. "Crystal structures and luminescent properties of terbium(III) carboxylates," *Inorg. Chim. Acta, 346*, **2003**, 187-196.

[a]Biju, S.; Reddy, M. L. P.; Cowley A. H.; Vasudevan, K. V. "Molecular ladders of lanthanide-3-phenyl-4-benzoyl-5-isoxazolonate and bis(2-(diphenylphosphino)phenyl)ether oxide complexes: The role of the ancillary ligand in the sensitization of Eu^{3+} and Tb^{3+} luminescence," *Cryst. Growth Des.*, *8*, **2009**, 3562-3569.

[b]Biju, S.; Reddy, M. L. P.; Cowley, A. H.; Vasudevan, K. V. "3-Phenyl-4-acyl-5-isoxazolonate complex of Tb^{3+} doped into poly-β-hydroxybutyrate matrix as a promising light-conversion molecular device," *J. Mater. Chem.*, *19*, **2009**, 5179-5187.

Biju, S.; Ambili Raj, D. B.; Reddy, M. L. P.; Jayasankar, C. K.; Cowley, A. H.; Findlater, M. "Dual emission from stoichiometrically mixed lanthanide complexes of 3-phenyl-4-benzoyl-5-isoxazolonate and 2,2'-bipyridine," *J. Mater. Chem.*, *19*, **2009**, 1425-1432.

Biju, S.; Ambili Raj, D. B.; Reddy, M. L. P.; Kariuki, B. M. "Synthesis, crystal structure, and luminescent properties of novel Eu^{3+} heterocyclic *β*-diketonate complexes with bidentate nitrogen donors," *Inorg. Chem., 45*, **2006**, 10651-10660.

Binnemans, K. "*Handbook on the Physics and Chemistry of Rare Earths,*" Elsevier, Amsterdam, **2005**, vol. 35, ch. 225, p. 107.

Binnemans, K. "Lanthanide-based luminescent hybrid materials," *Chem. Rev., 109*, **2009,** 4283-4374.

Bril, A.; De Jager-Veenis, A. W. "Quantum efficiency standard for ultraviolet and visible excitation," *J. Electrochem. Soc., 123*, **1976**, 396-398.

Brunet, E.; Juanes, O.; Rodriguez-Ubis, J. C. "Supramolecularly organized lanthanide complexes for efficient metal excitation and luminescence as

sensors in organic and biological applications," *Curr. Chem. Biol., 1*, **2007**, 11-39.

Bünzli, J.-C. G.; Piguet, C. *"Encyclopedia of Materials: Science and Technology,"* Buschow, K. H. J.; Cahn, R.W.; Flemings, M. C.B.; Ilschner, B.; Kramer, E. J.; Mahajan, S., Eds.; Elsevier Science Ltd, Oxford, **2001**, vol. 10, ch. 1.10.4, p. 4465.

Bünzli, J.-C.G.; Froidevaux, P.; Harrowfield, J. M. "Photophysical properties of lanthanide dinuclear complexes with *p*-tert-butylcalix[8]arene," *Inorg. Chem., 32*, **1993**, 3306.

Bünzli, J.-C.G.; Ihringer, F. "Photophysical properties of lanthanide dinuclear complexes with *p*-nitro-calix[8]arene," *Inorg. Chim. Acta, 246*, **1996**, 195.

Bußkamp, H.; Deacon, G. B.; Hilder, M.; Junk, P. C.; Kynast, U. H.; Leea, W. W.; Turnera, D. R. "Structural variations in rare earth benzoate complexes Part I. Lanthanum," *Cryst. Eng. Comm., 9*, **2007**, 394-411.

Cai, L. Z.; Chen, W. T.; Wang, M. S.; Guo, G. C.; Huang, J. S. "Syntheses, structures and luminescent properties of four new 1D lanthanide complexes with 2-thiopheneacetic acid ligand," *Inorg. Chem. Commun.*, *7*, **2004**, 611-613.

Cambridge Structural Database, version 5.27. http//www.ccdc.ac.uk.

Carlos, L. D.; de Mello Donega, C.; Albuquerque, R. Q.; Alves Jr. S.; Menezes, J. F. S.; Malta, O. L. "Highly luminescent europium(III) complexes with naphtoiltrifluoroacetone and dimethyl sulphoxide," *Mol. Phys., 101*, **2003**, 1037-1045.

Carnall, W. T. *"Handbook on the Physics and Chemistry of Rare Earths*," Gschneidner, K. A., Eyring, L., Eds.; Elsevier: Amsterdam, The Netherlands, **1987**; vol. 3, ch. 24, p. 171.

References

Charbonniere, L. J.; Balsiger, C.; Schenk, K. J.; Bünzli, J.-C.G. "Complexes of *p-tert*-butylcalix[5]arene with lanthanides: Synthesis, structure and photophysical properties**,**" *J. Chem. Soc., Dalton Trans.*, *3*, **1998**, 505.

Charbonniere, L. J.; Comby, S.; Imbert, D.; Sophie, C. A.; Bünzli, J. C. G.; Ziessel, R. F. "Influence of anionic functions on the coordination and photophysical properties of lanthanide(III) complexes with tridentate bipyridines," *Inorg. Chem., 43*, **2004**, 7369-7379.

Chatterton, N.; Bretonniere, Y.; Pecaut, J. Mazzanti, M. "An efficient design for the rigid assembly of four bidentate chromophores in water-stable highly luminescent lanthanide complexes," *Angew. Chem. Int. Ed.*, *44*, **2005**, 7595-7598.

Chen, B.; Wang, L.; Xiao, Y.; Fronczek, F. R.; Xue, M.; Cui, Y.; Qian, G. "A luminescent metal–organic framework with lewis basic pyridyl sites for the sensing of metal ions," *Angew. Chem. Int. Ed.*, *48*, **2009**, 500-503.

Chen, W.; Fukuzumi, S. "Ligand-dependent ultrasonic-assistant self-assemblies and photophysical properties of lanthanide nicotinic/isonicotinic complexes," *Inorg. Chem.*, *48*, **2009**, 3800-3807.

Chen, X. Y.; Bretonniere, Y.; Pecaut, J.; Imbert, D.; Bünzli, J.-C. G.; Mazzanti, M. "Selective self-assembly of hexameric homo- and heteropolymetallic lanthanide wheels: Synthesis, structure, and photophysical studies," *Inorg. Chem.*, *46*, **2007**, 625-637.

Chen, W. T.; Cai, L. Z.; Wang, M. S.; Guo, G. C.; Huang, J. S. "Syntheses, structures and luminescent properties of four new 1D lanthanide complexes with 2-thiophene acetic acid ligand," *Inorg. Chem. Commun.*, *7*, **2004**, 611-613.

Chen, X.; Pradhan, T.; Wang, F.; Kim, J. S.; Yoon, J. "Fluorescent chemosensors based on spiroring-opening of xanthenes and related derivatives," *Chem. Rev.*, *112*, **2012**, 1910-1956.

Colle, M.; Gmeiner, J.; Milius, W.; Hillebrecht, H.; Brütting, W. "Preparation and characterization of blue-luminescent tris(8-hydroxyquinoline)-aluminium (Alq3)," *Adv. Funct*. *Mater*., *13*, **2003**, 108-112.

Comby, S.; Imbert, D.; Anne-Sophie, C.; Bünzli, J.-C. G.; Charbonniere, L. J. Ziessel, R. F. "Influence of anionic functions on the coordination and photophysical properties of lanthanide(III) complexes with tridentate bipyridines," *Inorg. Chem., 43*, **2004**, 7369-7379.

Cotton, S. "*John Wiley & Sons Ltd, Lanthanide & Actinide Chemistry*," *Uppingham* School, Uppingham, Rutland*, UK*, **2006**, p. 51.

de Bettencourt-Dias, A. "Isophthalato-based 2D coordination polymers of Eu(III), Gd(III), and Tb(III): Enhancement of the terbium-centered luminescence through thiophene derivatization," *Inorg. Chem., 44*, **2005**, 2734-2741.

de Bettencourt-Dias, "Lanthanide-based emitting materials in light-emitting diodes," *Dalton Trans.*, *22*, **2007**, 2229-2241.

de Bettencourt-Dias, A.; Viswanathan, S. "Nitro-functionalization and luminescence quantum yield of Eu(III) and Tb(III) benzoic acid complexes," *Dalton Trans.*, **2006**, 4093-4103.

de Bettencourt-Dias.; Viswanathan, S. "Eu(III) and Tb(III) luminescence sensitized by thiophenyl-derivatized nitrobenzoato antennas," *Inorg. Chem.*, *45*, **2006,** 10138-10146.

de Faria, E. H.; Nassar, E. J.; Ciuffi, K. J.; Vicente, M. A.; Trujillano, R.; Rives, V.; Calefi, P. "New highly luminescent hybrid materials: Terbium pyridine-picolinate covalently grafted on kaolinite," *Appl. Mater. Interfaces*., *3*, **2011**, 1311-1318.

De Mello, J. C.; Wittmann, H. F.; Friend, R. H. "An improved experimental determination of external photoluminescence quantum efficiency," *Adv. Mater.*, *9*, **1997**, 230-232.

References

de Sa, G.F.; Malta, O.L.; de Mello Donega, C.; Simas, A.M.; Longo, R.L.; Santa-Cruz, P.A.; da Silva Jr, E.F. "Spectroscopic properties and design of highly luminescent lanthanide coordination complexes," *Coord. Chem. Rev., 196*, **2000**, 165.

Deacon, G. B.; Hein, S.; Junk, P. C.; Justel, T.; Lee, W.; Turner, D. R. "Structural variations in rare earth benzoate complexes Part II. Yttrium and Terbium," *Cryst. Eng. Comm.*, *9*, **2007**, 1110-1123.

Deacon, G. B.; Phillips, R. J. "Relationships between the carbon-oxygen stretching frequencies of carboxylato complexes and the type of carboxylate coordination," *Coord. Chem. Rev.*, *33*, **1980**, 227-250.

Dieke, G. H. "*Spectra and Energy Levels of Rare Earth Ions in Crystals*;" Wiley-Interscience: New York, **1968**.

Divya, V.; Biju, S.; Varma, R. L.; Reddy, M. L. P. "Highly efficient visible light sensitized red emission from europium tris[1-(4-biphenoyl)-3-(2-fluoroyl)propanedione] (1,10-phenanthroline) complex grafted on silica nanoparticles," *J. Mater. Chem.*, *20*, **2010**, 5220-5227.

Divya, V.; Freire, R. O.; Reddy, M. L. P. "Tuning of the excitation wavelength from UV to visible region in Eu^{3+}-β-diketonate complexes: Comparison of theoretical and experimental photophysical properties," *Dalton Trans.*, *40*, **2011**, 3257-3268.

Djerdj, I.; Cao, M.; Rocquefelte, X.; Cerny, R.; Jaglicic, Z.; Arcon, D.; Potocnik, A.; Gozzo, F.; Niederberger, M. "Structural characterization of a nanocrystalline inorganic-organic hybrid with fiberlike morphology and one-dimensional antiferromagnetic properties," *Chem. Mater.*, *21*, **2009**, 3356-3369.

Doeuff, S.; Henry, M.; Sanchez, C.; Livage, J. "Hydrolysis of titanium alkoxides: Modification of the molecular precursor by acetic acid," *Non-Cryst. Solids, 89*, **1987**, 206-216.

Donega, C. de M.; Junior, S. A.; de Sa, G. F. "Europium(III) mixed complexes with β-diketones and o-phenanthroline-N-oxide as promising light-conversion molecular devices," *Chem. Commun.*, *11, ***1996**, 1199-1200.

Eddaoudi, M.; Kim, J.; Rosi, N.; Vodak, D.; Wachter, J.; Keeffe, M. O'.; Yaghi, O. M. "Systematic design of pore size and functionality in isoreticular MOFs and their application in methane storage," *Science*, *295*, **2002**, 469-472.

Eddaoudi, M.; Kim, J.; Wachter, J. B.; Chae, H. K.; Keeffe, M. O'.; Yaghi, O. M. "Porous metal-organic polyhedra: 25 Å cuboctahedron constructed from 12 $Cu_2(CO_2)_4$ paddle-wheel building blocks," *J. Am. Chem. Soc.*, *123*, **2001**, 4368-4369.

Edwards, A.; Claude, C.; Sokolik, I.; Chu, T. Y.; Okamoto, Y. "Photoluminescence and electroluminescence of new lanthanide-(methyoxybenzoyl)benzoate complexes," *J. Appl. Phys.*, *82*, **1997**, 1841.

Eliseeva, S. V.; Bünzli, J. -C. G. "Lanthanide luminescence for functional materials and bio-sciences," *Chem. Soc. Rev., 39*, **2010,** 189-227.

Eliseeva, S. V.; Kotova, O. V.; Gumy, F.; Semenov, S. N.; Kessler, V. G.; Lepnev, L. S.; Bünzli, J.-C. G.; Kuzmina, N. P. "Role of the ancillary ligand *N*,*N*-dimethylaminoethanol in the sensitization of Eu^{3+} and Tb^{3+} luminescence in dimeric β-diketonates," *J. Phys. Chem. A, 112*, **2008**, 3614-3626.

Eliseeva, S. V.; Pleshkov, D. N.; Lyssenko, K. A.; Lepnev, L. S.; Bünzli, J.-C. G.; Kuzmina, N. P. "Novel 1D coordination polymer $\{Tm(Piv)_3\}_n$: Synthesis, structure, magnetic properties and thermal behavior," *Inorg. Chem.*, *50*, **2011**, 5137-5144.

Emeleus, H. J.; Sharpe, G. A. "*Advances in Inorganic Chemistry and Radiochemistry*," Vol. 20; Academic Press: London, **1977**.

Fiedler, T.; Hilder, M.; Junk, P. C.; Kynast, U. H.; Lezhnina, M. M.; Warzala, M. "Synthesis, structural and spectroscopic studies on the lanthanoid *p*-

aminobenzoates and derived optically functional polyurethane composites," *Eur. J. Inorg. Chem.*, **2007**, 291-301.

Fomina, I.; Dobrokhotova, Z.; Aleksandrov, G.; Emelina, A.; Bykov, M.; Malkerova, I.; Bogomyakov, A.; Puntus, L.; Novotortsev, V.; Eremenko, I. "Novel 1D coordination polymer $\{Tm(Piv)_3\}_n$: Synthesis, structure, magnetic properties and thermal behavior," *J. Solid State Chem.*, *185*, **2012**, 49-55.

Furmanova, N. G.; Razmanova, Z. P.; Soboleva, L. V.; Maslyanitsin, I. A.; Siegert, H.; Shigorin, V. D.; Shipulo, G. P. "Determination of crystal structure and determination of the quadratic optical susceptibility of formate lithium crystal structure determination and estimation of quadratic optical susceptibility yttrium formate," *Sov. Phys. Crystallogr.*, (Engl. Transl.) *29*, **1984**, 476-479.

George, M. R.; Golden, C. A.; Grossel, M. C.; Curry, R. J. "Modified dipicolinic acid ligands for sensitization of europium(III) luminescence," *Inorg. Chem., 45*, **2006**, 1739.

Grazulevicius, J. V.; Strohriegl, P.; Pielichowski, J.; Pielichowski, K. "Carbazole-containing polymers: Synthesis, properties and applications," *Prog. Polym. Sci., 28*, **2003**, 1297-1353.

Guseinova, M. K.; Antsishkina, A. S.; Koshits, M. A. P. "X-ray structural study of scandium formate," *J. Struct. Chem.*, (USSR) (Engl. Transl.) *9*, **1968**, 1040-1045.

Hilder, M.; Junk, P. C.; Kynast, U. H.; Lezhnina, M. M. "Spectroscopic properties of lanthanoid benzene carboxylates in the solid state: Part 1," *J. Photochem. and Photobiol. A: Chem.*, *202,* **2009**, 10-20.

Huang, F.; Zheng, Y.; Yang, Y. "Study on macromolecular metal complexes: Synthesis, characterization, and fluorescence properties of stoichiometric complexes for rare earth coordinated with poly(acrylic acid)," *J. Appl. Pol. Sci.*, *103*, **2007**, 351-357.

Jin, Q. H.; Li, X.; Zou, Y. Q. "Catena-poly[europium-tri-l-4-methyl-benzoato," *Acta Crystallogr., Sect. C, 57*, **2001**, 676-677.

John, A.; Yadav, P. J. P.; Palaniappan, S. "Clean synthesis of 1,8-dioxo-dodecahydroxanthene derivatives catalyzed by polyaniline-*p*-toluenesulfonate salt in aqueous media," *J. Mol. Catal. A: Chem.*, *248*, **2006,** 121-125.

Juan, P.; Xiaotian, G.; Jianbo, Y.; Yanhui, Z.; Ying, Z.; Yunyou, W.; Bo, S. "Synthesis and fluorescence studies on novel complexes of Tb(III) and Eu(III) with 4-(*9H*-carbazol-9-yl) benzoic acid," *J. Alloys Compd.*, *426*, **2006**, 363-367.

Kazuo, N. "*Infrared and Raman Spectra of Inorganic and Coordination Compounds*," third ed. [M], Chemical Industry Press, Beijing, **1986**, p. 237.

Kido, J.; Okamoto, Y. "Organolanthanide metal complexes for electroluminescent materials," *Chem. Rev., 102*, **2002**, 2357-2368.

Kistaiah, P.; Murthy, K. S.; Iyengar, L.; Rao, K. V. K.; "X-ray studies on the high pressure behaviour of some rare-earth formates," *J. Mater. Sci.*, *16*, **1981**, 2321-2323.

Kumar, N. S. S.; Varghese, S.; Rath, N. P.; Das, S. "Solid State optical properties of 4-alkoxy-pyridine butadiene derivatives: Reversible thermal switching of luminescence," *J. Phys. Chem. C.*, *112*, **2008**, 8429-8437.

Lam, A. W. H.; Wong, W. T.; Gao, S.; Wen, G. H.; Zhang, X. X. "Synthesis, crystal structure, and photophysical and magnetic properties of dimeric and polymeric lanthanide complexes with benzoic acid and its derivatives," *Eur. J. Inorg. Chem.,* **2003**, 149-163.

Lamture, J. B.; Zhou, Z. H.; Kumar, A. S.; Wensel, T. G. "Luminescence properties of terbium(III) Complexes with 4-substituted dipicolinic acid analogs," *Inorg. Chem.*, *34*, **1995**, 864.

References

Latva, M.; Takalo, H.; Mukkala, V. M.; Matachescu, C.; Rodriguez-Ubis, J. C.; Kanakare, J. "Correlation between the lowest triplet state energy level of the ligand and lanthanide(III) luminescence quantum yield," *J. Lumin.*, *75,* **1997**, 149-169.

Law, G.-L.; Wong, K.-L.; Lau, K.-K.; Tam, H.-L.; Cheah, K.-W; Wong, W.-T. "Synthesis, crystal structures, and photophysical properties of lanthanide complexes containing pyrrole-derivatized carboxylate ligands," *Eur. J. Inorg. Chem.,* **2007**, 5419-5425.

Lehn, J. M. "Perspectives in supramolecular chemistry–from molecular recognition towards molecular information processing and self-organization," *Angew. Chem. Int. Ed., 29*, **1990**, 1304-1319.

[a]Lenaerts, P.; Driesen K.; Van Deun, R.; Binnemans, K. "Covalent Coupling of Luminescent Tris(2-thenoyltrifluoroacetonato)lanthanide (III) complexes on a Merrifield Resin," *Chem. Mater., 17*, **2005**, 2148-2154.

[b]Lenaerts, P.; Storms, A.; Mullens, J.; D'Haen, J.; Gorller-Walrand, C.; Binnemans, K.; Driesen, K. "Thin films of highly luminescent lanthanide complexes covalently linked to an organic-inorganic hybrid material via 2-substituteed imidazo[4,5-f]-1,10-phenanthroline groups," *Chem. Mater., 17*, **2005**, 5194-5201.

Li, H.-F.; Yan, P.-F.; Chen, P.; Wang, Y.; Xu, H.; Li, G.-M. "Highly luminescent bis-diketone lanthanide complexes with triple-stranded dinuclear structure," *Dalton Trans.*, *41*, **2012**, 900-907.

Li, J.; Li, H.; Yan, P.; Chen, P.; Hou, G.; Li, G. "Synthesis, crystal structure, and luminescent properties of 2-(2,2,2-trifluoroethyl)-1-indone lanthanide complexes," *Inorg. Chem.*, *51*, **2012**, 5050-5057.

Li, Q.; Li, T.; Wu, J. "Luminescence of europium(III) and terbium(III) complexes incorporated in poly(vinylpyrolidone) matrix," *J. Phys. Chem. B.*, *105*, **2001,** 12293-12296.

Li, X.; Jin, L.; Lu, S.; Zhang, J. "Synthesis, structure and luminescence property of the ternary and quaternary europium complexes with furoic acid," *J. Mol. Struct.*, *604*, **2002,** 65-71.

Li, X.; Zhang, Z.-Y.; Wang, D.-Y.; Zou, Y.-Q. "Crystal structure of *catena-*hexakis(μ-4-methylbenzoato)didysprosium(III), Dy$_2$(C$_8$H$_7$O$_2$)$_6$," Z. Kristallogr.—*New Cryst. Struct.*, *220*, **2005**, 36-38.

Li, X.; Zhang, Z.-Y.; Zou, Y.-Q. "Synthesis, structure and luminescence properties of four novel terbium 2-fluorobenzoate complexes," *Eur. J. Inorg. Chem.,* **2005**, 2909-2918.

Li, X.; Zheng, X.; Jin, L.; Lu, S.; Qin, W. "Crystal structure and luminescence of a europium coordination polymer {[Eu(m-MOBA)$_3$.2H$_2$O]1/2(4,4'-bpy)}$_∞$," *J. Mol. Struct., 519*, **2000**, 85-91.

Li, X.; Zou, Y. Q. "Crystal structure of di(2,2'-bipyridine)tetra[μ-(4-methylbenzoato-O,O')]-di(4-methylbenzoato)disamarium(III), Sm$_2$(C$_8$H$_7$O$_2$)$_6$(C$_{10}$H$_8$N$_2$)$_2$," *Z. Kristallogr., 218*, **2003**, 448-450.

Li, X.; Zou, Y. Q.; Zheng, B.; Hu, H. M. "*Catena*-Poly[europium(III)-tri-μ-2,3-dimethoxybenzoato]," *Acta Crystallogr., Sect.C, 60*, **2004**, 197-199.

Li, Y.; Zheng, F. K.; Liu, X.; Zou, W. Q.; Guo, G. C.; Lu, C. Z.; Huang, J. S. "Crystal structures and magnetic and lumnescent properties of a series of homodinuclear lanthanide complexes with 4-cyano benzoic acid ligand," *Inorg. Chem., 45*, **2006**, 6308-6316.

Lill, D. T. de; Cahill, C. L. "An unusually high thermal stability within a novel lanthanide 1,3,5-cyclohexanetricarboxylate framework: synthesis, structure, and thermal data," *Chem.Commun.*, *47*, **2006**, 4946-4948.

Lucky, M. V.; Sivakumar, S.; Reddy, M. L. P.; Paul, A. K.; Natarajan, S. "Lanthanide luminescent coordination polymer constructed from unsymmetrical dinuclear building blocks based on 4-((1H-benzo[d]imidazol-1-yl)methyl)benzoic Acid," *Cryst. Growth. Des.*, *11*, **2011,** 857-864.

References

Ma, J. F.; Jin, Z. S.; Ni, J. Z. "Syntheses, characterization and crystal structures of the complexes of rare earth with *m*-methyl-benzoic acid," *Acta Chim. Sinica, 51*, **1993**, 265-272.

Melhuish, W. H. "Measurement of quantum efficiencies of fluorescence and phosphorescence and some suggested luminescence standards," *J. Opt. Soc. Am., 54*, **1964**, 183-186.

Morin, J. F.; Leclerc, M.; Ades, D.; Siove, A. "Polycarbazoles: 25 years of progress," *Macromol. Rapid Commun., 26*, **2005**, 761-778.

Mukkala, V.-M.; Kankare, J. J. "New 2,2′-bipyridine derivatives and their luminescence properties with europium(III) and terbium(III) ions," *Helv. Chim. Acta*, *75*, **1992**, 1578.

Nakamoto, K. "*Infrared and Raman Spectra of Inorganic and Coordination Compounds*," 4th ed.; Wiley: New York, **1986**.

Nie, D.; Chen, Z.; Bian, Z.; Zhou, J.; Liu, Z.; Chen, F.; Zhaob, Y.; Huang, C. "Energy transfer pathways in the carbazole functionalized *β*-diketonate europium complexes," *New J. Chem.*, *31*, **2007**, 1639-1646.

Ouchi, A.; Suzuki, Y.; Ohki Y.; Koizumi, Y. "Structure of rare earth carboxylates in dimeric and polymeric forms," *Coord. Chem. Rev.*, *92*, **1988**, 29-43.

Palsson, L.-O.; Monkman, A. P. "Measurements of Solid-State Photoluminescence Quantum Yields of Films Using a Fluorimeter," *Adv. Mater.*, *14*, **2002**, 757-758.

Pan, L.; Sander, M. B.; Huang, X.; Li, J.; Smith, M.; Bittner, E.; Bockrath, B.; Johnson, J. K. "Microporous metal organic materials: promising candidates as sorbents for hydrogen storage," *J. Am. Chem. Soc.*, *126*, **2004**, 1308-1309.

Pavithran, R.; Kumar, N. S. S.; Biju, S.; Reddy, M. L. P.; Junior, S. A.; Freire, R. O. "3-Phenyl-4-benzoyl-5-isoxazolonate complex of Eu³⁺ with tri-*n*-

octylphosphine oxide as a promising light-conversion molecular device," *Inorg. Chem.*, *45*, **2006**, 2184-2192.

Pavithran, R.; Reddy, M.L.P.; Alves, Jr. S.; Freire, R.O.; Rocha, G.B.; Lima, P.P. "Synthesis and luminescent properties of novel europium(III) heterocyclic *β*-diketone complexes with lewis bases: Structural analysis using the sparkle/AM1 model," *Eur. J. Inorg. Chem., 20*, **2005**, 4129-4137.

Polynova, T. N.; Smolyar, B. B.; Filippova, T. F.; Porai-Koshits, M. A.; Pirkes, S. B. "Crystal structure of neodymium 2-methoxybenzoate tetrahydrate Nd(2-CH/sub 3/OC/sub 6/H/sub 4/COO)/sub 3/ x 4H/sub 2/O," *Koord. Khim., 13*, **1987**, 130-135.

Quici, S.; Cavazzini, M.; Marzanni, G.; Accorsi, G.; Armaroli, N.; Ventura, B.; Barigelletti, F. "Visible and near-infrared intense luminescence from water-soluble lanthanide [Tb(III), Eu(III), Sm(III), Dy(III), Pr(III), Ho(III), Yb(III), Nd(III), Er(III)] complexes," *Inorg. Chem., 44*, **2005**, 529-537.

Quici, S.; Marzanni, G.; Forni, A.; Accorsi, G.; Barigelletti, F. "New lanthanide complexes for sensitized visible and near-IR light emission: synthesis, ^{1}H NMR, and X-ray structural investigation and photophysical properties," *Inorg. Chem., 43*, **2004**, 1294-1301.

Ramya, A. R.; Reddy, M. L. P.; Cowley, A. H.; Vasudevan, K. V. "Synthesis, Crystal Structure, and Photoluminescence of Homodinuclear Lanthanide 4-(Dibenzylamino)benzoate Complexes," *Inorg. Chem.*, *49*, **2010**, 2407-2415.

Rao, C. N. R.; Natarajan, S.; Vaidhyanathan, R. "Metal Carboxylates with Open Architectures," *Angew. Chem., Int. Ed.*, *43*, **2004**, 1466-1496.

Raphael, S.; Reddy, M. L. P.; Cowley, A. H.; Findlater, M.; "2-Thiopheneacetato-based one-dimensional coordination polymer of Tb^{3+}: Enhancement of

terbium-centered luminescence in the presence of bidentate nitrogen donor ligands," *Eur. J. Inorg. Chem.*, **2008**, 4387-4394.

Remya, P. N.; Biju, S.; Reddy, M. L. P.; Cowley, A. H.; Findlater, M. "1D molecular ladder of the ionic complex of terbium-4-sebacoylbis(1-phenyl-3-methyl-5-pyrazolonate) and sodium dibenzo-18-crown-6: Synthesis, crystal structure, and photophysical properties," *Inorg. Chem., 47*, **2008**, 7396-7404.

Roesky, H. W.; Andruh, M. "The interplay of coordinative, hydrogen bonding and π-π stacking interactions in sustaining supramolecular solid-state architectures. A study case of bis(4-pyridyl)- and bis(4-pyridyl-N-oxide) tectons," *Coord. Chem. Rev.*, *236*, **2003**, 91-119.

Rueff, J.-M.; Barrier, N.; Boudin, S.; Dorcet, V.; Caignaert, V.; Boullay, P.; Hix, G. B.; Jaffrès, P.-A. "Remarkable thermal stability of Eu(4-phosphonobenzoate): structure investigations and luminescence properties," *Dalton Trans.*, **2009**, 10614-10620.

Sabbatini, N.; Guardigli, M.; Lehn, J.-M. "Luminescent lanthanide complexes as photochemical supramolecular devices," *Coord. Chem. Rev.*, *123*, **1993**, 201-228.

Saleesh Kumar, N. S.; Varghese, S.; Rath, N. P.; Das, S. "Solid state optical properties of 4-alkoxy-pyridine butadiene derivatives: Reversible thermal switching of luminescence," *J. Phys. Chem. C*, *112*, **2008**, 8429-8437.

Samuel. A. P. S.; Xu. J.; Raymond. K. N. "Predicting efficient antenna ligands for Tb(III) emission," *Inorg. Chem.*, *48*, **2009**, 687.

Santos, P. C. R. S.; Nogueira, H. I. S.; Paz, F. A. A.; Ferreira, R. A. S.; Carlos, L. D.; Klinowski, J.; Trindade, T. "Lanthanide complexes of 2,6-dihydroxybenzoic acid: Synthesis, crystal structures and luminescent properties of [nBu_4N]$_2$[Ln(2,6-dhb)$_5$(H$_2$O)$_2$] (Ln = Sm and Tb)," *Eur. J. Inorg. Chem.*, *19*, **2003**, 3609-3617.

Seward, C.; Hu, N. X.; Wang, S. "1-D Chain and 3-D grid green luminescent terbium(III) coordination polymers: {Tb(O$_2$CPh)$_3$(CH$_3$OH)$_2$(H$_2$O)}$_n$ and {Tb$_2$(O$_2$CPh)$_6$(4,4'-bipy)}$_n$," *J. Chem. Soc., Dalton Trans.,* **2001**, 134-137.

Shah, B. K.; Neckers, D. C.; Shi, J.; Forsythe, E. W.; Morton, D. "Anthanthrene derivatives as blue emitting materials for organic lght-emitting diode applications," *Chem. Mater.*, *18*, **2006**, 603-608.

Shavaleev, N. M.; Eliseeva, S. V.; Scopelliti, R.; Bünzli, J.-C. G. "N-Aryl chromophore ligands for bright europium luminescence," *Inorg. Chem.,* *49*, **2010**, 3927-3936.

Sheldrick, G. M., *SHELL-PC Version 5; 03*, Siemens Analytical X-ray Instruments. Inc., Madison, WI, USA, **1994**.

Shi, M.; Li, F.; Yi, T.; Zhang, D.; Hu, H.; Huang C. "Tuning the triplet energy levels of pyrazolone ligands to match the ^{5}D$_0$ Level of europium(III)," *Inorg. Chem.*, *44*, **2005**, 8929-8936.

Shyni, R.; Biju, S.; Reddy, M. L. P.; Cowley, A. H.; Findlater, M. "Synthesis, crystal structures, and photophysical properties of homodinuclear lanthanide xanthene-9-carboxylates," *Inorg. Chem.*, *46*, **2007**, 11025-11030.

Sivakumar, S.; Reddy, M. L. P.; Cowley, A. H.; Butorac, R. R. "Lanthanide-based coordination polymers assembled from derivatives of 3,5-dihydroxy benzoates: Syntheses, crystal structures, and photophysical properties," *Inorg. Chem.*, *50*, **2011**, 4882-4891.

Sivakumar, S.; Reddy, M. L. P.; Cowley, A. H.; Vasudevan, K. V. "Synthesis and crystal structures of lanthanide 4-benzyloxy benzoates: Influence of electron-withdrawing and electron-donating groups on luminescent properties," *Dalton Trans.*, *39*, **2010**, 776-786.

References

Sivakumar, S; Reddy, M. L. P. "Bright green luminescent molecular terbium plastic materials derived from 3,5-bis(perfluorobenzyloxy)benzoate," *J. Mater. Chem.*, *22*, **2012**, 10852-10859.

Stanley, J. M.; Zhu, X.; Yang, X.; Holliday, B. J. "Europium complexes of a novel ethylenedioxythiophene-derivatized bis(pyrazolyl)pyridine ligand exhibiting efficient lanthanide sensitization," *Inorg. Chem.*, *49*, **2010**, 2035-2037.

Steemers, F. J.; Verboom, W.; Reinhoudt, D. N.; Tol, E. B. V.; Verhoeven, J. W. "New sensitizer-modified calix[4]arenes enabling Near-UV excitation of complexed luminescent lanthanide ions," *J. Am. Chem. Soc.*, *117*, **1995**, 9408-9414.

Teotonio, E. E. S.; Brito, H. F.; Felinto, M. C. F. C.; Thompson, L. C.; Young, V. G.; Malta, O. L.; "Preparation, crystal structure and optical spectroscopy of the rare earth complexes (RE^{3+} = Sm, Eu, Gd and Tb) with 2-thiopheneacetate anion," *J. Mol. Struct.*, *751*, **2005**, 85-94.

Teotonio, E. E. S.; Claudia, M.; Felinto, F.C.; Brito, H. F.; Malta, O. L.; Trindade, A. C.; Najjar, R.; Strek, W. "Synthesis, crystalline structure and photoluminescence investigations of the new trivalent rare earth complexes (Sm^{3+}, Eu^{3+} and Tb^{3+}) containing 2-thiophene carboxylate as sensitizer," *Inorg. Chim. Acta*, *357*, **2004**, 451-460.

Tsaryuk, V. I.; Zhuravlev, K. P.; Vologzhanina, A. V.; Kudryashova, V. A.; Zolin, V. F. "Structural regularities and luminescence properties of dimeric europium and terbium carboxylates with 1,10-phenanthroline (C.N. = 9)," *J. Photochem. Photobiol. A: Chem., 211*, **2010**, 7-19.

Tsaryuk, V.; Zhuravlev, K.; Zolin, V.; Gawryszewska, P.; Legendziewicz, J.; Kudryashova, V.; Pekareva, I. "Regulation of excitation and luminescence efficiencies of europium and terbium benzoates and 8-oxyquinolinates by modification of ligands," *J. Photochem. Photobiol. A: Chem.*, *177*, **2006**, 314-323.

Utochnikova, V.; Kalyakina, A.; Kuzmina, N. "New approach to deposition of thin luminescent films of lanthanide aromatic carboxylates," *Inorg. Chem. Comm.*, *16*, **2012**, 4-7.

Van Vleck, J. H. "The Puzzle of Rare-Earth Spectra in Solids," *J. Phys. Chem.*, *41*, **1937**, 67-80.

Viswanathan, S.; de Bettencourt-Dias, A. "Eu(III) and Tb(III) luminescence sensitized by thiophenyl-derivatized nitrobenzoato antennas," *Inorg. Chem.*, *45*, **2006**, 10138-10146.

Wang, Y. B.; Zheng, X. J.; Zhuang, W. J.; Jin, L. P. "Hydrothermal synthesis and characterization of novel lanthanide 2,2′-diphenyldicarboxylate complexes," *Eur. J. Inorg.Chem.,* **2003**, 1355-1360.

Wang, Y. B.; Zhuang, W. J.; Jin, L. P.; Lu, S. Z. "Solvothermal synthesis and structures of lanthanide-organic sandwich coordination polymers with 4,4'-biphenyldicarboxylic acid," *J. Mol. Struct., 705*, **2004**, 21-27.

Wu, Q. R.; Wang, J. J.; Hu, H. M.; Shangguan, Y. Q.; Fu, F.; Yang, M. L.; Dong, F. X.; Xue, G. L. "A series of lanthanide coordination polymers with 4′-(4-carboxyphenyl)-2,2′:6′,2″-terpyridine: Syntheses, crystal structures and luminescence properties," *Inorg. Chem. Comm.*, *14*, **2011**, 484-488.

Xiao, M.; Selvin, P. "Quantum yields of luminescent lanthanide chelates and far-red dyes measured by resonance energy transfer," *J. Am. Chem. Soc.*, *123*, **2001**, 7067-7073.

Xin, H.; Shi, M.; Gao, X. C.; Huang, Y. Y.; Gong, Z. L.; Nie, D. B.; Cao, H.; Bian, Z. Q.; Li, F. Y.; Huang, C. H. "The effect of different neutral ligands on photoluminescence and electroluminescence properties of ternary terbium complexes," *J. Phys. Chem. B., 108*, **2004**, 10796-10800.

Xu, H.; Wang, L.-H.; Zhu, X.-H.; Yin, K.; Zhong, G.-Y.; Hou, X.-Y.; Huang, W. "Application of chelate phosphine oxide ligand in Eu^{III} complex with mezzo triplet energy level, highly efficient photoluminescent, and

electroluminescent performances," *J. Phys. Chem. B.*, *110,* **2006,** 3023-3029.

Ye, H.-M.; Ren, N.; Zhang, J.-J.; Sun, S.-J.; Wang, J.-F. "Crystal structures, luminescent and thermal properties of a new series of lanthanide complexes with 4-ethylbenzoic acid," *New J. Chem.*, *34*, **2010**, 533-540.

Yong, Z.; Li, X.; Zou, Y. Q. "Synthesis, structure and luminescence properties of four novel terbium 2-fluorobenzoate complexes," *Eur. J. Inorg. Chem.*, *14*, **2005**, 2909-2918.

Yu, B.; Sun, B.; Zhao, Y.; Yan, X.-Q. "Study on the synthesis, characterization of structure and fluorescence properties of the solid complex of europium ion with 1,10-phenanthroline and 2-thiopheneglyoxylic acid**,**" *Spectrosc. Spectral Anal.*, *12*, **2004**, 1571-1574.

Yu, X.; Su, Q. "Photoacoustic and luminescence properties study on energy transfer and relaxation processes of Tb(III) complexes with benzoic acid," *J. Photochem. Photobiolog. A.*, *155*, **2003**, 73-78.

Yuan, L.; Li, Z.; Sun, J.; Zhang, K. "Synthesis and luminescence of zinc and europium α-thiophene carboxylate polymer," *Spectroch. Acta*, *59*, **2003,** 2949-2953.

Zhan, C.-H.; Wang, F.; Kang, Y.; Zhang, J. "Lanthanide-thiophene-2,5-dicarboxylate frameworks: Ionothermal synthesis, helical structures, photoluminescent properties, and single-crystal-to-single-crystal guest exchange," *Inorg. Chem.*, *51*, **2012**, 523-530.

Zhang, H.; Li, N.; Tian, C.; Liu, T.; Du, F.; Lin, P.; Li, Z.; Du, S. "Unusual high thermal stability within a series of novel lanthanide TATB frameworks: Synthesis, structure, and properties (TATB = 4, 4′, 4″-s-Triazine-2,4,6-triyl-tribenzoate)," *Cryst. Growth Des.*, *12*, **2012**, 670-678.

Zhang, J.; Li, X.; Jin, L.; Lu, S. "Synthesis, structure and luminescence property of the ternary and quaternary europium complexes with furoic acid," *J. Mol. Struct.*, *604*, **2002,** 65-71.

Zhang, X. -X.; Lam, A. W. -H.; Wong, W. -T.; Gao, S.; Wen, G. "Synthesis, crystal structure, and photophysical and magnetic properties of dimeric and polymeric lanthanide complexes with benzoic acid and its derivatives," *Eur. J. Inorg. Chem.*, *1*, **2003**, 149-163.

Zhang, J.; Wang, Y. W.; Dou, W.; Dong, M.; Zhang, Y. L.; Tang, Y.; Liu, W. S.; Peng, Y. "Synthesis, crystal structures, luminescent and magnetic properties of homodinuclear lanthanide complexes with a flexible tripodal carboxylate ligand," *Dalton Trans.*, *40*, **2011**, 2844-2851.

Zhang, Z.-H.; Wan, S.-Yi.; Okamura, T.-aki.; Suna, W.-Yin.; Ueyama, N. "Synthesis and crystal structure of two lanthanide complexes with benzene carboxylic derivatives," *Z. Anorg. Allg. Chem.*, *632*, **2006**, 679-683.

Zheng, Y.; Cardinali, F.; Armaroli, N.; Accorsi, G.; "Synthesis and photoluminescence properties of heteroleptic europium(III) complexes with appended carbazole units," *Eur. J. Inorg. Chem.*, **2008**, 2075-2080.

Zhu, Y.; Li, H.; Koltypin, Y.; Gedanken, A. "Preparation of nanosized cobalt hydroxides and oxyhydroxide assisted by sonicatio," *J. Mater. Chem.,* *12*, **2002**, 729-733.